Appendix E

A Uniform Moment Magnitude Earthquake Catalog and Background Seismicity Rates for the Wasatch Front and Surrounding Utah Region

By

Walter J. Arabasz, James C. Pechmann, and Relu Burlacu

University of Utah Seismograph Stations
Salt Lake City, Utah 84112

2016

Research supported by the State of Utah through a line-item appropriation to the University of Utah Seismograph Stations and by the U.S. Geological Survey (USGS), Department of the Interior, under USGS Cooperative Agreement Nos. G10AC00085 and G15AC00028. The views and conclusions contained in this document are those of the authors and should not be interpreted as necessarily representing the official policies, either expressed or implied, of the U.S. Government.

Suggested citation:

Arabasz, W.J., Pechmann, J.C., and Burlacu, R., 2016, A uniform moment magnitude earthquake catalog and background seismicity rates for the Wasatch Front and surrounding Utah region: Appendix E *in* Working Group on Utah Earthquake Probabilities (WGUEP), 2016, Earthquake probabilities for the Wasatch Front region in Utah, Idaho, and Wyoming: Utah Geological Survey Miscellaneous Publication 16-3, variously paginated.

CONTENTS

TABLES

FIGURES

ELECTRONIC SUPPLEMENTS

SUMMARY

This appendix describes full details of the construction and analysis of a refined earthquake catalog and the calculation of seismicity rates for the Wasatch Front and surrounding Utah region. A distillation of this appendix, with primary focus on a background earthquake model for the Wasatch Front region, appears as section 5 of the report of the Working Group on Utah Earthquake Probabilities (WGUEP, 2015). Anticipating other applications, the scope of this appendix, both in terms of the earthquake catalog and the calculation of seismicity rates, extends beyond the WGUEP study region to the larger "Utah Region" (lat. 36.75° to 42.50° N, long. 108.75° to 114.25° W).

The earthquake catalog we constructed for our target Utah Region unifies existing catalogs compiled or produced directly by the two primary agents of seismic monitoring of the region: the University of Utah Seismograph Stations (UUSS) and the U.S. Geological Survey (USGS). The catalog covers the time period from 1850 through September 2012. To avoid possible edge effects from "declustering" (i.e., the identification and removal of dependent events) along the periphery of our target region, we expanded the bounds of our catalog compilation to a larger rectangular area termed the Extended Utah Region (UTREXT, lat. 36.0º to 43.5º N, long. 108.0º to 115.0º W). The UTREXT thus encompasses the Utah Region (UTR), within which the WGUEP Region is embedded. The outer frame of the UTREXT surrounding the UTR is termed the Extended Border Region (EBR).

The following key products are presented in this appendix, which includes ten electronic supplements:

- A unified earthquake catalog for the Extended Utah Region, both clustered and declustered, with uniform moment magnitude, **M**, and quantified magnitude uncertainty, covering the time period from 1850 through September 2012
- A compilation of reliable moment magnitude data for 114 earthquakes ($3.17 \leq \mathbf{M} \leq 7.35$) within or near the UTREXT catalog region
- Eighteen region-specific conversion relationships to moment magnitude (16 new, two revised) for an assortment of instrumental magnitudes and shaking-intensity size measures reported for earthquakes in the catalog
- Electronic spreadsheets that allow examination of the stepwise construction of the earthquake catalog, including listings of available size measures for each earthquake in the final catalog and the basis of its measured or estimated moment magnitude and corresponding uncertainty
- Background earthquake models represented by unbiased, maximum-likelihood seismicity rate parameters for both the Wasatch Front (WGUEP) and Utah regions

Background earthquakes are those not associated with known faults and of a size generally below the threshold of surface faulting. The background earthquake model for the Wasatch Front region depicts the frequency-magnitude distribution of future mainshocks expected to occur on seismic sources other than the faults included in the WGUEP fault model. For the WGUEP study, the parameter of primary interest is the rate of future mainshocks of **M** 5.0 or

greater up to a maximum of **M** 6.75 ± 0.25. In addition to the background earthquake model for the WGUEP region, we also developed a similar model for the Utah Region.

To develop the desired background earthquake models, we first constructed an up-to-date earthquake catalog that meets the needs of state-of-practice seismic hazard analysis, namely, a catalog that: (1) is complete in terms of accounting for all known earthquakes in the magnitude range of interest; (2) assigns a uniform moment magnitude to each event; (3) identifies "dependent" events (foreshocks, aftershocks, and the smaller events of earthquake swarms) forming parts of earthquake clusters that can be removed for statistical analysis of mainshock recurrence parameters; (4) excludes non-tectonic seismic events such as blasts and mining-induced seismicity; (5) identifies human-triggered earthquakes for optional removal; and (6) quantifies the uncertainty and rounding error associated with the assigned magnitude of each earthquake.

We restricted attention to the UTR for the identification and removal of non-tectonic seismic events and human-triggered earthquakes from the earthquake catalog. Retaining any such events in the EBR has no practical effect on the resulting catalog of independent mainshocks in the UTR after declustering—but it means the catalog *outside* the UTR must be used with caution. Non-tectonic seismic events in the UTR consist primarily of surface blasts and mining-induced seismicity associated with underground coal mining in east-central Utah and underground mining of trona (a sodium evaporate mineral) in southwestern Wyoming. Human-triggered earthquakes are associated with deep fluid injection in three areas of the eastern UTR (outside the WGUEP Region) in the Utah-Colorado border region. These injection-induced earthquakes were retained in our catalog but not used in the calculations for earthquake rates in the UTR.

In order to get unbiased estimates of seismicity rate parameters for the background earthquake models, we used as a *general* guide the methodology framework outlined in the final report of a project co-sponsored by the Electric Power Research Institute (EPRI), the U.S. Department of Energy (DOE), and the U.S. Nuclear Regulatory Commission (NRC) (EPRI/DOE/NRC (2012). Key elements are the assignment of a uniform moment magnitude to each earthquake in the catalog, assessment of magnitude uncertainties, and the application of bias corrections based on those uncertainties to estimate unbiased recurrence parameters. Throughout, our definition of moment magnitude, **M**, follows Hanks and Kanamori (1979): $\mathbf{M} = 2/3 \log M_0 - 10.7$, where M_0 is the earthquake's scalar seismic moment in dyne-cm, generally determined from inversions of either long-period waveforms or surface-wave spectra.

Our unified catalog for the UTREXT contains more than 5300 earthquakes larger than about magnitude 2.5, but direct instrumental measurements of **M** are available for only 107 of them (excluding known and suspected mining-related seismic events). Using these observed values of **M** plus values for seven supplementary events, we developed eighteen conversion relationships to moment magnitude (16 new, two revised) for an assortment of shaking-intensity size measures (maximum Modified Mercalli intensity, MMI; total felt area; extent of area shaken at or greater than various levels of MMI) and instrumental magnitudes (including Richter local magnitude, coda or duration magnitude, and body-wave magnitude) that varied with time and reporting agency. Where multiple size measures were available for an individual earthquake without a measured **M**, we computed an inverse-variance-weighted mean of **M** values computed from conversion relations to get a best estimate of **M**.

Different approaches can be utilized to transform an earthquake catalog with a minor fraction of direct instrumental measurements of **M** into one with "uniform moment magnitude." In the methodology of EPRI/DOE/NRC (2012), the uniform estimate of moment magnitude is E[**M**], the "expected value of moment magnitude," given uncertainty in either the observed value of **M** or in the value of **M** estimated from one or more other size measures. It is important to note that E[**M**] is a statistical construct with the specific underlying purpose of estimating unbiased earthquake recurrence parameters. Further, the equations for E[**M**] in EPRI/DOE/NRC (2012) implicitly assume the consistent use of least-squares regression (LSR) in magnitude conversions.

We decided not to use the "E[**M**]" approach for three reasons. First, we wanted an earthquake catalog with uniform moment magnitude that could serve other general purposes. Because E[**M**] is a statistical construct, it does not serve the same purposes as **M** outside the context of estimating unbiased earthquake recurrence parameters. Second, the use of general orthogonal regression (GOR) is favored by many experts over LSR for magnitude conversions. Consequently, the use of LSR for consistency with the E[**M**] approach as applied in EPRI/DOE/NRC (2012) will not generally provide the best estimate of **M**. Third, by consistently using GOR instead of LSR for magnitude conversions, many of the complexities of the E[**M**] methodology in EPRI/DOE/NRC (2012) can be eliminated.

We call the alternative uniform moment magnitude used to construct our catalog a "best-estimate" moment magnitude. Our Best-Estimate Moment Magnitude (BEM) catalog assigns a value of moment magnitude to each earthquake that either is directly observed as **M** ($\mathbf{M}_{obs}$), is a conversion of one or more other size measures to **M** using empirical predictive equations based on GOR (which yield predicted values, $\mathbf{M}_{pred}$), or is a reported value of magnitude which we assume to be equivalent to **M** (termed $\mathbf{M}^{\sim}$). Where $\mathbf{M}_{obs}$ was reported for an earthquake, it was given precedence over other size measures in the catalog. Our focus in producing the unified earthquake catalog was on the uniformity and quality of magnitude, not on epicentral quality. Therefore the resulting catalog should not necessarily be considered the "best" available for purposes relating to the accuracy of earthquake locations.

Our approach to estimating earthquake recurrence parameters involves a standard procedure used in Probabilistic Seismic Hazard Analysis—namely, the use of the Weichert (1980) maximum-likelihood approach to fit a truncated exponential distribution to earthquake counts in magnitude bins. Two known potential sources of bias that can affect the seismicity-rate calculations are magnitude uncertainty and the discretization or rounding of magnitude values to some specified nearest decimal value. In this study, the effect of rounded magnitude values is shown to be insignificant and is ignored.

Quantifying magnitude uncertainty is necessary for three aspects of our analysis of background seismicity: (1) correcting for bias in earthquake recurrence rates; (2) specifying the error-variance ratio between dependent and independent variables when using GOR for magnitude conversions; and (3) using inverse-variance weighting when combining different size measures to get a robust estimate of moment magnitude for an individual earthquake. The magnitude of an earthquake is generally taken as the mean value of magnitude determinations of the same type made at multiple recording stations. In the absence of systematic and rounding errors, the mean value of the event magnitude can be viewed as having random errors that are normally distributed with zero mean and standard deviation, σ (Tinti and Mulargia, 1985; Veneziano and

Van Dyke, 1985b). Following these cited authors, we define the latter statistic σ as the *magnitude uncertainty*.

For each earthquake in the master catalog, we provide a value of uniform moment magnitude and its corresponding uncertainty σ. To determine σ, uncertainties were first assessed for observed values of **M** and for reported values of other size measures that were converted to **M** through regressions. For most of the entries in the master catalog, σ comes from the propagation of uncertainties involved in regressions or from inverse-variance weighting of multiple estimates of **M** from various size measures.

For conformity with procedures used by the USGS in earthquake catalog processing for the U.S. National Seismic Hazard Maps, we used the computer program *cat3w* developed by Dr. Charles Mueller of the USGS for declustering. The program implements the method of Gardner and Knopoff (1974), in which smaller earthquakes within fixed time and distance time windows of larger shocks are identified as dependent events. We verified the effectiveness of using *cat3w* to decluster our BEM catalog by (1) comparing space-time plots of the original and declustered versions of the catalog and (2) using the Kolmogorov-Smirnov (K-S) test to analyze data in critical magnitude bins.

A critical element for constructing the background earthquake models is the completeness period, T_C, for which the reporting of earthquakes at or above a given magnitude threshold in the earthquake catalog is complete. To determine T_C for different magnitude thresholds in the declustered catalog, we used cumulative recurrence curves (plots of the cumulative number of earthquakes above a given magnitude threshold versus time) together with general information on the space-time evolution of seismographic control, population, and newspapers.

Our BEM earthquake catalog for the UTREXT contains 5388 earthquakes ($\mathbf{M} \leq 6.63$). The declustered version contains 1554 independent mainshocks ($2.50 \leq \mathbf{M} \leq 6.63$) in the UTR and 660 independent mainshocks ($2.50 \leq \mathbf{M} \leq 6.59$) in the WGUEP Region. We provide descriptions, including the basis of their estimated moment magnitudes, for the 19 independent mainshocks of **M** 4.85 or larger in the UTR, nine of which are within the WGUEP Region.

The earthquake catalog database is presented in ten electronic supplements, each in the form of a Microsoft Excel workbook with multiple worksheets. Each workbook contains an explanatory "README" file to guide the reader. The electronic supplements allow examination not only of the final unified catalog but also its building blocks. These include merged, chronologically sorted, and edited individual line entries from the diverse USGS and UUSS source catalogs; tabulated available size measures for each event in the master catalog; and calculations behind the assigned value of uniform moment magnitude and corresponding uncertainty for each earthquake.

The culmination of the appendix is the calculation of seismicity rate parameters to represent background earthquake models for the WGUEP and Utah regions. We use the N^* approach originally proposed by Tinti and Mulargia (1985) to achieve unbiased earthquake recurrence parameters. N^* is a count of earthquakes in a specified magnitude interval, adjusted for magnitude uncertainty. We followed the EPRI/DOE/NRC (2012) steps of (1) calculating N^* from σ on an earthquake-by-earthquake basis (using $N^* = \exp\{-(b \ln(10))^2\sigma^2/2\}$), (2) summing N^* for earthquakes within specified magnitude intervals, (3) dividing each N^* sum by the period

of completeness for its respective magnitude interval, and (4) using the maximum-likelihood algorithm of Weichert (1980) to compute seismicity rate parameters from the equivalent N^* counts. For the N^* calculations, we used a *b*-value of 1.05 assessed from preliminary processing of the BEM catalog.

Expressed in terms of a truncated exponential distribution with a minimum magnitude, m_0, of 2.85 and an upper-bound magnitude, m_u, of 7.00, the cumulative annual rate of independent mainshocks in the WGEUP Region greater than or equal to $m_0 = 2.85$ is 7.70 with a standard error of 0.52. The *b*-value determined for the model is 1.06 with a standard error of 0.06. For the Utah Region, the cumulative annual rate greater than or equal to $m_0 = 2.85$ is 18.0 with a standard error of 0.81. The *b*-value determined for the model is 1.07 with a standard error of 0.04. These models predict average recurrence intervals for $\mathbf{M} \geq 5.0$ earthquakes of 25 yrs (90% conf. limits: 17 to 44 yrs) for the WGUEP Region and 11 yrs (90% conf. limits: 8 to 16 yrs) for the Utah Region.

INTRODUCTION

This appendix describes full details of the construction and analysis of a refined earthquake catalog and the calculation of seismicity rates for the Wasatch Front and surrounding Utah region (figure E-1). A distillation of this appendix, with primary focus on a background earthquake model for the Wasatch Front region, appears as section 5 of the report of the Working Group on Utah Earthquake Probabilities (WGUEP, 2015). This appendix is intended to serve as a stand-alone document. It repeats some of the content of section 5 of the WGUEP report but its scope extends to a significantly larger area than the Wasatch Front region defined for the WGUEP probabilistic forecast (herein termed "the WGUEP Region").

Spatial Extent of the Earthquake Catalog

The standard region for which the University of Utah Seismograph Stations (UUSS) has the responsibility for seismic monitoring and catalog reporting as part of the U.S. Advanced National Seismic System is termed the "Utah Region" (lat. 36.75° to 42.50° N, long. 108.75° to 114.25° W). Anticipating other applications beyond the WGUEP study, we undertook to develop an improved historical and instrumental earthquake record for the whole Utah Region that unifies existing catalogs compiled or produced directly by the two primary agents of seismic monitoring of the region: the UUSS and the U.S. Geological Survey (USGS).

The unified UUSS-USGS earthquake catalog that we constructed for our target Utah Region covers the time period from 1850 through September 2012. To avoid possible edge effects from "declustering" (i.e., the identification and removal of dependent events) along the periphery of our target region, we expanded the bounds of our catalog compilation to a larger rectangular area termed the Extended Utah Region (UTREXT, lat. 36.0º to 43.5º N, long. 108.0º to 115.0º W). The UTREXT thus encompasses the Utah Region (UTR), within which the WGUEP Region is embedded. The outer frame of the UTREXT surrounding the UTR is termed the Extended Border Region (EBR). The geographic boundaries of these regions are specified in table E-1 and their spatial relations are shown on figure E-1.

Background Earthquake Models

Background earthquakes are those not associated with known faults and of a size generally below the threshold of surface faulting. The background earthquake model for the Wasatch Front study region depicts the frequency-magnitude distribution of future mainshocks expected to occur on seismic sources other than the faults included in the WGUEP fault model. In terms of earthquake size, the WGUEP background earthquake model provides rates of future mainshocks of moment magnitude, **M**, 5.0 or greater up to a maximum of **M** 6.75 ± 0.25. We similarly construct a background earthquake model for the Utah Region as a whole. Our analyses of background seismicity involve more thorough and rigorous treatments of the earthquake record, magnitude estimates, and magnitude uncertainties than previously attempted, for example by Youngs and others (1987, 2000) and by Pechmann and Arabasz (1995).

In the WGUEP seismic source model (see WGUEP, 2015, section 2.1), background seismicity logically should exclude earthquakes that can be associated with faults included in the WGUEP model and also are above the minimum magnitude of earthquakes modeled on those faults. Based on figure 7.1-4 of WGUEP (2015), this minimum magnitude effectively is **M** ~5.9 (for rates $\geq 10^{-4}$ per year). In the case of the Wasatch Front Region—and, indeed, throughout the Intermountain seismic belt in Utah—few historical or instrumentally located earthquakes can confidently be associated with mapped surface faults (e.g., Arabasz *et al*., 1992, 2007). The only surface-rupturing earthquake in the Utah Region during the time period of the 1850–2012 catalog was the 1934 **M** 6.6 Hansel Valley, Utah, earthquake, and the surface fracturing associated with it may not have been primary tectonic surface faulting (Doser, 1989). The vast majority of the earthquakes in our catalog within the Utah Region appear to be background earthquakes on buried or unmapped secondary faults. For this reason we used our refined earthquake catalog, without removing any mainshocks near modeled faults, to calculate rates of background earthquakes for the WGUEP and Utah regions.

The desired background earthquake models for the Wasatch Front and Utah regions require an up-to-date earthquake catalog that meets the needs of state-of-practice seismic hazard analysis, namely, a catalog that: (1) is complete in terms of accounting for all known earthquakes in the magnitude range of interest; (2) assigns a moment magnitude to each event ; (3) identifies "dependent" earthquakes (foreshocks, aftershocks, and the smaller events of earthquake swarms) forming parts of earthquake clusters that can be removed for statistical analysis of mainshock recurrence parameters; (4) excludes non-tectonic seismic events such as blasts and mining-induced seismicity; (5) identifies human-triggered earthquakes for optional removal; and (6) quantifies the uncertainty and rounding error associated with the assigned magnitude of each earthquake.

Two U.S. studies exemplify the rigorous development and treatment of earthquake catalogs for calculating background seismicity rates: EPRI/DOE/NRC (2012), for the central and eastern United States, and Felzer (2007), for California. We have used the former study, first, as a *general* guide in developing an earthquake catalog with uniform moment magnitude for the Wasatch Front and Utah regions and, second, for methodology guidance in handling magnitude uncertainties for calculating unbiased seismicity rate parameters. In a later section, we describe how we depart from the EPRI/DOE/NRC (2012) methodology.

Key Products

The following key products are presented in this appendix, which includes ten electronic supplements:

- A unified earthquake catalog for the Extended Utah Region, both clustered and declustered, with uniform moment magnitude and quantified magnitude uncertainty, covering the time period 1850 through September 2012

  [Note: The Extended Utah Region was designed to facilitate declustering along the periphery of the Utah Region. Because we did not systematically identify and remove non-tectonic seismic events and human-triggered earthquakes in the Extended Border Region, the catalog outside the Utah Region must be used with caution.]

- A compilation of reliable moment magnitude data for 114 earthquakes ($3.17 \leq \mathbf{M} \leq 7.35$) within or near the UTREXT catalog region
- Eighteen region-specific conversion relationships to moment magnitude (16 new, two revised) for an assortment of instrumental magnitudes and shaking-intensity size measures reported for earthquakes in the catalog
- Electronic spreadsheets that allow examination of the stepwise construction of the earthquake catalog, including listings of available size measures for each earthquake in the final catalog and the basis of its measured or estimated moment magnitude and corresponding uncertainty
- Background earthquake models, in terms of unbiased, maximum-likelihood seismicity rate parameters, for both the Wasatch Front (WGUEP) Region and the Utah Region

Organization of the Appendix

We begin by outlining the steps taken to develop a unified earthquake catalog, after which we elaborate on our treatment of non-tectonic seismic events and human-triggered earthquakes. In subsequent major sections, we explain key issues of uniform moment magnitude and magnitude uncertainty, methodology for estimating unbiased earthquake recurrence parameters, and the handling of various size measures in the earthquake record together with magnitude conversions to moment magnitude. We then describe the resulting earthquake catalog, followed by descriptions of how dependent events were removed to achieve a "declustered" catalog of independent mainshocks and how we assessed periods of completeness for different magnitude ranges. Finally, we summarize the calculation of unbiased seismicity rate parameters that characterize background earthquake models for the Wasatch Front and Utah regions.

STEPS IN DEVELOPING A UNIFIED EARTHQUAKE CATALOG

To develop a unified earthquake catalog with uniform moment magnitude, the following basic steps were followed:

- Selection of a catalog region large enough for effective declustering around the edges of the region of interest
- Merging, chronological sorting, and editing of individual line entries from diverse USGS and UUSS source catalogs—accounting for all reported earthquakes, removing duplicates and non-tectonic events, and selecting the line entry with the preferred time and location for each unique earthquake event
- Compilation and evaluation of available size measures for each event in the master catalog
- Assessment of magnitude uncertainties and rounding errors for individual magnitudes
- Tabulation of available instrumental measurements of moment magnitude, **M**, for earthquakes in the catalog region
- Determination of conversion relationships between **M** and other available size measures using general orthogonal regression (for comparison, corresponding ordinary least-squares regressions were also done)
- Assignment of a uniform moment magnitude and corresponding uncertainty to each earthquake in the master catalog, based on either direct measurement or conversion from other size measures (duly accounting for the propagation of uncertainties)

Data Sources for the Unified Catalog

In aiming for a unified UUSS-USGS catalog, focus was placed on authoritative source catalogs compiled or produced directly by the UUSS and the USGS. For historical earthquakes, these catalogs are compilations based on various primary and secondary sources and documented by USGS and UUSS researchers. For instrumentally recorded earthquakes, the source catalogs consist of tabulations directly resulting from regional seismic monitoring by the UUSS since mid-1962 and from national-scale seismic monitoring by the USGS since 1973 (or in earlier decades by the U.S. Coast and Geodetic Survey).

The following source catalogs were assembled for sorting, merging, and editing: (1) the UUSS historical earthquake catalog (downloaded from UUSS files on March 21, 2013); (2) the UUSS instrumental earthquake catalog (downloaded from UUSS files on June 12 and 14, 2013); (3) a version of the USGS catalog used in the 2008 national seismic hazard maps, termed the "Western Moment Magnitude" (WMM) catalog, updated through 2010 and provided by C.S. Mueller of the USGS on June 6, 2011; (4) a USGS in-house catalog termed the "SRA" catalog (after Stover, Reagor, and Algermissen,1986) for the western U.S., downloaded from the USGS Earthquake Hazards Program website on February 1, 2012; (5) the USGS PDE online catalog, sorted for the UTREXT and downloaded on March 9, 2013; and (6) Stover and Coffman's (1993) tabulations of significant earthquakes in the U.S. The catalog of Pancha and others (2006), which was adopted extensively into the USGS WMM catalog that was provided to us, was not directly merged into the raw master catalog but was checked to ensure that all reported earthquakes were accounted for.

As outlined in table E-2, the master catalog comprises three subcatalogs, A, B, and C, corresponding to three different time periods. Break points correspond to the start of the UUSS instrumental catalog on July 1, 1962, and the end of the SRA catalog on December 31, 1986. The table indicates which source catalogs were merged and synthesized to form each subcatalog. The master catalog begins in 1850, the date of the earliest reported historical earthquake in the UTREXT, and ends on September 30, 2012. Minimum magnitudes vary with each source catalog. One of our aims was to try to achieve as long a record as possible in the UTR down to **M** 3.0 or smaller. To this end, all events in the UUSS instrumental earthquake catalog of magnitude 2.45 or larger (on whatever scale) were imported into the master catalog.

NON-TECTONIC SEISMIC EVENTS AND HUMAN-TRIGGERED EARTHQUAKES

We restricted attention to the UTR for the identification and removal of non-tectonic seismic events from the earthquake catalog. Retaining any such events in the EBR has no practical effect on the resulting catalog of independent mainshocks in the UTR after declustering—but it means the catalog *outside* the UTR must be used with caution. One notable non-tectonic event in the EBR that was removed from the master catalog was the Project Rio Blanco underground nuclear test (m_b USGS 5.4), 58 km northwest of Rifle, Colorado, on May 17, 1973.

Non-tectonic seismic events in the UTR primarily consist of seismicity associated with underground mining and surface blasts associated with quarrying and surface mining. We are not aware of any documented cases of reservoir-triggered seismicity in the UTR (see Smith and Arabasz, 1991, for an earlier review of induced seismicity in the Intermountain region). There is, however, uncertain evidence for *decreases* in seismicity within 40 km following the impounding of Glen Canyon (Lake Powell) and Flaming Gorge reservoirs (Simpson, 1976 and references therein).

Injection-induced earthquakes are another type of human-triggered seismicity in the UTR, but we treated these differently from mining-induced seismicity (MIS). MIS was considered to release predominantly non-tectonic stress and was removed at early stages of compiling the master catalog. Earthquakes induced by the injection of fluids into underground formations, on the other hand, more commonly release stored tectonic stress on preexisting faults and can contribute to seismic hazard (see Ellsworth, 2013). To give future hazard analysts the option of how to deal with earthquakes potentially induced by fluid injection, we retained them in the catalog. But as we explain presently, we removed such events from the declustered version of the catalog before calculating seismicity rate parameters for the UTR. The WGUEP Region is unaffected (see locations of circular areas on figure E-1).

Surface blasts are systematically identified and excluded from the UUSS source catalogs we used (see, for example, http://www.seis.utah.edu/EQCENTER/LISTINGS/overview.htm). In editing the merged UUSS-USGS catalogs, all unique events in the UTR that derived from one or more USGS sources and without a corresponding UUSS event line were carefully scrutinized for their validity. For the instrumental period (subcatalogs B and C), this scrutiny included cross-checking UUSS files of “manmade” seismic events to ensure that a solitary USGS-derived event in the merged catalog was not one which the UUSS had identified and removed as a blast.

To be clear, although we made diligent efforts to exclude surface blasts from the BEM earthquake catalog for the UTR, we relied on UUSS observatory practices for eliminating such events from the UUSS source catalogs that we used. We did not undertake an additional screening process and admit the possibility that our final earthquake catalog may still contain a few blasts near some known quarry and mine sites in the UTR. We judge that the total number of such events is small and inconsequential for the earthquake rate calculations in this study.

Seismicity Associated with Underground Mining

Known areas of prominent MIS in the UTR are identified on figure E-1 and their boundaries are specified in table E-1. These include two areas of extensive underground coal mining in east-central Utah labeled WP-BC, for the Wasatch Plateau-Book Cliffs coal-mining region, and SUFCO, for the Southern Fuel Company coal-mining area. Another area of prominent MIS labeled TRONA is for an area of underground trona mining in southwestern Wyoming.

Areas of Coal-Mining Seismicity in East-Central Utah

MIS caused by underground mining in the arcuate crescent of the Wasatch Plateau and Book Cliffs coalfields in east-central Utah (WP-BC and SUFCO areas on figure E-1) is a well-recognized phenomenon that has been studied since the 1960s (see reviews by Wong, 1993; Arabasz and others, 1997, 2007; and Arabasz and Pechmann, 2001). The region's largest mining seismic event to date ($\mathbf{M}_{obs}$ 4.16, Whidden and Pankow, 2012) was the August 6, 2007, Crandall Canyon mine collapse (Pechmann and others, 2008).

The boundaries of the WP-BC and SUFCO areas specified in table E-1 are standard ones used by the UUSS to encompass areas of abundant MIS in Utah's coal-mining region. A sort of the UUSS instrumental catalog for the period July 1, 1962–September 30, 2012, yielded 20,416 events in the WP-BC area; of these, 522 had M_L or $M_C \geq 2.45$. For the SUFCO area, the number of sorted events was 2680 of which 97 had M_L or $M_C \geq 2.45$. Because of the large numbers involved, all of the events within the WP-BC and SUFCO areas were removed prior to merging the UUSS and USGS instrumental catalogs in subcatalogs B and C (with three exceptions discussed below). For the historical earthquake period of subcatalog A, which chiefly predates the occurrence of significant MIS in Utah, events with epicenters within the MIS areas were examined individually. We removed three events as probable mining-related events (see the README file in the electronic supplement for merged subcatalog A).

A recurring question when MIS is removed from the WP-BC and SUFCO areas is whether these areas contain tectonic earthquakes as well as MIS. We have scrutinized the MIS data set in the UUSS instrumental catalog a number of times to address this issue (Arabasz and Pechmann, 2001; Arabasz and others, 2005; Arabasz and others, 2007). Three known tectonic events, identified on the basis of their focal depths and source mechanisms, have occurred within the WP-BC area and are retained in the BEM catalog: (1) June 2, 1996, 08:09 UTC, **M** 3.18 (Arabasz and Pechmann, 2001, p. 4-8); (2) July 14, 2008, 23:50 UTC, **M** 3.17 (Whidden and Pankow, 2012); and (3) November 10, 2011, 04:27 UTC, **M** 3.96 (UUSS unpublished data).

As a further check for this study, we sorted the UUSS catalog for the WP-BC and SUFCO areas (July 1, 1962–September 30, 2012; $M \geq 2.45$) and then searched for events with well-constrained focal depths that would confidently place them below shallow mining activity. We searched for

event solutions meeting the following quality criteria: (1) epicentral distance to the nearest station less than or equal to the focal depth or 5 km, whichever is larger, and (2) standard vertical hypocentral error (ERZ) of 2 km or less, as calculated by the location program. This search yielded only three events with a well-constrained depth greater than 2 km—two of the already known tectonic earthquakes and an event in 1970 that had been located with a restricted focal depth of 7.0 km. Thus, we believe that removing events in the WP-BC and SUFCO areas from the instrumental earthquake catalog—except for the three identified tectonic earthquakes—is adequately justified for this project, particularly for the magnitude threshold of **M** 2.85 that we ultimately use for our seismicity rate calculations. For seismic hazard or risk analyses involving lower magnitudes, a different approach may be advisable.

Trona-Mining Seismicity in Southwestern Wyoming

The association of seismicity with the underground mining of trona (a sodium evaporate mineral) in southwestern Wyoming was highlighted by the occurrence of a magnitude 5.2 (M_L UU, revised) seismic event on February 3, 1995. A collapse of part of the Solvay Mine was the dominant source of seismic radiation (Pechmann and others, 1995). Ground truth for associating an event of magnitude 4.3 (M_L UU) on January 30, 2000, with a roof fall in the Solvay Mine, was documented by McCarter (2001).

In order to identify suspected mine seismicity associated with trona mining in this region, we used information on the website of the Wyoming Mining Association (www.wma-minelife.com). Specifically, we used a "Known Sodium Leasing Area (KSLA) Map" (Anadarko Petroleum Corporation, 2005) showing the location of the principal areas of trona mining to demarcate a rectangular area specified in table E-1 that encompasses what we believe is predominantly, if not exclusively, trona-mining seismicity. Sixteen seismic events ($2.5 \le M_L$ UU ≤ 5.2) within the "TRONA" rectangle were sorted from the master catalog and are listed in table E-3. All were deleted from our merged subcatalogs B and C as non-tectonic events.

Some local seismic monitoring was initiated by operators of the Solvay Mine after the 1995 mine collapse, but these data are not integrated into the regional seismic monitoring from which our source catalogs were produced. As a result, both epicentral and focal-depth resolution in our source catalogs are relatively poor for the TRONA area, and we have little basis for discriminating tectonic events from mining events in the area less than about **M** 3.5.

Injection-Induced Earthquakes

There are two known areas in the UTR where injection-induced earthquakes are of significant number and size to be of concern for our purposes. These are as shown on figure E-1 as circular areas along the Colorado-Utah border, labeled PV for Paradox Valley and R for the Rangely oil field. A third area, labeled RW for the Red Wash oil field in northeastern Utah, adjoins the Rangely area and has a handful of events in the earthquake catalog that we suspect may also be injection-induced. For each of these areas, we chose a radial distance of 25 km, with center points given in table E-1, to sort out suspected injection-induced earthquakes in the catalog. The selected radius was intended to allow for epicentral location errors and is in reasonable agreement with available earthquake information for the Paradox Valley and Rangely source areas; it is somewhat arbitrary, however, for the Red Wash source area.

Table E-4 lists the mainshocks in each of the three areas of suspected injection-induced seismicity that we decided to remove from the declustered catalog before calculating seismicity rates for a background earthquake model for the UTR. Earthquakes in the Paradox Valley and Rangely areas that were earlier removed as dependent events are identified in footnotes in table E-4.

Paradox Valley

The U.S. Bureau of Reclamation (USBR) has thoroughly monitored, studied, and documented injection-induced seismicity in the Paradox Valley (PV) area (figure E-1) associated with its Colorado River Basin Salinity Control Project (e.g., Ake and others, 2005; Block and others, 2012). To divert the seepage and flow of salt brine into the Dolores River, a tributary of the Colorado River, the USBR extracts aquifer brine from nine shallow wells along the river in western Colorado and injects the brine under high pressure at a depth of 4.3 to 4.8 km below surface in a deep disposal well (Ake and others, 2005). According to these authors, injection testing occurred between July 1991 and March 1995, and continuous injection began in May 1996. Up-to-date summaries of the ongoing induced seismicity resulting from this injection are provided by Ellsworth (2013) and in Appendix K of a report by the Committee on Induced Seismicity Potential in Energy Technologies (2013).

Table E-4 lists 19 mainshocks with epicenters within the Paradox Valley (PV) source area, all later than 1996, identified for removal from the declustered catalog; two dependent events are noted in footnote 3 of the table. The three largest events occurred in June and July 1999 (**M** 3.66 and **M** 3.69, respectively) and in May 2000 (**M** 3.80). Since 2002, injection-induced earthquakes have occurred out to 16 km from the disposal well (figure K.1 in Committee on Induced Seismicity Potential in Energy Technologies, 2013).

We emphasize that the data for the earthquakes in table E-4 originate primarily from the UUSS source catalog; data for two come from the USGS PDE catalog. The USBR has continuously operated the Paradox Valley Seismic Network (PVSN) in the PV area since 1985 (Ake and others, 2005). Data from a few stations of the PVSN have been telemetered to the UUSS since 1989 to enhance seismographic control in the eastern part of the UTR, but operation of these stations was occasionally interrupted. Most (13 of 19) of the earthquake locations in table E-4 have hypocentral control from at least one PVSN station. Higher resolution earthquake locations from the PVSN are documented internally by the USBR but are not contained in national earthquake catalogs.

Rangely Oil Field

The Rangely oil field in northwestern Colorado is described by the Energy and Minerals Field Institute (EMFI, 2005) as “one of the oldest and largest oil fields in the Rocky Mountain region.” Reservoir rocks are part of a northwest-southeast anticline about 12 miles (19 km) long and 5 miles (8 km) wide (Gibbs and others, 1973). The case for induced seismicity associated with the injection of fluid in the Rangely oil field is well documented (Gibbs and others, 1973; Raleigh and others, 1976; Ellsworth, 2013). Secondary oil recovery using “water-flooding” in water-injection wells began in late 1957 and continued until 1986, when a tertiary recovery program using carbon dioxide (CO_2) injection was started (EMFI, 2005; Clark, 2012). The latter involves pumping CO_2 and water into the subsurface in alternating cycles (EMFI, 2005). Moran (2007)

reviews the occurrence of earthquakes in the Rangely area and includes a figure showing epicentral scatter within about 25 km of the center of the oil field.

The full catalog contains 17 earthquakes in the Rangely circular source area. Seven of these are independent mainshocks ($2.97 \leq \mathbf{M} \leq 4.26$) that we removed as suspected injection-induced earthquakes (table E-4). Another nine were identified as dependent events by the declustering algorithm (footnote 4, table E-4) and removed earlier. The remaining earthquake, which occurred on February 21, 1954 (20:20 UTC, **M** 3.67), predates fluid injection in the oil field and was retained in the catalog. All seven mainshocks marked for removal occurred during known periods of fluid injection in the Rangely field, either for secondary or tertiary oil recovery.

Red Wash Oil Field

Sparse information is available for correlating earthquake activity with fluid injection in the Red Wash oil field, and our decision to remove earthquakes in this source area from the declustered catalog as injection-induced is arguable. Their removal or inclusion has little effect on calculated seismicity rates for the UTR.

Fluid injection has been used at the Red Wash field as part of secondary and tertiary oil recovery (Schuh, 1993; Chidsey and others, 2003). The field's geocode coordinates (table E-1) place it about 30 km to the west of the northwestern end of the Rangely field. Given its proximity to the Rangely field, the Red Wash area plausibly may share a susceptibility to triggered earthquakes, perhaps on the same buried Pennsylvanian fault system identified at Rangely (Raleigh and others, 1976).

Table E-4 identifies five earthquakes in the Red Wash source area as suspected injection-induced events. (The source area also includes the smaller Wonsits Valley oil field; for convenience, we simply use "Red Wash" as the general identifier.) An earthquake of **M** 4.02 in 1967 also lies within the Rangely circular area. This earthquake is the most distal from the Red Wash center point and more likely is associated with fluid-injection activities at Rangely in the 1960s. The other four shocks ($\mathbf{M} \leq 3.92$) occurred between 1990 and 2000. In the process of routinely issuing UUSS press releases following shocks of magnitude 3.5 and larger in the Utah Region, we became familiar with these earthquakes at the times of their occurrence and also with their apparent spatial association with the Red Wash oil field.

UNIFORM MOMENT MAGNITUDE AND MAGNITUDE UNCERTAINTY

The primary purpose for compiling the earthquake catalog is to develop unbiased estimates of seismicity rate parameters for the background earthquake models. To achieve that goal, we used as a *general* guide the methodology framework outlined in the final report of a project co-sponsored by the Electric Power Research Institute (EPRI), the U.S. Department of Energy (DOE), and the U.S. Nuclear Regulatory Commission (NRC) (EPRI/DOE/NRC (2012). Key elements are the assignment of a uniform moment magnitude to each earthquake in the catalog, assessment of magnitude uncertainties, and the application of bias corrections based on those uncertainties to estimate unbiased recurrence parameters.

Uniform Moment Magnitude

We require an earthquake catalog with a uniform size measure for each event specified in terms of moment magnitude, **M**, defined by Hanks and Kanamori (1979):

$$\mathbf{M} = 2/3 \log M_0 - 10.7 \qquad \text{(E-1)}$$

where M_0 is the earthquake's scalar seismic moment in dyne-cm, generally determined from inversions of either long-period waveforms or surface-wave spectra. Moment magnitude is used in state-of-practice seismic hazard analyses for consistency with modern ground-motion prediction equations. Moreover, moment magnitude has become the size measure preferred by seismologists because it is the best indicator of an earthquake's true relative size and can be directly tied to physical properties of the earthquake source.

Our culled master catalog for the Extended Utah Region contains more than 5300 earthquakes larger than about magnitude 2.5, but direct instrumental measurements of **M** are available for only 107 of them (excluding known and suspected mining-related seismic events). Using these observed values of **M** plus values for seven supplementary events (see Electronic Supplement E-2), eighteen conversion relationships to moment magnitude were developed for this project (16 new, two revised) for an assortment of shaking-intensity size measures and instrumental magnitudes that varied with time and reporting agency. The principal instrumental magnitudes in the source catalogs are Richter local magnitude (M_L), coda or duration magnitude (M_C, M_D), and body-wave magnitude (m_b). The non-instrumental size measures that were converted to **M** are: the maximum value of Modified Mercalli Intensity, MMI (I_0); total felt area (FA); and the extent of area shaken at or greater than MMI IV, V, VI, and VII (A_{IV}, A_V, $A_{VI,}$ and A_{VII}). Where multiple size measures were available for an individual earthquake, we computed a weighted mean of these measures using inverse-variance weighting to get a best estimate of **M**.

Different Approaches to "Uniform Moment Magnitude"

Different approaches can be utilized to transform an earthquake catalog with a minor fraction of direct instrumental measurements of **M** into one with "uniform moment magnitude." In the methodology of EPRI/DOE/NRC (2012), the uniform estimate of moment magnitude is E[**M**], the "expected value of moment magnitude," given uncertainty in either the observed value of **M** or in the value of **M** estimated from one or more other size measures. It is important to note that E[**M**] is a statistical construct with a specific underlying purpose, namely: "to estimate [unbiased] earthquake recurrence parameters using standard techniques, such as the Weichert (1980) maximum likelihood approach using earthquake counts in magnitude bins" (EPRI/DOE/NRC, 2012, p. 3-12). Further, the equations for E[**M**] in EPRI/DOE/NRC (2012) implicitly assume the consistent use of ordinary least-squares regression in magnitude conversions (Robert R. Youngs, AMEC Foster Wheeler, verbal communication, September 5, 2013).

We decided not to use the "E[**M**]" approach for three reasons. First, we wanted an earthquake catalog with uniform moment magnitude that could serve other general purposes. Because E[**M**] is a statistical construct, it does not serve the same purposes as **M** outside the context of estimating unbiased earthquake recurrence parameters. Second, the use of general orthogonal regression (GOR) is favored by many experts over least-squares regression (LSR) for magnitude

conversions (e.g., Castellaro and others, 2006, Castellaro and Bormann, 2007, Lolli and Gasperini, 2012; see also Gasperini and Lolli, 2014). Consequently, the use of LSR for consistency with the E[**M**] approach as applied in EPRI/DOE/NRC (2012) will not generally provide the best estimate of **M**. Third, by consistently using GOR instead of LSR for magnitude conversions, many of the complexities of the E[**M**] methodology in EPRI/DOE/NRC (2012) can be eliminated.

We call the alternative uniform moment magnitude used to construct our catalog a "best-estimate" moment magnitude. Our Best-Estimate Moment Magnitude (BEM) catalog assigns a value of moment magnitude to each earthquake that is either (a) directly observed as **M** ($\mathbf{M}_{obs}$); (b) a conversion of one or more other size measures to **M** using empirical predictive equations based on GOR (which yield predicted values, $\mathbf{M}_{pred}$); or (c) a reported value of magnitude which we assume to be equivalent to **M** (termed $\mathbf{M}^{\sim}$). Details for constructing the BEM catalog and differences in treating this catalog versus an E[**M**] catalog for estimating earthquake recurrence parameters are explained in a later section, *Methodology for Estimation of Unbiased Recurrence Parameters*.

Magnitude Uncertainty

Quantifying magnitude uncertainty (defined presently) is necessary for three aspects of our analysis of background seismicity: (1) correcting for bias in earthquake recurrence rates (see Musson, 2012, and references therein); (2) specifying the error-variance ratio between dependent and independent variables when using GOR for magnitude conversions; and (3) using inverse-variance weighting when combining different size measures to get a robust estimate of moment magnitude for an individual earthquake.

The magnitude of an earthquake is generally taken as the mean value of magnitude determinations of the same type made at multiple recording stations. In the absence of systematic and discretization (rounding) errors, the mean value of the event magnitude can be viewed as having random errors that are normally distributed with zero mean and standard deviation, σ (Tinti and Mulargia, 1985; Veneziano and Van Dyke, 1985b). Following these cited authors, we define the latter statistic σ (interchangeably using the notation "sigM" in the electronic supplements) as the *magnitude uncertainty*. This term is equivalent to "magnitude accuracy" used by Kagan (2002, 2003).

For each earthquake in the master catalog, we provide a value of uniform moment magnitude and its corresponding uncertainty σ. As noted above, values of σ were also required for other purposes. To determine σ, uncertainties were first assessed for observed values of **M** and for reported values of other size measures that were converted to **M** through regressions. For most of the entries in the master catalog, σ comes from the propagation of uncertainties involved in regressions or from inverse-variance weighting of multiple estimates of **M** from various size measures.

Uncertainties in $\mathbf{M}_{obs}$ and Other Size Measures

Estimating uncertainties in original catalog magnitudes can be a challenging exercise. Example approaches include (1) making "an estimate of the global standard deviation σ (computed for earthquakes with at least three station estimates)" (Castellaro and others, 2006); (2) comparing

statistically independent magnitude estimates from two different catalogs (Kagan 2002, 2003); (3) bootstrapping of station magnitudes to estimate the magnitude error for individual earthquakes in a catalog (Felzer and Cao, 2007); and, when needed data are not available, (4) relying on nominal values of σ for a particular type of magnitude during different time periods (e.g., EPRI/DOE/NRC, 2012, p. 3-21). In this study, approaches (1), (2), and (4) were variously used. For clarity we explain how they were applied to estimate the values of σ specified in several tables.

σ as the average standard error: For some original magnitude types, a data set was assembled for earthquakes with at least three station measures. The sample standard deviation, *STDEV* (with denominator $N - 1$ for a sample size of N), was computed for each earthquake and then corrected for sample bias ($STDEV_{\text{corrected}}$). This correction was made, assuming a normal distribution, by using the bias corrections of Gurland and Trapathi (1971), as tabulated in Rohlf and Sokal (1981), as a function of sample size—in this case, the number of station measures (*Nsta*). For each individual earthquake, the standard error of the *event* magnitude, SE_{em}, was then calculated as the standard deviation of the mean, *SDOM*:

$$SE_{em} = SDOM = \frac{STDEV_{\text{corrected}}}{\sqrt{Nsta}} \tag{E-2}$$

The average standard error of event magnitudes, $\overline{\boldsymbol{SE_{em}}}$, i.e., the average *SDOM* for as large a number of earthquakes as feasible, was adopted as an estimate of the population standard error or magnitude uncertainty, σ, for the specified magnitude type.

Regarding the uncertainty in a *single-station measurement* of a magnitude type, it is useful to note that the average of sample $STDEV_{\text{corrected}}$ of station magnitudes for a sizeable number of earthquakes represents an estimate of the population standard deviation for a single-station magnitude. Dividing the latter by the square root of *Nsta* gives an estimate of σ for an event magnitude having *Nsta* as the number of station measures. We used this approach for some event magnitudes with *Nsta* < 3. Estimates of σ for some original magnitude types using the average-standard-error approach are given in table E-5 (see also table E-6a, added to help give the reader an overview of estimated uncertainties in original catalog magnitudes).

σ from statistics of two different catalogs: Indirect approaches are commonly used to assess magnitude uncertainty for some magnitude types, particularly for observed values of moment magnitude, $\mathbf{M}_{\text{obs}}$. Kagan (2002, 2003) uses error analysis to determine the magnitude uncertainty associated with some magnitude types by comparing reported values in two different catalogs. If the magnitude estimates are statistically independent, the uncertainty in the magnitude difference between the two catalogs is a linear combination of the squared magnitude uncertainties in the first catalog, σ_{M1}, and the second catalog, σ_{M2}, respectively:

$$\sigma_{\Delta M}^2 = \sigma_{M1}^2 + \sigma_{M2}^2 \tag{E-3}$$

where $\sigma_{\Delta M}$ is the standard deviation of the magnitude difference for matched earthquakes in the two catalogs. If one assumes that both catalogs have the same magnitude uncertainty, then $\sigma_{M1} = \sigma_{M2}$ can simply be computed by dividing the observed $\sigma_{\Delta M}$ by the square root of 2. Equation (E-3) can also be used to solve for σ_{M1} or σ_{M2} in cases where one or the other and $\sigma_{\Delta M}$ are

known. Estimates of σ for some original magnitude types using the two-catalog approach are given in table E-6 (see also table E-6a).

Nominal values of σ for $\mathbf{M}_{obs}$: When data were unavailable to assess σ for the instrumental moment magnitudes of specific earthquakes in this study, nominal values of σ for $\mathbf{M}_{obs}$ were adopted from the following tabulation in EPRI/DOE/NRC (2012, p. 3-21), which was constructed for a similar purpose: nominal $\sigma[\mathbf{M}|\mathbf{M}_{obs}] = 0.30$ for 1920–1959; 0.15 for 1960–1975; 0.125 for 1976–1984; and 0.10 for 1985–2008. Where these nominal uncertainty values were adopted for these time periods, they were assumed for both single **M** determinations and (in three cases) for the mean values of two **M** determinations.

Propagation of Uncertainties in Regressing $\mathbf{M}_{obs}$ vs. a Single Size Measure

A noteworthy methodology step in EPRI/DOE/NRC (2012) is shown in their equation (3.3.1-8), which with adapted notation is reproduced here as

$$\sigma^2[\mathbf{M}|X] = \sigma^2[\mathbf{M}_{obs}|X] - \sigma^2[\mathbf{M}|\mathbf{M}_{obs}] \quad \text{(E-4)}$$

In words, when one regresses observed values of moment magnitude, $\mathbf{M}_{obs}$, against another size measure X, the resulting uncertainty $\sigma^2[\mathbf{M}|X]$ (expressed as a variance) in true **M** given X equals $\sigma^2[\mathbf{M}_{obs}|X]$, the square of the standard error in the predicted value of **M** from the regression, minus or reduced by $\sigma^2[\mathbf{M}|\mathbf{M}_{obs}]$, the variance in the observed values $\mathbf{M}_{obs}$ used in the regression of $\mathbf{M}_{obs}$ versus X. From basic propagation of errors, this rule applies whether LSR or GOR is used.

Note: For all of our linear regressions, the statistic used to express the standard error in the predicted value of y is the standard error of estimate of y on x, $S_{y,x}$, given by

$$S_{y,x} = \sqrt{\frac{\sum_i^N (y_i - y_i')^2}{DOF}} \quad \text{(E-5)}$$

where y_i and y_i' are the observed and predicted values of y, respectively, for the ith data point and DOF is the number of degrees of freedom. Given N paired values of x and y, DOF is $N - 2$ for the linear regressions and $N - 3$ for the non-linear regressions (which have three constants).

Propagation of Uncertainties in Two-Step Regressions

For many earthquakes in the catalog, **M** was estimated using two sequential regression steps, for which the propagation of uncertainties had to be analyzed. Because direct measurements of **M** make up a small fraction of the earthquake catalog, we encountered secondary size measures, X_2, for which direct regression of $\mathbf{M}_{obs}$ versus X_2 was not feasible. However, in most cases we had a regression for $\mathbf{M}_{obs}$ versus a primary size measure X_1 (let us call it Regression A), and we were able to develop a regression for X_1 versus X_2 (let us call it Regression B). If values of X_1 are estimated from X_2 using Regression B and then substituted in Regression A to estimate **M**, the resulting uncertainty in **M**, $\sigma[\mathbf{M}|X_2]$ must be determined.

Our approach to this problem was to estimate the additional uncertainty resulting from the use of $X_1 = f(X_2)$ in Regression A, assuming that X_1 and X_2 are independent random variables and using

basic theorems for the linear combination of variances (e.g., Chapman and Schaufele, 1970, p. 131). Letting $\mathbf{M}_{obs} = a_1 X_1 + a_2$ for Regression A and letting $X_1 = b_1 X_2 + b_2$ for Regression B, where a_i and b_i are constants, the following equation was derived for the uncertainty in **M** calculated from Regression A with the substitution of $X_1 = f(X_2)$:

$$\sigma^2[\mathbf{M}|X_2] = \sigma^2[\mathbf{M}|X_1] + a_1^2 (\sigma^2[X_1|X_2] - \sigma^2 [X_1]) \quad \text{(E-6)}$$

where $\sigma^2[X_1|X_2]$ is the square of the standard error of estimate, $S_{y,x}$, from Regression B; $\sigma^2 [X_1]$ is the variance of values of X_1 used to develop Regression A; and $\sigma^2[\mathbf{M}|X_1]$ is the variance in true **M**, given X_1. The latter, as specified by equation (E-4), is

$$\sigma^2[\mathbf{M}|X_1] = \sigma^2[\mathbf{M}_{obs}|X_1] - \sigma^2[\mathbf{M}|\mathbf{M}_{obs}] \quad \text{(E-7)}$$

To give a concrete example, consider the case of $X_1 = M_L$ UU1 determined by the University of Utah and $X_2 = m_b$ PDE2 determined by the USGS. The conversion relationships based on general orthogonal regressions are given in tables E-8 and E-10. To estimate **M**, given m_b PDE2, we first use conversion relationship CR-9 to estimate M_L UU1 and then use conversion relationship CR-1. For this circumstance, $\sigma[\mathbf{M}|\ M_L$ UU1] = 0.139, $a_1 = 0.791$, $\sigma[M_L$ UU1$|\ m_b$ PDE2] = 0.429, and $\sigma[M_L$ UU1] = 0.07 (table E-10). The desired uncertainty, $\sigma[\mathbf{M}|m_b$ PDE2], is thus given by

$$\sigma[\mathbf{M}|m_b \text{ PDE2}] = \sqrt{0.139^2 + 0.791^2(0.429^2 - 0.07^2)} = 0.362 \quad \text{(E-8)}$$

Propagation of Uncertainties in Inverse-Variance Weighting

The procedure for finding the best estimate of a quantity x from several measured (or estimated) values, each with a corresponding uncertainty σ, is straightforward using a weighted average (see, for example, Taylor, 1982, p. 148–150). For the ith value, its weight w_i is the inverse of the variance associated with that value ($1/\sigma_i^2$); hence, inverse-variance weighting. Formulas from Taylor (1982) provide an instructive starting point:

$$x_{best} = \frac{\sum_i w_i x_i}{\sum_i w_i} \quad \text{(E-9)}$$

for which the uncertainty in x_{best} is given by

$$\sigma_{x_{best}} = \frac{1}{\sqrt{\sum_i w_i}} \quad \text{(E-10)}$$

Referring to equation (3.3.1-10) in EPRI/DOE/NRC (2012) and following notation in that report, if we seek a best estimate of uniform moment magnitude from a vector **X** of R observed size measures, for which X_i is a single measure of the vector **X**, then the combined variance, CV, for the complete inverse-variance weighted estimate is

$$\sigma^2[\mathbf{M}|\mathbf{X}] = \frac{1}{\sum_i \frac{1}{\sigma^2[\mathbf{M}|X_i]}} \quad \text{(E-11)}$$

which is readily seen to be an alternative expression of equation (E-10).

As explained earlier, we depart from the EPRI/DOE/NRC (2012) methodology by not using E[**M**] as our uniform estimate of moment magnitude. Equation (3.3.1-9) in that report specifies how to calculate the inverse-variance-weighted estimate of E[**M**]. In similar form, the equation we use to calculate a best estimate of **M** from multiple size measures using inverse-variance weighting is

$$\mathbf{M}_{best} = \sum_i^N \frac{\mathrm{CV}}{\sigma^2[\mathbf{M}|X_i]} \cdot \mathbf{M}|X_i \qquad \text{(E-12)}$$

where CV = $\sigma^2[\mathbf{M}|\mathbf{X}]$ is the combined variance from equation (E-1), $\mathbf{M}|X_i$ is the estimate of **M** (i.e., $\mathbf{M}_{\text{pred}}$ or $\mathbf{M}^{\sim}$), given X_i, and $\sigma^2[\mathbf{M}|X_i]$ is the variance from the latter estimate (we introduce "CV" to simplify notation and to help guide calculations in the electronic supplements).

Equation (3.3.1-9) of EPRI/DOE/NRC (2012) differs from equation (E-12) in that it includes a correction term, $+(R-1)\beta \cdot \mathrm{CV}$, where $\beta = b\ \ln\{10\}$. This correction term is obviated when the conversion of the X_i size measures to **M** is based on orthogonal regressions instead of least squares regressions.

METHODOLOGY FOR ESTIMATION OF UNBIASED RECURRENCE PARAMETERS

Our approach to estimating earthquake recurrence parameters involves a standard procedure used in Probabilistic Seismic Hazard Analysis—namely, the use of the Weichert (1980) maximum-likelihood approach to fit a truncated exponential distribution to earthquake counts in magnitude bins (see, for example, EPRI/DOE/NRC, 2012). In mathematical form, the truncated exponential distribution can be expressed (see Youngs and Coppersmith, 1985) as

$$N(m) = N(m_0)\ \frac{10^{-b(m\,-\,m_0)}\ -\ 10^{-b(m_u\,-\,m_0)}}{1\ -\ 10^{-b(m_u\,-\,m_0)}} \qquad \text{(E-13)}$$

where $N(m)$ is the number of earthquakes per year of magnitude m or larger, m_0 is the minimum magnitude, m_u is the upper bound magnitude, and b is the slope constant in the frequency-magnitude relation. Two known potential sources of bias that can affect the seismicity-rate calculations are magnitude uncertainty and the discretization or rounding of magnitude values to some specified nearest decimal value.

Correcting for Magnitude Uncertainty

The effect of magnitude uncertainty on calculations of earthquake rate parameters is described by Musson (2012), who reviews different approaches to correct for bias in frequency-magnitude relations. He also underscores the complexity of the issue. Basically, because of the exponential distribution of magnitude, observed magnitudes (measured with normally distributed errors) together with their counts in discrete bins can have "apparent" values that differ from their "true" values—typically shown using simulated earthquake catalogs.

As a conceptual guide, figure E-2 illustrates the equivalence of approaches proposed independently by Tinti and Mulargia (1985) and Veneziano and Van Dyke (1985b) to correct for magnitude uncertainty σ in calculating unbiased ("true") seismicity rates. [Note: The draft report

by Veneziano and Van Dyke (1985b) is difficult to access. Veneziano and Van Dyke's methodology was implemented and is described in EPRI (1988).]

Without dwelling on the mathematical equations (see Tinti and Mulargia, 1985; EPRI/DOE/NRC, 2012), the following key points can be grasped from figure E-2. First, in a frequency-magnitude plot, bias caused by magnitude uncertainty can equivalently be corrected either in the *x*-direction using an adjusted magnitude called **M*** ("M-star") or in the *y*-direction using an adjusted rate called *N** ("N-star"). Second, the sign of the necessary corrections depends on whether the starting data lie along the line based on values of $\mathbf{M}_{obs}$ or its equivalent, as is the case for the BEM catalog, or along the line based on values of E[**M**], as is the case for an E[**M**] catalog developed following the equations and steps of the EPRI/DOE/NRC (2012) methodology. EPRI/DOE/NRC (2012) showed that for catalogs with variable levels of magnitude completeness, the *N** approach performs better than the **M*** approach. Accordingly, we used the *N** approach in this study. The specific steps we followed are described in a later section, *N* Values and Seismicity Rate Parameters.*

Equivalence of Best-Estimate Moment Magnitudes to $\mathbf{M}_{obs}$

Our assertion that our best-estimate moment magnitudes are equivalent to $\mathbf{M}_{obs}$, in terms of where they lie in the frequency-magnitude space of figure E-2, is essential to establish because it is fundamental to how we apply correction terms for magnitude uncertainty vis-à-vis figure E-2. To begin, magnitudes in our BEM catalog determined as $\mathbf{M}_{obs}$ are straightforward and need no further comment.

Our second type of best-estimate moment magnitudes are estimates of **M** using the results of orthogonal regressions of $\mathbf{M}_{obs}$ vs. other size measures. In the E[**M**] methodology, a key element is that all least squares regressions of $\mathbf{M}_{obs}$ vs. other size measures yield estimates of **M** that lie along the E[**M**] line in figure E-2. This situation changes, however, if orthogonal regression is used. Based on guidance and numerical simulations from Gabriel Toro of Lettis Consultants International, Inc., one of the principal experts on the EPRI/DOE/NRC (2012) methodology team: if orthogonal regression is used, then the results should be treated as equivalent to $\mathbf{M}_{obs}$ and *N** should be calculated as if no regression was performed. This guidance was first provided to us during a WebEx online meeting convened by the USGS on September 5, 2013, to address methodology issues relating to the treatment of magnitude uncertainty for U.S. National Seismic Hazard Maps. As part of the teleconference, G. Toro distributed and discussed a PowerPoint presentation titled, "Uncertainty in magnitude: Numerical experiment with M_L [to] M_w using orthogonal regression." Confirmation of how to correctly handle results of orthogonal regressions was also provided to us by G. Toro in follow-up written communications during September 2013.

The third type of best-estimate moment magnitudes in our BEM catalog are those identified as $\mathbf{M}^{\sim}$. In this case, we followed guidance provided to us by Robert ("Bob") Youngs (AMEC Foster Wheeler, written communication, Aug. 8, 2013), another of the principal experts on the EPRI/DOE/NRC (2012) methodology team. According to his guidance, if one assumes that a magnitude scale is equivalent to **M**, then the measured magnitude values should be treated as "noisy **M** values." They thus lie along the $\mathbf{M}_{obs}$ line in figure E-2, above the line of "true" recurrence rates, and are corrected accordingly. This guidance from Bob Youngs was confirmed during the above-mentioned USGS teleconference on September 5, 2013.

Effect of Magnitude Rounding

The potential overestimation of seismicity rates due to the rounding of reported magnitudes in an earthquake catalog was examined by Felzer (2007). Note that the object of her study, an earthquake catalog for California, involved a substantial proportion of events in the early to middle 1900s whose assigned magnitudes (M_L) were rounded to the nearest 0.5. Further, because of an assumed equivalence between M_L and **M**, rounded values of M_L (except where a measured value of **M** was also available) translated directly into similarly rounded values of **M** in her moment-magnitude catalog, thus motivating the need for correction. In the EPRI/DOE/NRC (2012) study, the potential impact of rounding of data to the nearest 0.1 magnitude unit was examined using simulated data sets, and statistical tests showed that the effect of the rounding could be ignored.

In this study, all values of **M** are uniformly rounded to the nearest 0.01 magnitude unit as the result of calculating **M** either from a measured value of scalar seismic moment or from magnitude-conversion relationships, in which case the effects of rounding in original size measures are subsumed in the regressions. The only exceptions to rounding **M** to the nearest 0.01 magnitude unit in our BEM catalog are those associated with values of $\mathbf{M}^{\sim}$, which were reported to the nearest 0.1 magnitude. For the WGUEP region, none of the independent mainshocks has an $\mathbf{M}^{\sim}$ value within a completeness period that enters into our final seismicity-rate calculations; for the UTR, two such events enter into the seismicity-rate calculations. The effect of rounded magnitude values was judged to be insignificant in our calculations and was ignored. Felzer's (2007) correction for magnitude rounding, given a *b*-value of 1.05 (determined in our initial processing of the BEM catalog) and rounding to the nearest 0.01, would involve multiplying the number of earthquakes above the completeness threshold by 0.988.

MAGNITUDE CONVERSION RELATIONSHIPS

A major part of constructing our BEM catalog was the conversion of other size measures to a best estimate of **M**. Key steps involved (1) compiling reliable measurements of observed moment magnitude $\mathbf{M}_{obs}$ to form the basis for developing conversion relationships of other size measures to **M**; (2) using general orthogonal regression (GOR) to regress $\mathbf{M}_{obs}$ on other size measures, yielding $\mathbf{M}_{pred}$; and (3) inverse-variance weighting of multiple estimates of **M**, including $\mathbf{M}_{pred}$ from different size measures and occasionally $\mathbf{M}^{\sim}$. Where $\mathbf{M}_{obs}$ was reported for an earthquake, it was given precedence over other size measures in the catalog, following rules described below.

The magnitude conversion relationships developed in this study should be considered region-specific. Our primary goal was achieving uniform moment magnitude estimates in the UTR, so we focused our data selection on the UTR, expanding the use of data from the EBR only where necessary. In some cases we supplemented a particular data set with size measures from a few large earthquakes outside the UTREXT (see figure E-3). The region of applicability of individual conversion relationships is indicated in the tables.

Moment Magnitude Data

Observed moment magnitudes were compiled for 114 earthquakes ($3.17 \leq \mathbf{M} \leq 7.35$) in or near the UTREXT (figure E-3), including 107 in the master catalog and seven supplementary events. The latter include three mainshocks outside the UTREXT (Hebgen Lake, Montana, 1959; Borah Peak, Idaho, 1983; and Kelly, Wyoming, 2010) together with four earthquakes in the UTREXT in late 2012 and early 2013. Documentation of the moment magnitude data is provided in Electronic Supplement E-2. For each earthquake, the documentation includes hypocentral information, the source of the seismic moment from which $\mathbf{M}_{obs}$ was calculated using the definition of Hanks and Kanamori (1979), and an assessment of magnitude uncertainty. A breakdown by source of the 114 values of $\mathbf{M}_{obs}$ used in this study, or more precisely the reported values of M_0 from which $\mathbf{M}_{obs}$ was calculated, is given in table E-7. Reported seismic moments for known and suspected mining-related seismic events are excluded from the list and were not used in developing magnitude conversion relationships.

For earthquakes in 1989 and later, all values of $\mathbf{M}_{obs}$ were calculated from a *single* seismic moment. In cases where more than one reported value of M_0 was available, the selected value followed the hierarchy shown in the upper part of table E-7. Thus, if a seismic moment was reported by more than one source, the Global CMT (GCMT) catalog was given precedence, followed by Whidden and Pankow (2012) and so forth, down to the Oregon State University moment-tensor catalog. Most of the UUSS moment tensors (MTs) we used are for earthquakes within the UTR and are given priority above corresponding SLU MTs, chiefly because the UUSS MTs are more numerous in our region of interest and because we have a better understanding of their quality control.

As part of their study, Pechmann and Whidden (2013) found that values of $\mathbf{M}_{obs}$ (as we define it) from UUSS seismic moments (Whidden and Pankow, 2012; Whidden, unpublished) agree closely with those calculated from seismic moments reported by St. Louis University (Herrmann and others, 2011; SLU moment-tensor website), with mean $\Delta\mathbf{M} = 0.001$ and $\sigma_{\Delta M} = 0.071$ for 36 events (table E-6). In contrast, Pechmann and Whidden (2013) found a systematic difference between GCMT $\mathbf{M}_{obs}$ values and UUSS/SLU $\mathbf{M}_{obs}$ values. To compensate, we reduced all GCMT $\mathbf{M}_{obs}$ values in our catalog by 0.14, based on the average difference between GCMT and SLU $\mathbf{M}_{obs}$ values for 24 shallow earthquakes that occurred in the western U.S. between 1998 and 2013 ($\sigma_{\Delta M} = 0.076$; table E-6).

In our compilation of moment magnitude data, we excluded seismic moments published by Doser and Smith (1982) that were determined from long-period spectral levels of body waves for 19 earthquakes in the UTR prior to 1977. Shemeta (1989) discusses problems with the data used by Doser and Smith (1982), particularly single-station data at regional distances, which may account for the unusually high seismic moments relative to M_L determined by them for earthquakes of $M_L < 5.0$. For five of the excluded seismic moments, including those for the three largest shocks, we used available values of M_0 that were determined from inversions of either long-period waveforms or surface-wave spectra. Based on values of $\mathbf{M}_{obs}$ from these other data, together with additional values of $\mathbf{M}_{pred}$, we infer that Doser and Smith (1982) systematically overestimated M_0 for shocks less than about $\mathbf{M}$ 5.75.

We examined values of $\mathbf{M}_{obs}$ that were calculated from seismic moments reported by Oregon State University (OSU) for earthquakes in the UTR during 1995–1998 and judged them to be

reliable. In three cases, a corresponding $\mathbf{M}_{obs}$ was available from Whidden and Pankow (2012), and the paired values were virtually identical. In seven other cases, $\mathbf{M}_{obs}$ from the OSU data agreed closely with $\mathbf{M}_{pred}$ from M_L determined by the UUSS. OSU moment tensors elsewhere in the Intermountain Seismic Belt, north of the UTR, appeared to yield $\mathbf{M}_{obs}$ systematically lower than $\mathbf{M}_{pred}$ from UUSS M_L data and were not used.

General Orthogonal Regression vs. Least Squares Regression

Castellaro and others (2006) discuss the underlying assumptions for least squares regression (LSR), most notably that the uncertainty in the independent (predictor) variable is at least an order of magnitude smaller than that in the dependent (response) variable. They point out that this assumption is seldom satisfied in magnitude conversions. For unbiased regression parameters, Castellaro and others (2006) show that general orthogonal regression (GOR) is superior to LSR for magnitude conversions when both dependent and independent variables are affected by uncertainty. GOR requires that the ratio η of the dependent variable variance (σ_y^2) to the independent variable variance (σ_x^2) be known. If η is unknown, assuming a value of 1 and using simple orthogonal regression still generally performs better than LSR (Castellaro and Bormann, 2007).

In this study, we were able to measure or reasonably estimate the uncertainties in both dependent and independent variables involved in our magnitude conversions, allowing us to apply GOR. GOR calculations for the linear conversion relations were performed in Excel spreadsheets using equations from Castellaro and others (2006), corrected for typographic errors that we confirmed by comparison with the original equations in Fuller (1987) that Castellero and others (2006) referenced. For the one non-linear conversion relation that we determined, CR-12, we carried out the GOR using a generalization of the method of Cheng and Van Ness (1999, p. 10) for two predictor variables (described in Pechmann and others, 2010).

Presentation of Magnitude Conversion Results

Up to this point, we have laid the methodology groundwork for presenting and discussing our magnitude conversion relationships (CRs), which entail considerable detail. We summarize much of this detail in tables. We begin with overviews of available magnitude data and the CRs we developed and then proceed to discuss the individual CRs, some under grouped headings.

Overview of Reported Magnitudes

Figure E-4 gives a schematic overview of the magnitude types reported in the source catalogs for the UTREXT. These data shaped our efforts to pursue conversion relationships to a uniform moment magnitude. For the historical period prior to July 1962 (subcatalog A), instrumentally-determined magnitudes are relatively sparse. Seismic moments are available for the 1934 Hansel Valley, Utah, earthquake and its largest aftershock, and an assortment of instrumental magnitudes is available for 68 earthquakes between 1917 and 1962. Most of these are M_L magnitudes determined at Pasadena for earthquakes in the southwestern part of the UTREXT between 1936 and 1962. An early 1917 magnitude comes from Wiechert seismographs operating at Reno, Nevada (Jones, 1975). Thus, size estimates for historical earthquakes prior to July 1962 rely greatly upon non-instrumental information. Size measures that we converted to **M** were: the maximum value of Modified Mercalli Intensity, MMI (I_0); total felt area (FA); and

the extent of area shaken at or greater than MMI IV, V, VI, and VII (A_{IV}, A_V, A_{VI}, and A_{VII}, respectively).

For the instrumental period from July 1962 through September 2012 (subcatalogs B and C), figure E-4 shows a gradually increasing availability of **M** with time. But most of the available data require reliance upon other instrumental magnitudes that varied with time and reporting agency. The instrumental magnitudes in the source catalogs that we converted to **M** come primarily from the UUSS and the USGS, and secondarily from the International Seismological Centre, ISC. They are Richter local magnitudes (M_L), coda or duration magnitudes (M_C, M_D), or body-wave magnitudes (m_b). There are ten values of M_S reported by the USGS for earthquakes in the UTREXT between 1984 and 2008, which we discuss but did not attempt to convert to **M**. The remainder of the magnitude data consists of more than a dozen other miscellaneous magnitude types for which data were inadequate for conversion to **M**. These magnitude types appear as the sole instrumental magnitude available for 188 earthquakes in the master catalog. We discuss them under the label **M**˜.

Overview of Magnitude Conversion Relationships

Using the available data represented on figure E-4, we developed 16 new CRs and refined two CRs earlier developed by Pechmann and Whidden (2013). For each of these 18 magnitude conversions, we performed both GOR and LSR, with results shown for comparison on each regression plot that we present. Table E-8 summarizes the GOR results, which provide the basis for estimates of **M** that enter into our BEM catalog. For the convenience of others who may wish to pursue the alternative E[**M**] approach using our data and the correction terms in EPRI/DOE/NRC (2012), we summarize our LSR results in table E-9.

Throughout, counterpart CRs in the tables and figures for GOR and LSR are given the same ID, but the letter "a" is appended to the CR-ID for the LSR results (e.g., CR-1a). Our discussion of the CRs focuses on the GOR results.

Based on our discussions with Gabriel Toro and Bob Youngs, practitioners are advised to consistently use either GOR or LSR in developing magnitude conversion relations. Otherwise, neither the BEM nor E[**M**] approaches to correcting event counts for magnitude uncertainty, as we have described them, can be used correctly without other complicated adjustments.

Regression statistics related to the CRs are presented in table E-10 for each GOR and in table E-11 for each LSR. Terms specific to GOR in table E-10 include σ_y and σ_x, the uncertainties in the dependent and independent variables, respectively, and η, the ratio of $\sigma_y{}^2$ to $\sigma_x{}^2$. In both tables E-10 and E-11, ID is the CR-ID in table E-8 or E-9; $S_{y,x}$ is the standard error of estimate of y on x; σ[**M**|X] is the uncertainty in true **M**, given the size measure X; and R^2 is the coefficient of determination for the regression. The minimum and maximum values of the independent variable x for each LSR, given in table E-11, are the same as for its counterpart GOR in table E-10.

Plots for each of the 13 regressions in tables E-10 and E-11 and for two model fits relating M_L magnitudes determined by the USGS to M_L magnitudes of the UUSS are shown in figures E-5 through E-15. A summary of the miscellaneous magnitudes encountered in the merged source catalogs for which data were insufficient to develop conversion relationships to **M** is presented in

table E-13. The table also gives the value of σ that we assessed for each of these magnitude types and its basis.

Except for CR-12 (and 12a), which has a non-linear form that follows EPRI/DOE/NRC (2012), all the conversion relationships to **M** that we developed are linear, as justified by the resulting correlation coefficients for our linear regressions and, for some relationships, by antecedent studies. M_L, M_C (or M_D), and m_b are commonly shown to be linearly correlated with **M**, at least over limited ranges of **M** up to 3.0 to 3.5 magnitude units (e.g., Braunmiller and others, 2005; EPRI/DOE/NRC, 2012). The same is true for the logarithm of the area shaken at or greater than a specified MMI in the western U.S. (Hanks and Johnston, 1992; Toppozada and Branum, 2002). In developing some of the CRs we chose to limit the size range of the data points used (CRs 8, 8a, 9, 9a, 10, 10a) or to use segmented linear regression (CRs 13 and 14 , along with their LSR counterparts). For CRs 8, 9, and 10 (and their LSR counterparts), which involve values of m_b PDE during specified time periods, the extrapolation of the CRs outside the defined segments of the independent variable is risky—as evident from inspection of figures E-9, E-10, and E-11.

For the linear regressions, the square root of R^2 listed in tables E-10 and E-11 yields the linear correlation coefficient R, which provides one basis for justifying the linear models. Using a standard table for the probabilities of correlation coefficients (e.g., Appendix C in Taylor, 1982) one can quantitatively assess the linear correlation of two variables. Such a table gives the probability $P_N(|R| \geq |R_o|)$ that N measurements of two uncorrelated variables would result in a coefficient R as large as observed, R_o. Small P_N indicates a likely correlation. If $P_N(|R| \geq |R_o|) \leq 0.05$, the correlation is deemed *significant*; if ≤ 0.01, then *highly significant* (Taylor, 1982, p. 248). Based on the N and R^2 statistics in tables E-10 and E-11, the evidence for linear correlation is highly significant for every one of the linear regressions.

$\mathbf{M_{pred}}$ from UUSS $\mathbf{M_L}$ Magnitudes

Richter local magnitude, M_L, measured on paper (and later synthetic) Wood-Anderson (W-A) seismograms, has been reported by the UUSS since mid-1962. Figure E-4 indicates two periods of M_L UU. M_L UU1 designates revised M_L values in the UUSS catalog since 1981 described by Pechmann and others (2007). M_L UU2 designates M_L values predating 1981 and based exclusively on paper seismograms from up to four W-A stations in Utah, as described by Griscom and Arabasz (1979). Empirical M_L station corrections determined by Pechmann and others (2007) minimize differences between M_Ls calculated from paper and synthetic W-A records and were designed to ensure uniformity of UUSS M_L values since 1962. The reason for distinguishing M_L UU1 from M_L UU2 is a change in magnitude uncertainty.

CR-1, 1a: Pechmann and Whidden (2013) used 65 data pairs for earthquakes predominantly in the UTR to regress $\mathbf{M}_{obs}$ (as defined herein) on M_L UU. The data consist of 64 paired values from 1983–2013 and one from 1967, and are plotted on figure E-5. The regression results reported here are a refinement of those given by Pechmann and Whidden (2013). In the refined regressions, GCMT $\mathbf{M}_{obs}$ values were reduced by 0.14, for reasons explained earlier in the section *Moment Magnitude Data*. For CR-1, the value of 0.139 for $\sigma[\mathbf{M}|M_L \text{ UU1}]$ comes from $S_{y,x} = 0.1473$ from the GOR reduced by the average uncertainty of 0.05 for the values of $\mathbf{M}_{obs}$ used in the GOR [see equation (E-4) and table E-10].

CR-2, 2a: A conversion relationship from M_L UU2 to **M** is based on the uniformity of M_L UU1 and M_L UU2 except for their differing magnitude uncertainty. Accordingly, we developed a two-step conversion, using CR-1, in which a larger σ of 0.24 for M_L UU2 (see footnote 3 in table E-5) is accounted for. Equation (E-6) yields a value of 0.229 for the uncertainty σ[**M**|M_L UU2] (table E-8). The calculation follows the example of equation (E-8), using the value of 0.24 for σ[M_L UU1|M_L UU2].

$\mathbf{M_{pred}}$ from UUSS $\mathbf{M_C}$ Magnitudes

Coda or duration magnitudes reported by the UUSS have changed with time, as indicated on figure E-4. This change is chiefly due to changes in recording methods—from paper seismograms used from July 1962 through September 1974 (M_C UU3) to 16-mm film recorders used from October 1974 through December 1980 (M_C UU2) to digital recording starting in January 1981 (M_C UU1). UUSS coda-magnitude scales for all three periods have been calibrated to the UUSS M_L scale (Griscom and Arabasz, 1979; Pechmann and others, 2010).

CR-3, 3a: The M_C scale calibrated by Pechmann and others (2010), which we designate M_C UU1, is the result of major efforts to automate and homogenize coda magnitudes determined by the UUSS from digital recordings since 1981. Pechmann and Whidden (2013) used 63 data pairs for earthquakes predominantly in the UTR from 1983 to 2013 to regress $\mathbf{M}_{obs}$ on M_C UU1 (figure E-6). Just as for CR-1, the regression results reported here are a refinement of those given by Pechmann and Whidden (2013). For CR-3, the value of 0.225 for σ[**M**|M_C UU1] comes from $S_{y,x}$ = 0.2310 from the GOR reduced by the average uncertainty of 0.05 for the values of $\mathbf{M}_{obs}$ used in the GOR [see equation (E-4) and table E-10].

CR-4, 4a: A conversion relationship from M_C UU2 (measured on 16-mm Develocorder film) to **M** is based on the calibration of M_C UU2 to M_L UU with a standard error of estimate of 0.27 (Griscom and Arabasz, 1979). A two-step conversion was developed, using CR-1, in which the larger σ of 0.27 for M_C UU2 is accounted for. Equation (E-6) yields a value of 0.249 for the uncertainty σ[**M**|M_C UU2] (table E-8). The calculation follows the example of equation (E-8), using the value of 0.27 for σ[M_L UU1|M_C UU2].

CR-5, 5a: A conversion relationship from M_C UU3 (measured on short-period, vertical-component Benioff seismograms) to **M** is based on the calibration of M_C UU3 to M_L UU with a standard error of estimate of 0.28 (Griscom and Arabasz, 1979). A two-step conversion was developed, using CR-1, in which the larger σ of 0.28 for M_C UU3 is accounted for. Equation (E-6) yields a value of 0.256 for the uncertainty σ[**M**|M_C UU3] (table E-8). The calculation follows the example of equation (E-8), using the value of 0.28 for σ[M_L UU1|M_C UU3].

$\mathbf{M_{pred}}$ from USGS $\mathbf{M_L}$ Magnitudes

M_L magnitudes designated "ML GS" appear in the USGS SRA catalog for earthquakes as early as 1969. Because this start time predates 1973, when the National Earthquake Information Center (NEIC) was transferred from the National Oceanic and Atmospheric Administration to the USGS, the designation "ML GS" for the pre-1973 earthquakes is confusing—but, more importantly, we are uncertain how those magnitudes were actually calculated.

Information from Bruce Presgrave (USGS, written communication, Nov. 29, 2012) is central to our understanding of M_L GS as it was reported by the USGS beginning in 1974 until sometime in

2011, when the USGS/NEIC began to compute M_L from synthetic horizontal W-A seismograms using its *Hydra* earthquake processing system. The following is an excerpt from Bruce Presgrave's written communication:

> Our magnitude we call ML (GS) has been the same from [1974] until we started using Hydra routinely for nearly all local events about 1 year ago. 'Our' (GS) ML was computed from the largest amplitude on the vertical short-period seismogram, with the amplitude adjusted to what it would have been on a Wood-Anderson instrument (i.e., nominal 2800 magnification). This was a two-stage process, either manually or by computer. First, we'd use the instrument calibration to convert from trace to ground amplitude, then convert that ground amplitude back to an amplitude at 2800 magnification. If the event were in or close to an area where a regional network (such as yours) was using ML off a true W-A instrument, we would often adjust the magnitude so that our values agreed more closely to what you or Caltech or Berkeley (etc.) might get. This usually involved adding 0.3 to 0.5 to the ML we computed off the vertical instrument.

Other relevant information in the written communication includes: (1) an evolution from the brief initial use of paper records to data from 16-mm film recorders to digital data, beginning about 1981; and (2) the routine calculation of M_L as an average, using data from any calibrated station available at NEIC that was within 5.4 degrees of the hypocenter. By Presgrave's account, the USGS/NEIC procedures used to determine M_L from 1974 to 2012 were basically pragmatic. Nevertheless, we found a good empirical correlation of M_L GS values to M_L UU values in the UTR (figure E-7) and in the EBR (figure E-8) that enabled conversion relationships to **M**.

CR-6, 6a: A conversion relationship from M_L GS to **M** applicable to the UTR for 1974−2012 is based on a comparison of M_L GS to M_L UU. Figure E-7 shows data for 69 data pairs for this time period. Because of the basic equivalence of both magnitude scales (Richter's amplitude-distance corrections are used for both), and given the apparent linear correlation between them, we adopted a simple offset model for which M_L UU = M_L GS − 0.11 ± 0.245 (1 std. deviation). An examination of a subset of the data (12 paired values) for the 1974−1980 period indicated a slightly larger offset of − 0.16 ± 0.34, but given the sparse data, we chose to use the grouped data for the entire 1974−2012 period.

A two-step conversion to **M** was then developed using CR-1 for the second step, as indicated in table E-8. Equation (E-6) yields a value of 0.232 for the uncertainty σ[**M**|M_L GS] (table E-8). The calculation follows the example of equation (E-8), using the value of 0.245 for σ[M_L UU1|M_L GS].

In completing the BEM catalog, we encountered four earthquakes in the UTR during 1970−1973 for which M_L GS (2.6−3.2) was the only instrumental magnitude available; we applied CR-6 to estimate **M** for these earthquakes.

CR-7, 7a: Similar to our approach for CR-6, we developed a conversion relationship from M_L GS to **M** applicable to the EBR for 1981−2012. Figure E-8 shows 280 data pairs for this region and time period. There were no data pairs for earthquakes prior to 1981, and the data set is heavily dominated by numerous aftershocks of the Draney Peak, Idaho, earthquake of February 3, 1994 ($\mathbf{M}_{obs}$ = 5.66), and of the Wells, Nevada, earthquake of February 21, 2008 ($\mathbf{M}_{obs}$ = 5.91).

For the 280 data pairs, we adopted a simple offset model, for which M_L UU = M_L GS + 0.09 ± 0.242 (1 std. deviation).

A two-step conversion to **M** was then developed using CR-1 for the second step, as indicated in table E-8. Equation (E-6) yields a value of 0.230 for the uncertainty σ[**M**|M_L GS] (table E-8). The calculation follows the example of equation (E-8), using the value of 0.242 for σ[M_L UU1|M_L GS].

In completing the BEM catalog, we encountered nine earthquakes in the EBR during 1969−1973 for which M_L GS (2.7−4.0) was the sole available size measure; we applied CR-7 to estimate **M** for these earthquakes.

$\mathbf{M_{pred}}$ from $\mathbf{m_b}$ PDE Magnitudes

The magnitude m_b PDE (also designated m_b GS after 1973) refers to teleseismic short-period body-wave magnitudes reported in the Preliminary Determination of Epicenters (PDE) bulletins published by the USGS/NEIC and its predecessors. Dewey and others (2003, 2004, 2011, including pdf copies of the corresponding poster presentations provided to us by J. Dewey, USGS) describe time-varying changes in m_b PDE, which they associate with temporal changes in procedures and data used at the NEIC in calculating this magnitude. We used their observations for earthquakes less than magnitude 6 to help us distinguish three periods for which m_b PDE in the UTREXT appears to differ. The periods are illustrated on figure E-4 and designated in table E-8 as m_b PDE1 (1991–2012), m_b PDE2 (1978–1990), and m_b PDE3 (1963–1977).

We chose 1991 as the start for m_b PDE1. This is the year in which the USGS inaugurated the U.S. National Seismograph Network, providing broadband digital data to the NEIC from a rapidly growing number of stations from which m_b began to be increasingly calculated from filtered data simulating the output of a short-period seismometer (Dewey and others, 2003). At about 1990, Dewey and others (2004) saw evidence of a decrease in m_b PDE values of about 0.2 magnitude unit when comparing m_b PDE with m_b predicted from local magnitudes such as M_L at Pasadena and Berkeley.

The change from m_b PDE3 to m_b PDE2 in 1978 marks when the USGS/NEIC sharply reduced the use of amplitudes and periods measured at regional distances between 5° and 15° (these tend to increase event m_b) to calculate m_b PDE for shallow-focus U.S. earthquakes (Dewey and others, 2003, 2004). During the period prior to 1978, other factors contributing to the heterogeneity of m_b PDE3 for smaller earthquakes include: computations from a relatively small number of stations; changes in the distribution of contributing stations, such as the closing of VELA arrays in the early 1970s (including UBO in Utah); and the measurement of amplitudes and periods from the first three cycles of the initial P-wave rather than from a larger time window (Dewey and others, 2003, 2004).

CR-8, 8a: The magnitude conversion from m_b PDE1 to **M** for the period 1991–2012 is the most straightforward of the three m_b PDE conversions. The availability of a sufficient number of data pairs allows a direct regression of $\mathbf{M}_{obs}$ on m_b PDE1 (figure E-9). Figure E-9 shows a divergence of data points for the smallest earthquakes, which is understandable for measurements of m_b made at teleseismic distances. We truncated the data set and limited the regressions to $m_b > 3.5$.

Of the 23 data pairs included in the regressions, 14 are for earthquakes in the UTR; nine, in the EBR.

For CR-8, the value of 0.207 for σ[**M**|m_b PDE1] comes from $S_{y,x}$ = 0.2154 from the GOR reduced by the average uncertainty of 0.06 for the values of $\mathbf{M}_{obs}$ used in the GOR[see equation (E-4) and table E-10].

CR-9, 9a: A conversion relationship from m_b PDE2 to **M** for the UTR for 1978−1990 is based on a regression of M_L UU or M_C UU (when M_L UU was not available) against m_b PDE2. Figure E-10 shows data for 23 data pairs for this time period. Just as for m_b PDE1, we truncated the data set, here limiting the regressions to 21 data pairs for $m_b \geq 3.5$. (The dependent variable is M_L UU for 16 of the 21 data pairs and M_C UU for five.) For the GOR, $S_{y,x}$ = 0.4292 (table E-10).

A two-step conversion to **M** was then developed using CR-1 for the second step (with the simplifying assumption that M_C UU = M_L UU), as indicated in table E-8. Equation (E-6) yields a value of 0.362 for the uncertainty σ[**M**|m_b PDE2] (table E-8). The calculation follows the example of equation (E-8), using the value of 0.429 for σ[M_L UU1|m_b PDE2].

CR-10, 10a: A conversion relationship from m_b PDE3 to **M** for the UTR for 1963−1977 is based on a regression of M_L UU or M_C UU (when M_L UU was not available) against m_b PDE3. Figure E-11 shows data for 110 data pairs for this time period. The scattered data reflect heterogeneity in m_b PDE during the 1960s and 1970s, attributable to factors discussed earlier. The data suggest a non-linear relationship with m_b, which is systematically larger than UUSS local magnitude below m_b 5.0 (see also Griscom and Arabasz, 1979). The data shown on figure E-11 were the most problematic m_b PDE data to deal with, but pursuing a magnitude conversion relationship was important because m_b PDE was the only instrumental magnitude available in the master catalog during 1963−1977 for 50 earthquakes in the EBR and 13 shocks in the UTR. All had magnitudes in the 3 and 4 range. We trimmed the data set as shown on figure E-11 ($3.3 \leq m_b$ PDE ≤ 5.0) and performed linear regressions on the 103 remaining data pairs. (The dependent variable is M_L UU for 59 of the 103 data pairs and M_C UU for 44.) For the GOR, $S_{y,x}$ = 0.5369 (table E-10).

A two-step conversion to **M** was then developed using CR-1 for the second step (with the simplifying assumption that M_C UU = M_L UU), as indicated in table E-8. Equation (E-6) yields a value of 0.443 for the uncertainty σ[**M**|m_b PDE3] (table E-8). The calculation follows the example of equation (E-8), using the value of 0.537 for σ[M_L UU1|m_b PDE3]. Because of this relatively large σ, we applied CR-10 only when m_b PDE3 was the sole instrumental magnitude available.

$\mathbf{M_{pred}}$ from ISC $\mathbf{m_b}$ Magnitudes

Teleseismic short-period body-wave magnitudes, m_b, have been reported by the ISC since 1964. In July 2012 when we extracted data from the ISC catalog (International Seismological Centre, 2010), the catalog was current to April 2010. Compared to m_b PDE, m_b ISC provides a more stable reference, affected by fewer procedural changes with time. In exploring the ISC data set it became apparent that m_b ISC was an attractive additional size measure for earthquakes in the UTR, independent of those in the source catalogs we had merged, particularly for shocks in the

magnitude 4 and 5 range. For data quality, we used only values of m_b ISC based on five or more stations (Nsta ≥ 5).

CR-11, 11a: A conversion relationship from m_b ISC (Nsta ≥ 5) to **M** is based on 13 data pairs shown on figure E-12 for earthquakes between 1967 and 2010. All of the earthquakes are in the UTR except for one: the Wells, Nevada, earthquake of February 21, 2008 ($\mathbf{M}_{obs}$ 5.91). For CR-11, the value of 0.295 for σ[**M**|m_b ISC] in table E-8 comes from $S_{y,x}$ = 0.3053 from the GOR reduced by the average uncertainty of 0.08 for the values of $\mathbf{M}_{obs}$ used in the GOR [see equation (E-4) and table E-10].

$\mathbf{M}_{pred}$ from Maximum Modified Meralli Intensity, I_0

The historical source catalogs for the UTREXT (subcatalog A) rely heavily on observations of Modified Mercalli Intensity (MMI) for estimates of earthquake size. (We use Roman and Arabic numerals interchangeably for MMI.) The maximum observed intensity is not necessarily identical to epicentral intensity, I_0, but is commonly assumed to be equivalent (e.g., Rogers and others, 1976). The maximum intensity reported by Stover and Coffman (1993) is the value closest to the epicenter. As noted in EPRI/DOE/NRC (2012), one can argue from the isoseismal maps in Stover and Coffman (1993) that the maximum intensity is typically very close to the epicenter.

In this study, we assume an approximate equivalence between maximum observed MMI and I_0. For the I_0-$\mathbf{M}_{obs}$ pairs that we used in our regressions, associated with earthquakes between 1934 and 2012, we scrutinized the epicentral distance associated with the maximum reported intensity for each earthquake. For older earthquakes, two useful resources were the annual publications of *U.S. Earthquakes* for 1934–1985 and the National Geophysical Data Center's *U.S. Earthquake Intensity Database* for 1683 to 1985 (www.ngdc.noaa.gov/hazard/int_srch.shtml). For earthquakes in the UTREXT since 2001, our primary resource was the USGS "Did You Feel It?" (DYFI) website (http://earthquake.usgs.gov/earthquakes/dyfi/, see also Atkinson and Wald, 2007).

For all but two of the I_0-$\mathbf{M}_{obs}$ pairs, the maximum intensity was observed within 20 km epicentral distance. One of the exceptions was an I_0-$\mathbf{M}_{obs}$ pair (5, 4.00) for an earthquake on July 14, 2006, near Georgetown, Idaho, for which I_0 = 5 was observed at Grace, Idaho, 25 km distant. The other presumed exception was an I_0-$\mathbf{M}_{obs}$ pair (6, 5.20) for the Southern Wasatch Plateau, Utah, earthquake of January 30, 1989; in this case, it was unclear whether I_0 = 6 was observed at the nearby town of Salina (population ~2400), 26 km distant, or at a closer site. Where I_0 (maximum MMI) came from DYFI data, we only used values of I_0 based on five or more responses within 20 km epicentral distance. We were able to evaluate proximity based on our familiarity with the location of population centers, without relying on the DYFI distances which are calculated relative to the centers of zip code areas.

For historical shocks in Utah of MMI V or greater, Rogers and others (1976) showed that estimated magnitude (M) plotted vs. I_0 reasonably followed Gutenberg and Richter's (1956) relation $M = 1 + 2/3\ I_0$. This same relation was used by Arabasz and McKee (1979) in compiling the UUSS historical earthquake catalog for the UTR. Gutenberg and Richter (1956) based their relation chiefly on data for $I_0 \geq$ V, with a single data point for I_0 = IV (see their figure 6). With

more modern data, the empirical scaling of I_0 with M is observed to be non-linear with a change in slope below $I_0 = V$ (e.g., EPRI/DOE/NRC, 2012, chapter 3, and references therein).

Mindful that I_0 was the only available size measure for most of the events in the pre-instrumental time period, we took care when merging the source catalogs to indicate a preferred value of I_0. USGS sources were given precedence, and the following order of priority was adopted: (1) Stover and Coffman (1993), two experienced compilers who had examined and revised maximum MM intensities in the process of producing multiple reports and publications on U.S. earthquakes, (2) the USGS-SRA catalog, and (3) the UUSS historical earthquake catalog.

For developing a conversion relationship from I_0 to **M**, we started with our compilation of $\mathbf{M}_{obs}$ and sought corresponding values of I_0 observed at small epicentral distance. In this exercise our assigned values of I_0 came exclusively from USGS (or predecessor) sources. Throughout, priority was given to Stover and Coffman (1993). For 1934–1985, supplementary values of I_0 came from annual editions of *U.S. Earthquakes*. Supplementary values of I_0 for 1986–2012 came from the USGS/NEIC PDE catalog and (for earthquakes in the UTREXT since 2001) the USGS DYFI website. If I_0 reported in the PDE catalog differed from DYFI data, we used the latter if well-founded.

CR-13, 13a: Data for converting $I_0 \geq V$ to **M** are plotted on figure E-13, showing the expected change in slope below $I_0 = 5$. For $I_0 \geq V$, the 24 data pairs are fit with a linear model. Our aim was to develop a region-specific relationship for the UTR, and 20 of the data pairs are for earthquakes within the UTR between 1934 and 2012. To provide control at the upper end of the regression, we added I_0-$\mathbf{M}_{obs}$ pairs for four shocks outside the UTR with the following (I_0, $\mathbf{M}_{obs}$) values: (1) 1959 Hebgen Lake, Montana (10, 7.35); (2) 1983 Borah Peak, Idaho (9, 6.82); (3) 1994 Draney Peak, Idaho (7, 5.66); and (4) Wells, Nevada (8, 5.93).

For the GOR (CR-13) we treated the independent variable I_0 as quasi-continuous, measured as discrete integers but with an uncertainty of 0.5. As shown in table E-10, values of 0.4474 and 0.429 were computed for $S_{y,x}$ and $\sigma[\mathbf{M}|I_0 \geq V]$, respectively. For our final CR-13 (table E-8), we adopted 0.5 as a nominal value for $\sigma[\mathbf{M}|\ I_0 \geq V]$, corresponding to what EPRI/DOE/NRC (2012) determined applying LSR to a much larger data set.

Conversion relationships for magnitude versus I_0 can differ regionally. Relationships in California (e.g., Toppozada, 1975; Gutenberg and Richter, 1956) differ significantly from that determined by EPRI/DOE/NRC (2012) for the central and eastern United States (CEUS). Comparisons must be made with care, taking into account the regression method, the type of magnitude being regressed, and the data available to control the regression, particularly at higher intensities. Keeping these issues in mind, the predicted magnitude for a given I_0 in the CEUS appears to be about a half to one magnitude unit lower than what would be predicted in California for the same I_0 in the range of V to VIII. For the Utah Region, figure E-13 shows that our conversion relationships CR-13 and CR-13a are close to Gutenberg and Richter's (1956) relation for California—rather than suggesting something transitional between California and the CEUS.

CR-14, 14a: Our conversion of $I_0 < V$ to **M** must be viewed as provisional and approximate. We wanted a relationship to estimate **M** for numerous earthquakes in the master catalog whose only reported size measure was MMI 2, 3, or 4. The earthquakes in question occurred before the

start of periods of complete reporting for these smaller shocks, so our seismicity-rate calculations are unaffected. Our approach is shown on figure E-14. To enlarge the data set for $I_0 < V$ shown on figure E-13, we added data pairs for earthquakes in the UTR in which the magnitude is $\mathbf{M}_{pred}$ from M_L UU ≥ 2.75 and I_0 is from DYFI data (black open circles in figure E-14). We then performed GOR on the expanded data set using data for $I_0 = 3$ or larger and including $I_0 = 5$ data for control. Just as for CR-13, we treated the independent variable I_0 as quasi-continuous, measured as discrete integers but with an uncertainty of 0.5. Our preferred GOR relationship (CR-14, table E-8) is labeled "GOR constrained" on figure E-14. This regression line is constrained to pass through the (x,y) value (5,4.05) predicted from CR-13 for $I_0 \geq 5$, thus tying conversions for I_0 above and below 5. For the constrained GOR, $\sigma[\mathbf{M}|\ I_0 < V]$ is 0.308, but we adopt the nominal value of 0.5 (see table E-8), just as for CR-13.

To explore whether CR-14 could reasonably be extrapolated to $I_0 = 2$, we further added data pairs for earthquakes in the UTR in which the magnitude is $\mathbf{M}_{pred}$ from M_L UU < 2.75 and I_0 is from DYFI data (red open circles in figure E-14). Note that this magnitude range is below the limit of data for CR-1 (figure E-5). These added data were not used in any of the regressions but are shown on figure E-14 for illustration. Overall, the data on figure E-14 indicate it is reasonable to use CR-14 (GOR constrained) to estimate **M** for $I_0 < 5$ in the UTR. It also appears reasonable to extrapolate CR-14 to $I_0 = 2$. Again, we emphasize that our use of CR-14 is provisional and approximate.

$\mathbf{M}_{pred}$ from the Logarithm of the Total Felt Area

Regressions of magnitude M on the logarithm of the macroseismic felt area, whether total felt area (FA) or the area shaken at or greater than a specified level of MMI (A_{MMI}, e.g., A_{VI}) generally provide more robust estimates of M than regressions of M on I_0 (Toppozada, 1975; Toppozada and Branum, 2002; see also Hanks and others, 1975). We first describe a conversion relationship for FA (CR-12) and then describe relationships for A_{VII}, A_{VI}, A_V, and A_{IV} (CR-15 to CR-18). All areas are measured in km^2.

CR-12, 12a: There are theoretical reasons why the scaling of log(FA) or ln(FA) with **M** is expected to be non-linear (Frankel, 1994). An updated data set of **M** versus ln(FA) for the central and eastern United States (EPRI/DOE/NRC, 2012, Fig. 3.3-44) clearly displays this non-linearity. To develop a conversion relationship from FA to **M**, we followed the model used by EPRI/DOE/NRC (2012): $\mathbf{M} = c_0 + c_1 \times \ln(FA) + c_2 \sqrt{FA}$, where c_0, c_1, and c_2 are constants.

Figure E-15 shows a plot of ln(FA)-$\mathbf{M}_{obs}$ data pairs, truncated at ln(FA) = 8 (i.e., FA ~3000 km^2), that we regressed to fit the above model. Above the truncation point, there are 26 data pairs, predominantly for shocks in the UTR. For additional control on the regression we included data for four shocks outside the UTR with the following (ln(FA), $\mathbf{M}_{obs}$) values: (1) 1959 Hebgen Lake, Montana (13.98, 7.35); (2) 1983 Borah Peak, Idaho (13.66, 6.82); (3) 1994 Draney Peak, Idaho (12.14, 5.66); and (4) a 2001 earthquake near Soda Springs, Idaho (10.76, 5.17).

The FA values for 12 of the 26 earthquakes come from isoseismal maps—as measured and reported by Stover and Coffman (1993) for ten and as measured by ourselves for two. For the remainder, the FA values come from measurements we made on Community Internet Intensity Maps (CIIMs) from the DYFI website. We systematically searched the DYFI archives for CIIMs associated with earthquakes in the UTR that were based on at least 50 responses (the

resulting median was ~160) and had sufficient zip-code "granularity" such that the interior of the felt area encompassed several or more zip codes. For the selected CIIMs, we outlined the felt area with an elliptical or curvilinear boundary, taking into account the known distribution of towns in rural areas and using judgment to transect zip codes at the periphery of the felt area with only one or a few responses.

In order to determine an uncertainty in ln(FA) for our measured felt areas, we converted all 26 FA values into equivalent circular areas, each with an effective radius. Examining both the historical and DYFI data, we assessed an uncertainty of ± 20 percent in the effective radius for an individual earthquake. Taking the geometric mean of the asymmetric error in the plus and minus directions gave us an uncertainty of 0.4 in ln(FA) for use in the GOR. The corresponding mean uncertainty for $\sqrt{\text{FA}}$ is 55 km for our data set of 26 earthquakes.

The GOR and LSR fits to our adopted non-linear model for $\mathbf{M}_{obs}$ vs. ln(FA), shown on figure E-15, are nearly identical and are well constrained by the data. To explore the implied trend of the regressions below ln(FA) = 8, we added data pairs for five small earthquakes (open circles, figure E-15) for which **M** is $\mathbf{M}_{pred}$ from M_L UU and FA was measured from DYFI data. These data are consistent with the trend of CR-12 at its lower end.

For CR-12, the value of 0.339 for σ[**M**|ln(FA)] in table E-8 comes from $S_{y,x}$ = 0.3535 from the GOR reduced by the average uncertainty of 0.10 for the values of $\mathbf{M}_{obs}$ used in the GOR [see equation (E-4) and table E-10].

In applying CR-12, it became apparent that FA values reported for early historical shocks were underestimated and unreliable. Toppozada (1975) noted the difficulty of determining FA for pre-1932 events because of sparse population and because weakly felt ground shaking may not have been considered noteworthy. Stover and Coffman (1993) report FA to the nearest 1000 km^2; their values of FA for older smaller earthquakes are low compared to modern DYFI data. For these reasons, we did not use any measurement of FA for historical earthquakes earlier than 1930, and our truncation of CR-12 at ln(FA) = 8 excludes FA values less than ~3000 km^2.

$\mathbf{M}_{pred}$ from the Logarithm of the Area Shaken at or Greater than MMI IV–VII

We turn now to A_{MMI}, the area shaken at or greater than a specified MMI, as a further means of estimating **M** from observations of macroseismic felt area. Table E-12 summarizes a region-specific data set that we compiled for A_{MMI} using available isoseismal maps for 22 earthquakes. The table is divided into three parts, indicating: (1) A_{MMI} used to develop CRs for A_{VII}, A_{VI}, $A_{V,}$ and A_{IV} that are displayed on figure E-16; (2) A_{MMI} used in applying the resulting CRs, contributing to the best-estimate moment magnitudes; and (3) A_{MMI} that was measured but not used for earthquakes after 1962. The data are predominantly from the UTR; however, the $\mathbf{M}_{obs}$-A_{MMI} pairs for the regressions include data from two earthquakes in the UTREXT (Draney Peak, Idaho, and Wells, Nevada) and two earthquakes outside the UTREXT (Hebgen Lake, Montana, and Borah Peak, Idaho).

Using the isoseismal maps indicated in table E-12, contours were digitized for the desired MMI isoseismals. These contours were not available for some earthquakes because of grouped intensities; in some other cases, the desired isoseismal was incomplete. Areas within the

digitized contours were then measured using a spatial mapping tool in *ArcGIS*, a geographic information system (GIS). Measured areas in table E-3 are rounded to the nearest 10 km^2.

Using data from the ten earthquakes for which $\mathbf{M}_{obs}$ was available, we developed direct magnitude conversion relationships by regressing $\mathbf{M}_{obs}$ on $\log(A_{MMI})$, following Toppozada (1975) and Toppozada and Branum (2002). For the ranges of magnitude and $\log(A_{MMI})$ considered, the $\mathbf{M}_{obs}$-A_{MMI} pairs for each of the MMI thresholds display a linear relationship, and the regressions are well constrained (figure E-16). Parameters for the four CRs based on GOR, CR-15 to CR-18, are given in table E-8, and regression statistics are given in table E-10. For the GORs, we estimated an uncertainty of 0.18 in $\log(A_{MII})$ in a way equivalent to how we estimated uncertainty in ln(FA). We used 0.18 as the nominal value for σ_x in all four GORs (table E-10).

We adopted a generic value of 0.35 for $\sigma[\mathbf{M}|\log(A_{MMI})]$ for CR-15 through CR-18 (table E-8) based on evaluating the regression statistics in table E-10. Actual values of $\sigma[\mathbf{M}|\log(A_{MMI})]$ in table E-10 include 0.339 for CR-16, 0.357 for CR-17, and much smaller equivalent values for CR-15 and CR-18. There is also a value of 0.339 for $\sigma[\mathbf{M}|\ln(FA)]$, reflecting scatter associated with a larger sample of areas of shaking. The generic value of 0.35 seems reasonable and was intended, in part, to allow for more scatter likely to be seen in larger samples of A_{VII} through A_{IV}. If multiple estimates of **M** from A_{MMI} were available, we computed the mean of those estimates and treated it as a single estimate with $\sigma = 0.35$.

$\mathbf{M}^{\sim}$, Magnitude Types Assumed to be Equivalent to M

In earlier sections we introduced $\mathbf{M}^{\sim}$, a magnitude type assumed to be equivalent to **M** and one of our three kinds of best-estimate moment magnitudes. Here we address the magnitude types that fall into the category of $\mathbf{M}^{\sim}$ and briefly discuss their relative significance. On the one hand, they are essential for achieving an estimate of **M** for every earthquake in the master catalog. On the other hand, they have an insignificant influence on our seismicity-rate calculations.

In merging diverse source catalogs, a practical problem arose with miscellaneous magnitudes that are the sole instrumental magnitude available for a number of earthquakes and for which there were inadequate data to develop magnitude conversions to **M**. Such magnitudes are among the earliest appearing in the master catalog (figure E-4). Table E-13 lists and describes these magnitudes and gives a breakdown in terms of their number, magnitude range, time period, region, and event type. Perhaps the most relevant information appears at the end of the table where one sees that of the 188 earthquakes having $\mathbf{M}^{\sim}$ as their sole magnitude, 129 are in the EBR and only 13 are mainshocks in the UTR. Of those 13 mainshocks, only two have $\mathbf{M}^{\sim}$ values within periods of completeness that enter into our seismicity-rate calculations for the UTR; no $\mathbf{M}^{\sim}$ values enter into the rate calculations for the WGUEP Region.

To be clear, the magnitude types listed in Table E-13 were used to estimate **M** for a particular earthquake only if no other instrumental magnitude was reported for which we had developed a CR. In such cases, for practicality, the sole available magnitude type was assumed to be equivalent to **M** and its reported value was treated as a "noisy" **M** value (see earlier section, *Equivalence of Best-Estimate Moment Magnitudes to $\mathbf{M}_{obs}$*). The assumption of equivalence to **M** can be reasonably justified for magnitude scales such as M_SGR, MLPAS, MLBRK, and the Wiechert magnitude at Reno, MxJON, which Jones (1975) calibrated against magnitude values published by Gutenberg and Richter (1949).

For each of the magnitude types in table E-13, we assign an uncertainty σ and give the basis for the assessment. We note that none of the 19 magnitude types in table E-13 is calculated directly from other earthquake size estimates using a magnitude conversion equation determined by least-squares regression. Consequently, for the purpose of magnitude corrections, we judged it more appropriate within the methodology framework outlined on figure E-2 to treat these 19 magnitude types as noisy **M** values rather than as E[**M**] values.

We caution the reader that our $\mathbf{M}^{\sim}$ approach may not always be appropriate for every problematic magnitude type. In our study, as noted above, only two $\mathbf{M}^{\sim}$ values in our catalog enter into our seismicity-rate calculations for the UTR and none for the WGUEP Region. In other studies where a substantial number of assigned $\mathbf{M}^{\sim}$ values influence such calculations, the hazard analyst will have to determine whether and how to correct those $\mathbf{M}^{\sim}$ values for magnitude uncertainty, according to the magnitude type (see Musson, 2012).

M_S Magnitudes

The instrumental earthquake catalog (merged subcatalogs B and C) contains only ten reported values of M_S (4.0 to 6.1) for earthquakes in the UTREXT, all determined by the USGS between 1984 and 2008. An earlier value of 3.4 in 1963 reported as "M_S GS" is of uncertain origin and accuracy. For the ten events with USGS determinations of M_S GS, corresponding values of $\mathbf{M_{obs}}$ are available for the six largest, and other magnitudes are available for the remainder, so there was no compelling need in this study for a conversion relationship from M_S to **M**. For researchers interested in this issue, the available data suggest approximate equivalence between M_S GS and **M** above approximately magnitude 5.5 (up to the saturation point of the M_S scale) but a nonlinear relationship over the range of magnitude 4 to 5.5, such as the quadratic equation determined by EPRI/DOE/NRC (2012) for a larger M_S-**M** dataset in the central and eastern United States.

RESULTS OF CATALOG COMPILATION

This section is the culmination of steps outlined at the outset under *Steps in Developing a Unified Earthquake Catalog*. The earthquake catalog database, comprising the full final catalog and its building blocks, is contained in ten electronic supplements. We first give the reader an explanatory guide to those supplements and then give a narrative overview of the final catalog, including descriptions of the largest mainshocks ($\mathbf{M} \geq 4.85$) in the UTR.

It should be emphasized that our focus in producing the unified earthquake catalog was on the uniformity and quality of magnitude, not on epicentral quality. Therefore the resulting catalog should not necessarily be considered the "best" available for purposes relating to the accuracy of earthquake locations. In selecting a preferred epicenter from duplicate entries in the merged catalogs, we made qualitative judgments but did not undertake any formal comparison of solution qualities for the reported epicenters.

For non-instrumentally located earthquakes in subcatalog A (pre-July 1962), we generally selected the location given in the UUSS source catalog, which coincides with the site of the maximum reported MMI. For subcatalogs B and C (post-June 1962), the UUSS location was preferred for epicenters within the UTR. For epicenters in the EBR, a USGS location was

generally preferred. However, for some events in the EBR immediately bordering the Utah Region and for most of the 1994 Draney Peak aftershock sequence, for which the UUSS installed local seismographs, the UUS location was selected. In our compilation of earthquakes in the UTR with an observed moment magnitude (see Electronic Supplement E-2), we adopted and annotated locations based on special study, when available. Most of the assigned focal depths are the centroid depth from an indicated moment-tensor inversion. When available, the depth from a specified well-constrained hypocentral solution was substituted.

We remind the reader that we did not systematically identify and remove non-tectonic seismic events and human-triggered earthquakes in the EBR. For this reason, the catalog outside the Utah Region must be used with caution.

Earthquake Catalog Database (Electronic Supplements)

The earthquake catalog database is presented in ten electronic supplements (E-1 to E-10), each in the form of a Microsoft Excel workbook with multiple worksheets. Each workbook contains an explanatory "README" file to guide the reader. The electronic supplements allow examination not only of the final unified catalog but also its building blocks. The building blocks include merged, chronologically sorted, and edited individual line entries from the diverse USGS and UUSS source catalogs; tabulated available size measures for each event in the master catalog; and calculations behind the assigned value of uniform moment magnitude and corresponding uncertainty for each earthquake.

In brief, electronic supplement E-1 contains the final catalog. E-2 summarizes the moment-magnitude data that were used to determine $\mathbf{M}_{obs}$ and as the basis for magnitude conversions from other size measures. E-3, E-4, and E-5 document how we merged and edited subcatalogs A, B, and C, respectively, as part of compiling a master catalog of unique earthquake events. E-6 to E-9 contain worksheets keyed to the seven general kinds of best-estimate moment magnitude explained below under "Mag Type" in the summary for E-1. For each magnitude type listed, a building-block file was created within E-6 to E-9. Exports from these building-block files in a uniform format were ultimately combined and chronologically sorted to create the final BEM catalog. Electronic supplement E-10 documents counts both of the actual and equivalent number (N*) of earthquakes, binned by magnitude, for independent mainshocks in the WGUEP and Utah regions.

Electronic Supplement E-1 (BEM Earthquake Catalog)

This workbook contains the Best-Estimate Moment Magnitude (BEM) earthquake catalog for the entire UTREXT, both in its clustered and declustered versions (explained and described in the next major section). For each earthquake line, the following information is given in successive columns (fields), following the structure of the USGS western moment magnitude (WMM) catalog:

BEM	Best-estimate moment magnitude
Long W, Lat N	Longitude and latitude (in degrees) of earthquake location
Depth	Earthquake focal depth (km)

Year, Mo, Day, Hr, Min, Sec — Earthquake origin date and time expressed in Coordinated Universal Time (UTC), or equivalently in Greenwich Mean Time (GMT) prior to 1960. In converting local standard time to UTC (or GMT), we accounted for advances in standard time that took place prior to the institution of Daylight Saving Time in 1967. These occurred during World War I (between March 31 and October 27, 1918, and between March 30 and October 26, 1919) and during World War II (between February 9, 1942, and September 30, 1945). These adjustments explain time differences of 1 hour with some event lines in USGS source catalogs.

sigM — Standard deviation of normally distributed errors in the best-estimate moment magnitude, used to compute N^*.

Round — Rounding error in the listed best-estimate moment magnitude

Mag Type — Descriptor indicating the basis for the best-estimate moment magnitude:

Mobs = $\mathbf{M}_{obs}$, observed moment magnitude from a direct instrumental measurement of seismic moment

M˜|[source] = $\mathbf{M}^{\sim}$, a magnitude type assumed to be equivalent to **M** (source indicates the origin of the reported magnitude)

Mpred|I_0 = Predicted moment magnitude, $\mathbf{M}_{pred}$, from converting maximum MMI, I_0, to **M**

Mpred|Xi = $\mathbf{M}_{pred}$ from converting a single instrumental size measure, X_i, to **M**

Mpred|Xvar = $\mathbf{M}_{pred}$ from inverse-variance weighting of $\mathbf{M}_{pred}$ values from two or more instrumental size measures

Mpred|Xnon = $\mathbf{M}_{pred}$ from inverse-variance weighting of $\mathbf{M}_{pred}$ values from two or more non-instrumental size measures

Mpred|Xmix = $\mathbf{M}_{pred}$ from inverse-variance weighting of $\mathbf{M}_{pred}$ values from a mix of instrumental and non-instrumental size measures

N^* — Equivalent earthquake count assigned to an individual earthquake that accounts for the effects of magnitude uncertainty in computing unbiased earthquake recurrence parameters. $N^* = \exp\{-\beta^2 \text{sigM}^2/2\}$, where $\beta = b\ln(10)$. A *b*-value of 1.05, assessed from preliminary processing of the BEM catalog, is used for all the N^* calculations.

Electronic Supplement E-2 (Moment Magnitude Data)

This workbook was introduced earlier in the section *Moment Magnitude Data*. For each of the 114 values of $\mathbf{M}_{obs}$ used in this study, documentation is provided for the source of the seismic moment from which we calculated $\mathbf{M}_{obs}$, using the definition of Hanks and Kanamori (1979). Hypocentral information and an assessment of magnitude uncertainty are also provided. Data for $\mathbf{M}_{obs}$ associated with earthquakes in the UTR and the EBR, respectively, and with seven supplementary events are presented in separate worksheets. Another worksheet presents data for $\mathbf{M}_{obs}$ associated with four known or suspected mining-related events in the UTR. These seismic events are excluded from the BEM catalog and their $\mathbf{M}_{obs}$ values were not used in this study.

Electronic Supplements E-3 to E-5 (Merged Subcatalogs A, B, and C)

In these three workbooks the reader can track separately for subcatalogs A, B, and C, respectively, the merging, chronological sorting, culling, and editing of individual line entries from the diverse USGS and UUSS source catalogs. For each subcatalog, multiple worksheets guide the reader through three successive compilations: (1) a merged and filtered raw compilation with the source of each event line identified ("filtered" means that mining-induced seismicity in the UUSS source catalog was removed prior to merging); (2) an expanded version of (1) in which duplicate line entries are identified, a preferred epicenter selected, and comments added; and (3) a culled version that contains event lines representing unique earthquake events, each with a preferred epicenter and a listing of all reported size measures.

Electronic Supplement E-6 (Worksheets for Mobs, M˜, Mpred|I_0)

This workbook contains three relatively straightforward worksheets in the format of the final catalog. The first is a tabulation of 107 earthquakes in the UTREXT for which values of $\mathbf{M}_{obs}$ are available, along with data distilled from electronic supplement E-2. The second worksheet lists all event lines in subcatalogs A, B, and C for which **M˜** is the only available *instrumental* size measure (for historical shocks, an **M˜** measurement was given priority over I_0); the Mag Type descriptor (e.g., M˜|MLPAS) indicates the source of the reported magnitude (see table E-13). The third worksheet lists all event lines (1850–1966, plus one event in 1974) for which I_0 is the only available size measure. An extra column gives the preferred value of I_0 that was identified when editing the merged subcatalogs. With this added information, one can examine the calculation of $\mathbf{M}_{pred}|I_0$ in the spreadsheet's first column that uses either conversion relationship CR-1, for $I_0 \geq V$, or CR-14, for $I_0 < V$ (see table E-8).

Electronic Supplements E-7 to E-9 (Worksheets for Mpred|Xnon, Xmix, Xvar, or Xi)

The workbooks for electronic supplements E-7, E-8, and E-9 deal with all earthquakes in the master catalog whose size information does not belong to one of the three categories of E-6 (i.e., $\mathbf{M}_{obs}$, **M˜**, or solitary I_0). The workbooks show all available size measures for the individual earthquakes, propagated forward from the merged subcatalogs. Added information documents how we used these size measures to determine **M** and σ for each earthquake utilizing the conversion relationships of table E-8. Editing comments and annotations are included.

In these workbooks, our general approach was to use all available size measures to achieve a best estimate of **M** with the following exceptions: (1) We ignored measurements of total felt area for historical earthquakes earlier than 1930 for reasons discussed earlier (see *M_{pred} from the Logarithm of the Felt Area*). (2) For earthquakes after 1963, only instrumental magnitudes were used in inverse-variance weighting. (3) Because of the relatively large uncertainty associated with converting m_b PDE3 to **M** (see figure E-11), we used m_b PDE3 only when it was the sole magnitude available.

Electronic supplement E-7 includes calculations for $\mathbf{M}_{pred}|X_{non}$ (inverse-variance weighting of $\mathbf{M}_{pred}$ values from non-instrumental size measures) and $\mathbf{M}_{pred}|X_{mix}$ (inverse-variance weighting of $\mathbf{M}_{pred}$ values from a mix of non-instrumental and instrumental size measures). The calculations

apply to 16 earthquakes between 1900 and 1962. $\mathbf{M}_{pred}|X_{non}$ was used for 14 earthquakes between 1900 and 1961, and $\mathbf{M}_{pred}|X_{mix}$ was used for the 1959 Arizona-Utah border earthquake and for the 1962 Magna earthquake (both discussed presently as part of a description of the largest mainshocks in the UTR).

Electronic supplements E-8 and E-9 pertain to subcatalogs B and C, respectively. They document the calculation of $\mathbf{M}_{pred}$ for the majority (70%) of individual earthquakes in the BEM catalog based either on $\mathbf{M}_{pred}|X_i$ (the conversion of a single instrumental size measure, X_i, to **M**) or $\mathbf{M}_{pred}|X_{var}$ (inverse-variance weighting of $\mathbf{M}_{pred}$ values from two or more instrumental size measures).

Errata Relating to Electronic Supplements E-8 and E-9

After completing the final BEM catalog and rate calculations, we discovered that some of the values of σ used in the conversions of m_b PDE (labeled "sigM mb PDE") in the workbooks of electronic supplements E-8 and E-9 were not the final correct values listed in table E-8. Specifically, instead of 0.362 for the two-step σ for CR-9, our calculations used 0.346; and instead of 0.443 for the two-step σ for CR-10, our calculations used 0.401. We examined what effect these small errors might have on earthquake data for the UTR, the area of interest for this study, and we found the effect to be negligible.

The discrepancy between 0.346 and 0.0362 for CR-9 (for m_b PDE2, 1978–1990) affected calculations for seven mainshocks in the UTR. Of these, the best-estimate moment magnitude remained the same for six and changed by 0.01 magnitude unit for one; *N** remained the same for five and decreased by 0.002 for two. These two tiny changes in *N** entered into the rate calculations for the WGUEP Region but not the UTR (because of the date of the earthquakes vis-à-vis periods of completeness).

The discrepancy between 0.401 and 0.443 for CR-10 (for m_b PDE3, 1963–1977) affected calculations for three mainshocks in the UTR. For all three, the best-estimate moment magnitudes remained the same but *N** decreased by 0.061. These *N** values did not enter into the rate calculations for either the WGUEP Region or the UTR because the shocks were not within periods of completeness.

Electronic Supplement E-10 (*N Counts for the WGUEP and Utah Regions)**

This workbook contains worksheets that allow the reader to track counts of *N** listed in tables E-18 and E-19 for the WGUEP and Utah regions, respectively. For each region, there are two worksheets. The first contains the appropriate geographic sort of the declustered version of the BEM catalog. The second has a color-coded display of the sorted earthquakes showing their grouping into magnitude bins 0.7 unit wide (beginning with $\mathbf{M} \geq 2.85$ up to **M** 7.00) along with counts both of the actual and equivalent number (*N**) of earthquakes in each magnitude bin. Within each color-coded magnitude bin, event lines are chronologically sorted and the period of completeness is demarcated. For the Utah Region, injection-induced earthquakes are excluded, as indicated in table E-4.

Overview of Best-Estimate Moment Magnitude (BEM) Catalog

Our unified and uniform earthquake catalog for the Utah Extended Region, i.e., the BEM catalog, contains 5388 earthquakes ($2.06 \leq \mathbf{M} \leq 6.63$) covering the period from 1850 through September 30, 2012. Only six of the shocks are smaller than **M** 2.50. Figure E-17 shows an epicenter map for all events in the total master catalog. The complete BEM catalog includes mainshocks, foreshocks, aftershocks, and earthquake swarms. Non-tectonic seismic events such as blasts and mining-induced seismicity are excluded.

After the removal of dependent events from the earthquake catalog resulting in a declustered version, the BEM catalog contains 1554 independent mainshocks ($2.50 \leq \mathbf{M} \leq 6.63$) in the UTR and 660 independent mainshocks ($2.50 \leq \mathbf{M} \leq 6.59$) in the WGUEP Region. (The count of 1554 mainshocks includes the 30 injection-induced earthquakes in table E-4). Corresponding epicenter maps are shown on figures E-18 and E-19, respectively.

Largest Mainshocks (M ≥ 4.85) in the Utah and WGUEP Regions

The declustered version of the BEM catalog, 1850 through September 2012, contains 19 independent mainshocks of **M** 4.85 or larger in the UTR, nine of which are within the WGUEP Region. Numbering of these earthquakes, keyed to table E-14, is shown on figures E-18 and E-19. Table E-14 summarizes basic information for each of these earthquakes, including the date and origin time, location, best-estimate moment magnitude and corresponding uncertainty σ, and the type of BEM on which **M** is based. Some description of these significant earthquakes is warranted, particularly regarding the basis of the estimated moment magnitudes.

An online resource (http://www.quake.utah.edu/lqthreat/nehrp_htm/eqtbl-date.shtml) provides historical information for most of these earthquakes, including newspaper articles, photographs, individual accounts, and excerpts from publications. Note that our present study provides more up-to-date information on magnitude estimates.

In the following descriptions of individual earthquakes where epicenters and focal depths are referred to, see table E-14. Estimates of moment magnitude from other size measures, $\mathbf{M}_{pred}$, are from the conversion relationships in table E-8. For convenience here, we simply refer to these values as **M**.

1. 1884, Nov. 10. Near Paris, Idaho (M 5.58): Historical accounts of this earthquake in the Idaho-Utah-Wyoming tri-state area, one of the earliest damaging shocks in the UTR and WGUEP regions, have been studied and analyzed by Evans and others (2003), whose preferred epicenter we adopt. The distribution of felt reports described by Evans and others (2003) suffers from incompleteness and irregularity typical for this early time period. These authors report a failed attempt, due in part to anomalous ground shaking at large epicentral distances, to use Bakun and Wentworth's (1997) inversion method to estimate magnitude from the available felt observations. Our best-estimate moment magnitude, **M** 5.58 ± 0.50, is based on I_0 = VII assessed by Stover and Coffman (1993). Our attempts to use the felt observations reported by Evans and others (2003) proved problematical. The felt area of 70,000 km^2 reported by Evans and others (2003) gives **M** 5.03; their suggestion of a felt area possibly as large as 210,000 km^2, based on the addition of a single felt report, gives **M** 5.77. Figure 3 of Evans and others (2003) indicates A_V of about 1650 km^2, implying **M** 3.84.

2. 1901, Nov. 14. Tushar Mountains, Utah (M 6.63): This damaging earthquake in central Utah rivals the 1934 Hansel Valley earthquake as the largest historical earthquakes in the UTR since pioneer settlement. Williams and Tapper (1953) summarize macroseismic effects, including extensive rockslides and rock falls in the Tushar Mountains betweeen Beaver and Marysvale. No surface faulting was observed. We adopt an epicenter that lies at the mid-point of the area shaken at MMI VIII or greater on Hopper's (2000) isoseismal map. Our best-estimate moment magnitude, **M** 6.63 ± 0.29, is based on inverse-variance weighting of **M** values from I_0 = VIII assessed by Stover and Coffman (1993) and from measures of A_{VI} and A_{VII} in table E-12. The assigned magnitude of this earthquake is just slightly larger than that of the 1934 Hansel Valley mainshock (**M** 6.59 ± 0.30). Comparison of the measures of A_{VI} and A_{VII} for the 1901 and 1934 earthquakes (table E-12) supports the assessment that the 1901 central Utah earthquake was comparable in size or slightly larger than the 1934 Hansel Valley earthquake.

3. 1902, Nov. 17. Pine Valley, Utah (M 6.34): Williams and Tapper (1953) summarize damage reports and felt effects for this earthquake centered in Pine Valley, north of St. George in southwest Utah. Our best-estimate moment magnitude, **M** 6.34 ± 0.50, is based on I_0 = VIII assessed by Stover and Coffman (1993). The asssigned epicenter is from the UUSS catalog, corresponding to coordinates for Pine Valley, based in turn on MMI effects described by Williams and Tapper (1953). Their FA of 10,000 square miles (25,900 km^2) is undoubtedly underestimated, and the lack of an isoseismal map leaves I_0 as the sole size measure.

4. 1909, Oct. 6. Hansel Valley, Utah (M 5.58): Williams and Tapper (1953) note that this earthquake in northern Utah generated waves in Great Salt Lake (GSL) that passed over the Lucin cut-off (a 19-km-long railroad trestle that crosses GSL in an east-west direction) and rolled over a bath house pier at Saltair at the southern end of GSL. Based on the distribution of towns reporting the mainshock, these authors expressed a high degree of confidence that the earthquake originated in Hansel Valley, located at the northern end of GSL. Our assigned epicenter, from the USGS SRA catalog, is on the western side of Hansel Valley on the Hansel Valley fault and ~15 km north of Great Salt Lake. Our best-estimate moment magnitude, **M** 5.58 ± 0.50, is based on I_0 = VII assessed by Stover and Coffman (1993). A felt area of 78,000 km^2 reported by Stover and Coffman (1993), likely an underestimate because of the time period, gives **M** 5.09. Felt reports are inadequate to estimate A_{MMI}. If our assigned location and estimated magnitude are correct, then the large water waves generated in Great Salt Lake could plausibly be explained by an earthquake-induced landslide underneath or into the lake.

5. 1910, May 22. Salt Lake City, Utah (M 5.28): Williams and Tapper (1953) describe effects of this local earthquake in the Salt Lake Valley, which damaged several buildings and toppled many chimneys in Salt Lake City. For consistency with the isoseismal map of Hopper (2000, figure 4), our selected epicenter is from the USGS SRA catalog. Our best-estimate moment magnitude, **M** 5.28 ± 0.29, is based on inverse-variance weighting of two **M** values: an **M** value calculated from I_0 = VII assessed by Stover and Coffman (1993) and a mean **M** value calculated from A_V and A_{VI} (table E-12). A_{VII} gives **M** significantly lower than the other size measures and was judged to be poorly constrained and imprecise.

6. 1921, Sept. 29. Elsinore, Utah (M 5.45): This earthquake was the first and largest of three strong earthquakes that occurred between September 29 and October 1, 1921, causing considerable damage in the small town of Elsinore in the Sevier Valley in central Utah (Pack,

1921; Williams and Tapper, 1953; Stover and Coffman, 1993). Our adopted epicenter for the mainshock is from the UUSS catalog and corresponds to the location of Elsinore.

Estimating the sizes of the three earthquakes poses a challenge. Hopper (2000) noted the contrast between their relatively high maximum intensities (MMI = VIII, VII, VIII, as assessed by Stover and Coffman, 1993) and their very rapid intensity attenuation, concluding that they were probably extremely shallow events. (See Arabasz and Julander, 1986, regarding a discontinuity in seismicity and geological structure at about 6 km depth beneath the Elsinore area.) Isoseismal maps published by Hopper (2000) for the three events are at a small scale, but contours for MMI $\geq$ VII for the first shock and MMI $\geq$ VI for the second and third shocks appear to be reasonably constrained by the distribution of towns surrounding Elsinore. Given the early date, FA may be underestimated.

For the first and largest event, our best-estimate moment magnitude, **M** 5.45 ± 0.29, is based on inverse variance weighting of **M** values from A_{VII} (estimated at 400 km^2, **M** 5.01, from the isoseismal map of Hopper, 2000) and from I_0 = VIII (**M** 6.34). Stover and Coffman (1993) and the SRA catalog list a magnitude of "5.20Ukn PAS" for this earthquake. We were unable to find the source of this magnitude and decided not to use it; the earthquake predates the start of seismographic reporting from Caltech in October 1926 (Hileman and others, 1973). (Note: Pasadena is ~750 km from Elsinore.)

The second and third shocks in the sequence were smaller than the first. Stover and Coffman (1993) list maximum MMI = VIII for the third shock, but information in Pack (1921) and Hopper (2000) indicates a size smaller than for the first shock. Based on estimating A_{VI} at 300 km^2 from isoseismal maps of Hopper (2000) for both the second and third shocks, together with Stover and Coffman's (1993) maximum MMI values, our best-estimate moment magnitudes from inverse-variance weighting for the second and third shocks are 4.42 ± 0.29 and 4.67 ± 0.29, respectively. Our magnitudes for all three earthquakes are significantly lower than earlier estimates based on MMI alone.

7. 1934, Mar. 12. Hansel Valley, Utah (M 6.59): This well-known earthquake, which occurred in a sparsely populated area north of Great Salt Lake in northern Utah, is distinguished as the only historical shock to date in the UTR known to have produced surface faulting (see Smith and Arabasz, 1991, for a general review; Neumann, 1936, for a summary of macroseismic effects; and Shenon, 1936, for documentation of geologic effects of the earthquake). MMI was assessed at VIII by Stover and Coffman (1993).

Our best-estimate moment magnitude, **M** 6.59 ± 0.30, is based on $\mathbf{M}_{obs}$ from the geometric mean of two values of M_0 (8.5 x 10^{25} dyne-cm and 8.8 x 10^{25} dyne-cm) reported by Doser (1989) from the inversion of *P* and *S* waveforms recorded at teleseismic and regional distances. This **M** is basically identical to Gutenberg and Richter's surface-wave magnitude (M_S GR) of 6.6 commonly cited for this earthquake (e.g., Stover and Coffman, 1993). A_{MMI} values given in table E-12 yield an average **M** of 6.39. Our adopted epicenter is from Doser (1989), based on a relocation attributed to J.W. Dewey (USGS, written communication to D. Doser, 1986). A focal depth of 9 km indicated in table E-14 is the average of two values (9.7 ± 1.4 km and 8.5 ± 2.0 km) determined by Doser (1989) from her waveform inversions.

8. 1937, Nov. 19. Nevada-Utah-Idaho tri-state area (M 5.40): Reports from varied sources point to the occurrence of a significant earthquake on this date at approximately 00:50 (GMT) in the general vicinity of the Nevada-Utah-Idaho tri-state border, but with an uncertain epicenter. Neumann (1940a) reports this as an earthquake near Wells, Nevada, based on felt reports there, and as a "rather widespread shock" felt as far away as Salt Lake City. The summary of instrumental epicenters located by the U.S.Coast and Geodetic Survey for 1937 (Neumann, 1940b) does not have any entry for a local earthquake in the U.S. on November 18 or 19, 1937.

Jones (1975) gives an instrumental epicenter (unclear whether determined at Reno or at Berkeley) at 42.1º N, 113.9º W, which we adopt. Stover and Coffman (1993) and Slemmons and others (1965, table B) give the same epicenter. Our best-estimate moment magnitude, **M** 5.40 ± 0.37, is an **M**˜ value based on a Wiechert magnitude determined at Reno, Nevada (Jones, 1975).

Epicentral distances estimated by Jones (1975) from Fresno and Reno, presumably based on $S - P$ intervals, are more consistent with the assigned epicenter than for a location closer to Wells, Nevada. However, this epicenter is inconsistent with felt observations reported by Neumann (1940a) and Williams and Tapper (1953). The epicenter is: 142 km from Wells (MMI not specified), where the felt effects apparently were strongest (but not indicative of immediate proximity to a magnitude 5 earthquake); 85 km from Lucin, Utah (MMI = IV); 44 km from Grouse Creek, Utah (MMI = III); and 152 km from Wendover, Utah (MMI not specified). From the felt observations, the earthquake appears to have originated in the general vicinity of the Nevada-Utah-Idaho tri-state border, likely in northeasternmost Nevada (to the southwest of our adopted epicenter) in the area surrounded by Wells, Lucin, Grouse Creek, and Wendover.

9. 1950, Jan. 18. Northwestern Uinta Basin (M 5.30): Information on this earthquake comes primarily from *United States Earthquakes 1950* (Murphy and Ulrich, 1952) and USGS sources. Both the location and size of this earthquake are uncertain. The shock was instumentally located by the U.S. Coast and Geodetic Survey (USCGS) at 40.5° N, 110.5° W, east of the Wasatch Front along the south flank of the Uinta Mountains. Stover and Coffman (1993) and the USGS SRA catalog list the USCGS epicenter. Our best-estimate moment magnitude, **M** 5.30 ± 0.20, is based on **M**˜ (Ukn PAS) reported both by Stover and Coffman (1993) and the USGS SRA catalog.

Murphy and Ulrich (1952) describe the location of the shock as "near Soldier Summit, Utah" (39.929° N, 111.083° W), which is 80 km southwest of the instrumental location and seemingly inconsistent with the description of weak shaking (MMI I to III) in Price, 40 km southeast of Soldier Summit. In aggregate, the irregularity of felt intensities (V at Grand Junction, Colo., 235 km distant; IV at Duchesne, Utah, 38 km distant; IV at Sego, Utah, 177 km distant; IV at Fruita, Colo., 214 km distant; and IV at Moab, Utah, 229 km distant) invites comparison with a shock of **M** 4.68 that occurred on September 30, 1977, almost at the same location (40.458° N, 110.484° W) as the USCGS epicenter for the 1950 earthquake. The 1977 earthquake similarly resulted in irregular felt effects in the Colorado Plateau (see *United States Earthquakes 1977*: Coffman and Stover, 1979). If the two earthquakes indeed occurred in the same area, stronger felt effects reported for the 1977 shock suggest that the 1950 earthquake may have been smaller than **M** 5.30.

10. 1959, July 21. Arizona-Utah border (M 5.55): This slightly damaging earthquake within the Colorado Plateau is well established in the historical earthquake record of the UTR. Felt effects on both sides of the Arizona-Utah border are described in *United States Earthquakes 1959* (Eppley and Cloud, 1961). Our assigned epicenter is from Stover and Coffman (1993). No instrumental M_0 is available for this earthquake, but it is one of three in the UTR for which Bakun (2006) estimated moment magnitude based on an MMI intensity attenuation model for the Basin and Range Province. Instrumental values of $\mathbf{M}_{obs}$ are available for the other two earthquakes: the Cache Valley earthquake of August 1962 and the Pocatello Valley earthquake of March 1975. Our best-estimate moment magnitude, **M** 5.55 ± 0.14, is based on inverse-variance weighting of a value of $\mathbf{M}^{\sim}$ (5.60 MLPAS), reported by Stover and Coffman (1993) and in the USGS SRA catalog, and Bakun's (2006) estimated moment magnitude of 5.5 using the USGS epicenter. We treated Bakun's estimate as a noisy estimate of **M**, using his stated uncertainties.

11. 1962, Aug. 30. Cache Valley, Utah (M 5.75): This damaging earthquake in northern Utah was one of the first to occur in the UTR after the start of regional seismographic monitoring by the University of Utah in July 1962. Damage and felt effects are described in *United States Earthquakes 1962* (Lander and Cloud, 1964). Westaway and Smith (1989) undertook a special study of this earthquake, including a revision of the mainshock's hypocenter and a determination of a moment tensor from inversion of long-period teleseismic body waveforms. Our assigned epicenter and focal depth are from their study. Our best-estimate moment magnitude, **M** 5.75 ± 0.15, is based on $\mathbf{M}_{obs}$, where M_0 is the geometric mean of two measurements: 7.1×10^{24} dyne-cm made by Wallace and others (1981) and $3.1 \pm 0.2 \times 10^{24}$ dyne-cm made by Westaway and Smith (1989).

12. 1962, Sept. 5. Magna, Utah (M 4.87): Six days after the **M** 5.75 shock in Cache Valley, this damaging earthquake occurred 140 km to the south in the Salt Lake Valley. Damage and felt effects are described in *United States Earthquakes 1962* (Lander and Cloud, 1964). Our assigned epicenter and focal depth are from the UUSS catalog. For reasons described earlier (see *Moment Magnitude Data*), a seismic moment determined by Doser and Smith (1982), corresponding to **M** 5.02, was judged to be unreliable (likely an overestimate). In the absence of a reliable seismic moment and because of the occurrence of this earthquake soon after the mid-1962 start of regional seismic monitoring in Utah, we decided to use all available size measures, including non-instrumental ones, to estimate **M**. Available instrumental size measures consist of a single-station M_L UU value of 5.0 (revised), an M_L PAS value of 5.0 (Earthquake Notes, Bulletin of the Seismological Society of America, v. 53, no. 1, p. 215), and an m_b GS value of 5.1. We did not use the latter measurement because our m_b GS regression for this period is poorly constrained (see figure E-11) and the reported value of 5.1 is just outside the bounds of our regression (if used, the conversion relationship would yield **M** 4.88) .

Our best-estimate moment magnitude, **M** 4.87 ± 0.13, is based on inverse-variance weighting that combines $\mathbf{M}_{pred}$ values from M_L UU (**M** 4.81), M_L PAS ($\mathbf{M}^{\sim}$ 5.0), FA (**M** 4.81), I_0 = VI (Stover and Coffman, 1993, **M** 4.81), and A_{MMI} (using the mean of **M** 4.56 and **M** 4.99, calculated from A_V and A_{VI}, respectively). The weighted and individual estimates of **M** are fairly consistent and indicate a size slightly smaller than **M** 5.0 for the 1962 Magna earthquake.

13. 1963, July 7. Juab Valley, Utah (M 5.06): This earthquake in Juab Valley in central Utah reached MMI VI (Stover and Coffman, 1993) and produced slight damage. Damage and felt effects are described in *United States Earthquakes 1963* (von Hake and Cloud, 1965). Our adopted epicenter for this earthquake is from the UUSS catalog. Our best-estimate moment magnitude, **M** 5.06 ± 0.15, is from Patton and Zandt's (1991) moment-tensor solution for this earthquake, determined from the inversion of regional surface-wave data. The focal depth we list for this shock is also from Patton and Zandt (1991).

14. 1966, Aug. 16. Nevada-Utah border (M 5.22): A vigorous earthquake sequence with characteristics of an earthquake swarm occurred from August 1966 into early 1967 in the sparsely populated, southern Nevada-southwestern Utah border area. The largest event, which occurred at the start of the sequence on August 16, 1966, at 18:02 (UTC), is described by Rogers and others (1991) and referred to as the Caliente/Clover Mountains earthquake. Our assigned epicenter is from the UUSS catalog. A joint-hypocenter-determination location at 37.395° N, 114.206° W by Rogers and others (1991), 9 km south-southwest of the UUSS epicenter, still lies within the UTR. Felt effects are described by von Hake and Cloud (1968). Stover and Coffman (1993) assess a shaking intensity of MMI V at Caliente, the closest town (population ~1100) at a distance 28 km from the epicenter of Rogers and others (1991) and 36 km from our UUSS epicenter.

The only available measurement of seismic moment for this earthquake is one by Doser and Smith (1982), corresponding to **M** 5.33. However, for reasons described earlier (see *Moment Magnitude Data*), their M_0 was judged to be unreliable (likely an overestimate). Our best-estimate moment magnitude, **M** 5.22 ± 0.20, is from inverse-variance weighting of $\mathbf{M}_{pred}$ values from two available instrumental size measures: a revised, single-station M_L UU of 5.2 (**M** 4.96) and an m_b ISC of 5.4 from 19 stations (**M** 5.53). The data we have reviewed do not support a magnitude as high as 5.7 to 6.1 reported by Rogers and others (1991) and attributed to the University of California at Berkeley. In addition to the instrumental size measures described above, the area shaken is also indicative of a smaller size. Our measurement of A_V (table E-12) gives **M** 5.25, and the total felt area of 66,000 km^2 estimated by Stover and Coffman (1993) gives **M** 4.99.

In the declustered version of the BEM catalog, the **M** 5.22 earthquake on August 16 at 18:02 (UTC) was originally flagged as a foreshock to a following event on August 17 at 23:07 (UTC) that had a magnitude of $\mathbf{M}^{\sim}$ 5.5, based on an M_L determined at Berkeley. Knowing that the August 16 shock was the largest in the sequence (Rogers and others, 1991, and UUSS data), we re-assigned it to be the mainshock and eliminated the August 17 event as an aftershock. Our best estimate of the mainshock's size suggests that values of $\mathbf{M}^{\sim}$ from MLBRK in the BEM catalog may overestimate **M** by a half magnitude unit or more. Except for two earthquakes in the EBR in 1972 and 1984, all $\mathbf{M}^{\sim}$ entries in the BEM catalog from MLBRK are for aftershocks of the August 16, 1966, earthquake. (It is unclear which stations of the Berkeley array were used to determine the M_L values we used as $\mathbf{M}^{\sim}$; we estimate that the Berkeley stations would be roughly in the 500–700 km distance range from the 1966–1967 Nevada-Utah border earthquakes.)

15. 1967, Oct. 4. Marysvale, Utah (M 5.08): This earthquake caused minor damage within and near the southern Sevier Valley in central Utah and was widely felt. Felt and damage effects are described by von Hake and Cloud (1969). Our best-estimate moment magnitude, **M** 5.08 ± 0.15, is based on Patton and Zandt's (1991) moment tensor for this earthquake, determined from

the inversion of regional surface-wave data. The focal depth we list for this shock is also from Patton and Zandt (1991); our assigned epicenter is from the UUSS catalog. For comparison with other size measures, a three-station M_L UU of 5.4 (revised) yields **M** 5.12. A_{MMI} measures (table E-12) indicate a slightly larger size: the average **M** from A_V, A_{VI}, and A_{VII} is 5.36.

16. 1975, Mar. 28. Pocatello Valley, Idaho (M 6.02): This earthquake, which occurred in a rural valley on the Idaho-Utah border, is the largest to date in the UTR since the beginning of regional seismographic monitoring by the UUSS in July 1962. Details of the foreshock-mainshock-aftershock sequence are described by Arabasz and others (1981). Damage and felt effects are described by Coffman and Stover (1977) and by Cook and Nye (1979). Our assigned epicenter is from the UUSS catalog; the focal depth, from Arabasz and others (1981). Our best-estimate moment magnitude, **M** 6.02 ± 0.06, is based on the geometric mean of four measurements of M_0 from Battis and Hill (1977), Williams (1979), Bache and others (1980), and Wallace and others (1981). The value of $\sigma = 0.06$ is the standard error of the mean calculated from the four values of $\mathbf{M}_{obs}$, after correcting their standard deviation for sample size. A_{MMI} measures (table E-12) are consistent with $\mathbf{M}_{obs}$: the average **M** from A_{IV}, A_{VI}, and A_{VII} is 6.03.

17. 1988, Aug. 14. San Rafael Swell, Utah (M 5.02): This earthquake occurred within the Colorado Plateau of east-central Utah, triggering numerous rockfalls within 40 km of the epicenter. Case (1988) describes geologic and felt effects, and Pechmann and others (1991) describe details of the foreshock-mainshock-aftershock sequence. Our assigned epicenter for the mainshock is from the UUSS catalog; the focal depth of 17 km is from Pechmann and others (1991). Despite its size and date, no instrumental measurements of M_0 are available for this earthquake. Our best-estimate moment magnitude, **M** 5.02 ± 0.13, is based on inverse-variance weighting of $\mathbf{M}_{pred}$ values from four instrumental size measures: M_L UU = 5.17 (**M** 4.94); M_C UU = 4.92 (**M** 4.80); m_b GS = 5.5 (**M** 5.07); and m_b ISC = 5.4 (**M** 5.53).

18. 1989, Jan. 30. Southern Wasatch Plateau, Utah (M 5.20): This shock is often paired with the San Rafael Swell earthquake. It occurred just five months later and 70 km to the southwest within the Basin and Range-Colorado Plateau transition in central Utah. Both shocks had mid-crustal focal depths and occurred on buried Precambrian basement faults, perhaps reflecting regional left-lateral shear (Pechmann and others, 1991). Stover and Coffman (1993) briefly describe felt effects of the1989 mainshock, referencing unpublished USGS intensity data for 1989. Pechmann and others (1991) present and discuss seismological data for the foreshock-mainshock-aftershock sequence; our assigned epicenter and a focal depth of 25 km are from that study.

Our best-estimate moment magnitude, **M** 5.20 ± 0.10, is based on a seismic moment from the Global CMT Catalog (Ekström and Nettles, undated; Dziewonski and others, 1990). As noted earlier (see *Moment Magnitude Data*), we reduce $\mathbf{M}_{obs}$ from Global CMT seismic moments by 0.14.

19. 1992, Sept. 2. St. George, Utah (M 5.50): As of this writing, this earthquake in southwestern Utah was the most recent of $\mathbf{M} \geq 5.0$ in the UTR. The shock damaged buildings within and near the epicentral area and triggered a destructive landslide 44 km away near the town of Springdale (Jibson and Harp, 1995). Geologic effects of the earthquake are described by Black and others (1995), ground shaking and felt effects by Olig (1995), and seismological data by Pechmann and others (1994).

Our best-estimate moment magnitude, **M** 5.50 ± 0.10, is based on a seismic moment from the Global CMT Catalog (Ekström and Nettles, undated; Dziewonski and others, 1993). As noted earlier (see *Moment Magnitude Data*), we reduce $\mathbf{M_{obs}}$ from Global CMT seismic moments by 0.14. Pechmann and others (2007) determined a mean $\mathbf{M}_{obs}$ of 5.54 from seven reported measurements of M_0. Our measurements of A_{MMI} (table E-12) from Olig's (1995) isoseismal map give an average **M** 5.99 from A_V and A_{VI}. Our assigned epicenter for the earthquake is from the UUSS catalog; the focal depth is from the Global CMT solution.

IDENTIFICATION AND REMOVAL OF DEPENDENT EVENTS (DECLUSTERING)

Spatial and temporal clustering is common in natural seismicity. Statistical techniques are required to decompose or "decluster" an earthquake catalog into "main" events that are random and independent in a statistical sense and "dependent" events that relate non-randomly to the main events. Declustering algorithms variously use magnitude-dependent space-time windows, specific cluster models, or stochastic approaches to remove dependent events from an earthquake catalog (e.g., van Stiphout and others, 2012).

The terminology we adopt warrants comment. We define foreshocks, aftershocks, and the smaller events of earthquake swarms to be "dependent" events, following common usage in the published literature relating to declustering and without implying the nature of the dependency. (Veneziano and Van Dyck, 1985a, prefer the adjective "secondary" as a less specific qualifier for such events.) We use the companion term "main" events or "mainshocks" for isolated events and the largest events of earthquake clusters. For specificity, we alternatively refer to the set of main events identified by our selected declustering algorithm as "independent mainshocks," assuming they occur as part of a Poisson process.

Declustering Algorithm Used

For conformity with procedures used by the USGS for earthquake catalog processing associated with the U.S. National Seismic Hazard Maps (see Petersen and others, 2008), we used the computer program *cat3w* developed by C.S. Mueller of the USGS. This program implements the declustering method of Gardner and Knopoff (1974), in which smaller earthquakes within fixed time and distance windows of larger shocks are identified as dependent events (using our terminology). The program *cat3w* uses the window values published by Gardner and Knopoff (1974). Although the Gardner and Knopoff (1974) declustering technique is a relatively simply one, its recent application to seismicity throughout the central and eastern U.S. produced results very similar to those from a stochastic declustering method (EPRI/DOE/NRC, 2012).

For our purposes, we made three modifications to *cat3w* that are hard-coded in the computer program. First, we reduced the minimum magnitude from 4.0 to 2.5. Second, we modified the eastern limit of a geographic sorting boundary so that the entire extended Utah region would be included. Third, we slightly changed the boundaries of sort areas that *cat3w* uses to exclude coal-mining related seismicity in Utah to correspond exactly to the standard boundaries used by the UUSS. We did this so that *cat3w* would not remove events, judged by us to be tectonic, *outside* our defined MIS areas.

Table E-15 summarizes declustering results for each of the spatial domains of the BEM catalog. The relative proportion of independent mainshocks to dependent events in each of the domains should be viewed with caution because it varies significantly with time, particularly before and after the start of regional instrumental monitoring in the early 1960s. The larger proportion of dependent events in the EBR chiefly results from an intense aftershock sequence following the **M** 5.66 Draney Peak, Idaho, earthquake of February 3, 1994; other major contributors are aftershocks of the **M** 5.91 Wells, Nevada, earthquake of February 21, 2008, and events of a swarm sequence near the Nevada-Utah border whose largest event was a shock of **M** 5.22 on August 16, 1966.

Checks on Effectiveness of Declustering

Space-Time Plots

To check the effectiveness of using *cat3w* to decluster our BEM catalog, we first compared space-time plots of the clustered and declustered versions of the catalog to satisfy ourselves that the declustering results were reasonable. Comparative plots are shown in figures E-20 and E-21 for the WGUEP Region and in figures E-22 and E-23 for the Utah Region. In each of the space-time plots, times of earthquake occurrence from 1960 through September 2012 are plotted as a function of latitude and distinguished by earthquake size. We chose 1960 as the starting point of the time range because dependent events are more systematically recorded and amenable to study during the instrumental part of the earthquake catalog. The magnitude bins used in the plots correspond to those analyzed later with respect to completeness and earthquake rates (the only shocks of $\mathbf{M} \geq 6.5$ in the catalog occurred before 1960). The start dates of periods of complete reporting for the three lower magnitude bins are plotted as vertical dashed lines on the declustered versions of the space-time plots.

For the WGUEP Region plots, the declustered version (figure E-21), compared with the clustered version (figure E-20), indicates a favorable outcome: clustered earthquakes have been thinned out in the space-time vicinity of larger shocks, and earthquakes identified as mainshocks have the appearance of being randomly scattered (using the periods of completeness as a visual guide). This observation is qualitatively consistent with a temporal Poisson process. Spatially, rates of occurrence are inhomogeneous and can be seen to be relatively higher in the northern part of the WGUEP Region, north of about latitude 41.5°N. The latitude-vs.-time plots suffer from being two-dimensional, but they serve the purpose of enabling a visual assessment of whether there is a reasonable balance between leaving too many grouped shocks and unduly decimating the catalog.

Comments similar to the above apply to the Utah Region plots (figures E-22 and E-23) in terms of the declustering outcome. In this larger region, spatial inhomogeneity of earthquake occurrence is more evident. Background earthquake activity is relatively higher in the northern and southern parts of the Utah Region and discernibly lower between about latitude 41.5°N and about latitude 39.5°N—the part of Utah's northerly-trending seismic belt that roughly coincides with the five central active segments of the Wasatch fault. This feature of Utah's seismicity is well known (see, for example, Smith and Arabasz, 1991).

Kolmogorov-Smirnov (K-S) Tests

As a quantitative check on whether the declustered catalog for the WGUEP region was Poissonian, we used the Kolmogorov-Smirnov (K-S) test to analyze data in the three lowest magnitude bins plotted on figure E-21, comparing the observed cumulative distribution function (CDF) of inter-event times to that expected for a Poisson distribution (see analogous example of traffic-gap data in Benjamin and Cornell, 1970, p. 470–472). The reason for analyzing the three lowest magnitude bins is that they have sufficient data and are the most sensitive to choices of space-time windows used in the declustering. The data analyzed were restricted to the periods of completeness indicated on figure E-21.

To illustrate the K-S test, figures E-24a and E-24b graphically display data for the two lowest magnitude bins. The K-S statistic**,** *D*, indicated on the plots is the largest absolute difference between the CDF for the observed declustered data and the expected CDF for a Poisson distribution, given the mean inter-event time from the observed sample. The test statistic *D* is 0.042 for $2.85 \leq \mathbf{M} \leq 3.54$ (182 inter-event times), 0.133 for $3.55 \leq \mathbf{M} \leq 4.24$ (38 inter-event times), and for the third magnitude bin (not shown), 0.466 for $4.25 \leq \mathbf{M} \leq 4.94$ (8 inter-event times). Following Benjamin and Cornell (1970), *D* in each case was found to be less than the critical value at the 5 percent significance level, α, for *rejecting* the null hypothesis that the observed CDF is Poissonian (we interpolated some of the values of the critical statistic in table A7 of Benjamin and Cornell, 1970). As expected, *D* values for the clustered CDFs in each of the three magnitude bins exceeded their critical values for $\alpha = 0.05$, indicating that these distributions were not Poissonian.

We similarly used K-S tests to analyze declustered data for the Utah Region shown on figure E-23, again analyzing the three lowest magnitude bins and restricting data to the periods of completeness shown on the figure. Graphical results are displayed on figures E-24c and E-24d. The test statistic *D* is 0.033 for $2.85 \leq \mathbf{M} \leq 3.54$ (427 inter-event times), 0.064 for $3.55 \leq \mathbf{M} \leq 4.24$ (76 inter-event times), and for the third magnitude bin (not shown), 0.181 for $4.25 \leq \mathbf{M} \leq 4.94$ (17 inter-event times). Here too, *D* in each case was found to be less than the critical value at the 5 percent significance level for rejecting the null hypothesis that the observed CDF is Poissonian. Just as for the WGUEP Region, *D* values indicated that all the Utah Region's clustered CDFs were non-Poissonian distributions.

In sum, our testing gives us confidence that the declustered BEM earthquake catalog can be used to develop reliable background earthquake models for the WGUEP and Utah regions. Despite its relative simplicity, the declustering approach of Gardner and Knopoff (1974) that we implemented using the computer program *cat3w* yielded satisfactory results.

PERIODS OF COMPLETENESS

A critical element for constructing the background earthquake models is the completeness period, T_C, for which the reporting of earthquakes at or above a given magnitude threshold in the earthquake catalog is complete. For the WGUEP study, the parameter of the model ultimately of primary concern to the Working Group is the annual rate of occurrence of independent mainshocks of $\mathbf{M} \geq 5.0$ within the *entire* WGUEP Region. Accordingly, this region was treated

as a single domain for assessing periods of completeness. We similarly treated the UTR as a single domain for assessing the periods of completeness for its background earthquake model.

To determine T_C for different magnitude thresholds in the declustered catalog, we used cumulative recurrence curves (CRCs) together with general information on the space-time evolution of seismographic control, population, and newspapers. A CRC is a plot of the cumulative number of earthquakes above a given magnitude threshold versus time. The use of a probabilistic approach, which allows the analysis and use of variable completeness throughout an entire earthquake record (see, for example, EPRI/DOE/NRC, 2012, or Felzer, 2007) was beyond the scope of this study. According to Grünthal and others (1998, as quoted in and cited by Hakimhashemi and Grünthal, 2012), the CRC method is "very simple but rather robust."

Seismographic Monitoring

Seismographic monitoring of the Utah Region by the University of Utah has progressively evolved since June 29, 1907, when a pair of Bosch-Omori horizontal-pendulum seismographs were installed on the university campus in Salt Lake City (Arabasz, 1979). Significant milestones in the UUSS instrumental coverage of the region include the beginning of a skeletal statewide network in Utah of onsite-recording seismographs in July 1962, the start of a regional telemetered seismic network in October 1974, and the start of digital network recording in January 1981 (see Arabasz et al, 1992, and Smith and Arabasz, 1991, for representative maps of seismographic coverage and historical background). Major expansion and modernization of the University of Utah's regional seismic network during the last two decades have enhanced the quality and precision of earthquake locations and magnitudes, but they have not materially affected the completeness of the earthquake record above the lowest threshold of interest here ($\mathbf{M} \geq 2.85$).

Early Historical Earthquake Record

The historical earthquake record for the Utah Region effectively begins with the arrival of Mormon pioneers in the Salt Lake Valley in July 1847, under the leadership of Brigham Young, and the establishment soon thereafter of the first newspaper in Utah in 1850. Other explorers and fur trappers reached the present Utah Region before 1847, but their written records contain no mention of local earthquakes, and there is no known oral history of specific earthquakes felt by Native Americans in the region before the coming of white settlers. The first documented earthquake in the Utah Region occurred on February 22, 1850 (Arabasz and McKee, 1979).

The completeness of Utah's historical earthquake record is influenced by the pattern of settlement after 1847. After reaching the Salt Lake Valley, Brigham Young promptly initiated and directed an extensive program of exploring and colonizing. Between July 1847 and May 1869, when the First Transcontinental Railroad was completed at Promontory Summit north of Great Salt Lake, more than 60,000 Mormon pioneers crossed the plains to settle in Utah (Wahlquist, 1981). For convenience, we use the areas and boundaries of present-day states in describing historical geography.

By the time of Brigham Young's death in 1877, Mormon settlements extended throughout the Intermountain Seismic Belt in the UTR (figure E-1) as well as into outlying parts of Utah and other parts of the UTR in southeastern Idaho, southwestern Wyoming, and northern Arizona (see

Wahlquist, 1981, and Arrington, 1994). Settlements in the region were also founded by railroads, mining companies and non-Mormons (Wahlquist, 1981; Arrington, 1994).

There are useful summaries, figures, and tabulations pertaining to the timing and geographical extent of permanent settlements in the UTR in Wahlquist (1981). The website Utah Digital Newspapers (http://digitalnewspapers.org/about/county_map/) provides the names, dates, and locations of newspapers in the region. We use these sources of information to support arguments for assessing T_C for the magnitude bins of larger earthquakes in the WGUEP and Utah regions, extending backward into historical time.

Population Distribution and Growth in the UTR

To help the reader understand some of our later arguments, we elaborate on the distribution and historical growth of population in the UTR. The variability of modern population density in the UTR is illustrated in the map on figure E-25. Referring to the numbered localities on the map, salient features include: concentrated population in a northerly-trending belt in Utah's Wasatch Front area (1) extending into southeastern Idaho (2); a southwesterly-trending band of population centers extending from the Sanpete Valley (3) in central Utah through the Sevier Valley (4) and Beaver Basin (5) to population centers in the vicinities of Cedar City (6) and St. George (7) in southwestern Utah; a roughly elliptical populated area in the Uintah Basin of northeastern Utah (8); diffusely scattered population centers in southwestern Wyoming (9); and relatively sparse population in Utah's southeast quadrant, where the interior of the Colorado Plateau (10) is bordered by a roughly circular ring of scattered population centers in central and southern Utah (11, 12), northern Arizona (13), northwestern New Mexico (14), and western Colorado (15). Using this modern population map for reference, together with information in Wahlquist (1981), we can characterize the distribution of population in the UTR at earlier stages in 1850, 1860, and 1880—particularly in relation to the Intermountain Seismic Belt (compare figures E-18 and E-25).

Population Distribution in 1850

In 1850, there were at least 37 permanent settlements in Utah, concentrated along the Wasatch Front between Brigham City and Payson and extending west of the Salt Lake Valley into neighboring Tooele Valley (see localities a–d on figure E-25). Again referring to the numbered localities on figure E-25, there also were outlying settlements in Manti (3) in central Utah and near Cedar City (6) in southwestern Utah. These early settlements, combined with the presence of Fort Bridger (16) in southwestern Wyoming established in 1842, and Fort Hall (17) in southeastern Idaho, established in 1834, provided a significant capability for detecting and reporting strong earthquake ground shaking in the WGUEP Region in 1850.

Population Distribution in 1860

A tabulation of more than 400 settlements in Utah with a Mormon ward or branch, including their date of settlement, is given in Wahlquist (1981, page 91). Of the 397 permanent settlements listed, one-third were established by the end of 1860. Utah settlements in 1860 are shown on a map on page 114 of Wahlquist (1981). Importantly, Utah's population during the 1850s expanded from the Wasatch Front area into central and southwestern Utah (along the trend of localities 3, 4, 5, 6, and 7 on figure E-25). Fillmore (locality 18, figure E-25) was also

established in the 1850s as the first capital of the Utah Territory. By 1860, the continuity of population centers along Utah's main seismic belt—in southwestern, central, and northern Utah—was effectively complete.

Population Distribution in 1880

The distribution of communities in Utah in 1880 is illustrated by a map on page 114 in Wahlquist (1981). The map in question is a plot for 1890, but companion data on page 91 of the same publication indicate that 277 (93%) of the 297 communities whose locations are plotted had actually been settled by 1880. These same data indicate that 70% of Utah's permanent communities had been established by 1880. Except for the Uintah Basin and southeasternmost Utah, the general distribution of population in Utah by that time does not differ greatly from that in 1950 or 1970 (compare maps for 1890, 1950, and 1970 on pages 114 and 115 in Wahlquist, 1981).

During the 1860s and 1870s, Mormon expansion beyond Utah had also led to population coverage of the border regions of the UTR in southern and southeastern Idaho, southwestern Wyoming, eastern Nevada, northern Arizona, and northwestern New Mexico (see Wahlquist, 1981, p. 92–93). This additional population coverage, partly reflected in the location of population centers on figure E-25, is germane to capabilities for the detection and reporting of earthquake ground shaking in the UTR in 1880.

Population Distribution and Sampling of Earthquake Ground Shaking

For our use in later arguments, figure E-25 also provides information for visually comparing population distribution and the expected extent of ground shaking of MMI IV or greater, depicted by circular areas equal to A_{IV} predicted for shocks of **M** 4.95 to **M** 6.45. Our purpose in using A_{IV} is to convey the likelihood not only of detecting earthquake ground shaking but also of having sufficient geographic sampling to estimate **M**.

For reference, ground shaking associated with a level of IV on the MM intensity scale is described by Stover and Coffman (1993, p. 3) as follows: "Felt by many to all. Trees and bushes were shaken slightly. Buildings shook moderately to strongly. Walls creaked loudly. Observer described the shaking as 'strong.'" This characterization of effects, which these USGS authors use as a guide for assigning intensity level IV, represents a slight modification of the MM intensity scale outlined by Wood and Neumann (1931).

Table E-17 gives the radii of the equivalent circular areas for A_{IV}. The table also gives the equivalent radii for an approximation of *total* felt area, FA. As noted in the table, the values of A_{IV} were calculated using the results of a general orthogonal regression of $\log(A_{IV})$ on $\mathbf{M}_{obs}$, but FA was approximated by simply inverting the non-linear conversion relationship CR-12 in table E-8. Note that for each magnitude, the equivalent radius of the expected total felt area is roughly double (1.7–2.3 times) the radius for A_{IV}, which greatly increases the chance that an earthquake of a particular magnitude would be reported at multiple localities.

Data and Basis for Completeness Periods

Table E-16 summarizes the completeness periods (T_C) we assessed for the WGUEP and Utah regions. In our rate calculations, we use magnitude bins with a range of 0.7 magnitude unit. The table also provides T_C for magnitude bins with a range of 0.5 magnitude unit for those wishing to use alternative bins in other applications. For each specified magnitude threshold, $T_C = t_e - t_0$, where t_e and t_0 are the end and start dates, respectively, of the completeness period. In this study, t_e uniformly is the end of our earthquake catalog on September 30, 2012.

In the remainder of this section, we explain how we chose t_0 for the various magnitude thresholds we analyzed—based either on a pick from a CRC, on joint consideration of a CRC and other arguments, or solely on other arguments (for $\mathbf{M} \geq 5.95$). CRCs for the WGUEP and Utah regions are presented in figures E-26 and E-27, respectively. To help the reader navigate table E-16 in conjunction with the figures, we will use the same font-type notation for dates as used in table E-16 when discussing our selection of t_0 for the various magnitude bins (e.g., **1986**, ***1908***, *1850*). Also, for convenient shorthand, we will refer to the magnitude bins by the lower end of their range and use "W" for the WGUEP Region and "U" for the UTR (e.g., 2.85W, 3.55U, etc.).

t_0 from CRCs (1963–1986)

For our picks of t_0 from a CRC (indicated by a date in regular bold type in table E-16), we estimated t_0 by inspecting the CRC, superposing a trend line for the most recent time period (assuming stationarity of earthquake rate), and visually picking the point on the CRC backward in time at which the linear trend deviates significantly. The deviation is typically, but not always, a decrease in rate. Our primary objective in selecting each t_0 was to bracket a completeness period whose earthquake rate was convincingly uniform and reliable, particularly for magnitude thresholds below 4.95. For the latter data, the completeness periods we picked from the CRCs should be considered conservative minimum values of T_C. In other words, our selected t_0 does not necessarily mark when network sensitivity changed to enable uniform reporting above that magnitude threshold. For some CRCs, statistical tests of rate information allow T_C to be lengthened, but a t_0 earlier than the one we adopted is not as visually compelling on the CRC.

To check our picks of t_0 from CRCs, the reader can simply examine table E-16 and then refer to the corresponding CRC. For example, for 2.85W, t_0 = **1986**, which can be seen as the labeled pick on figure E-26a. Our direct picks range from **1963** (3.95W, 4.25U) to **1986** (2.85W, 2.85U). The selected dates are internally consistent, and they are consistent with maps of the evolution of seismographic coverage in the UTR. (Besides referring to the maps cited earlier, we also examined annual station maps in UUSS reports.) Our assessments of T_C indicate completeness since 1963 for $\mathbf{M} \geq 3.95$ in the WGUEP Region and for $\mathbf{M} \geq 4.25$ in the UTR.

t_0 from CRCs and Other Arguments (1908, 1880)

1908: In table E-16, two values of t_0 (indicated in italicized bold type: ***1908, 1880***) are based on joint consideration of CRCs and other arguments. For the earthquake record before 1963, the CRC for 18 shocks of $\mathbf{M} \geq 4.95$ in the UTR (4.95U, figure E-27h) suggests completeness and a fairly uniform rate of occurrence extending back to the first decade of the 1900s. The CRC for

the smaller WGUEP Region (4.95W, figure E-26h) is consistent with this conclusion. The installation of seismographs on the University of Utah campus in June 1907 is significant. We believe that any shock of **M** ≥ 4.95 in the UTR after the start of local seismographic recording on that date would not have escaped reporting. Based on this argument and the CRCs, we assign ***1908*** as the t_0 for both 4.95U and 4.95W.

The distribution of population and newspapers in Utah by 1908 and the expected extent of ground shaking of MMI IV or greater (figure E-25) support the expectation that any shock in the UTR of **M** ≥ 4.95 after 1908 would be reported and its size reasonably estimated. These supporting arguments are strongest for Utah's main seismic belt but are admittedly weaker for southeastern Utah. By 1908, local newspapers were being continuously published in 24 of Utah's 29 counties. Three of the exceptions are in southeastern Utah. In Garfield County, publishing began in 1913; in San Juan County, in 1919; and in Kane County, in 1929. Regarding the two other exceptions, local newspaper publishing began in 1909 in Duchesne County in the Uintah Basin and in 1910 in Morgan County in north-central Utah.

1880: The second t_0 value based on joint consideration of CRCs and other arguments is ***1880***. The CRC for 11 shocks of **M** ≥ 5.45 in the UTR (5.45U, figure E-27i) suggests completeness and a fairly uniform rate of occurrence extending back to about 1880 (the first shock in the sample occurred in 1884). The CRC for for the smaller WGUEP Region (5.45W, figure E-26i) also supports this conclusion. Data for the slightly higher threshold of **M** ≥ 5.65 are more sparse (5.65U, figure E-27j, and 5.65W, figure E-26j); however, by extension, completeness for **M** ≥ 5.45 must also apply to **M** ≥ 5.65.

We use figure E-27i as the starting point to argue for ***1880*** as the t_0 for **M** ≥ 5.45 in the UTR, which would logically lead to the same t_0 for 5.45W, 5.65U, and 5.65W. Supporting arguments can be made from the distribution of population in 1880, discussed earlier, and (to a lesser extent) of newspapers. In 1880 newspapers were being continuously published only in the Wasatch Front area. The extent of observed ground shaking caused by the **M** 5.58 earthquake near Paris, Idaho, at the northern end of the UTR in November 1884 (Evans and others, 2003) and the predicted extent of A_{IV} from a shock of **M** 5.45 (figure E-25) also support the expectation that earthquakes of this size in the UTR would be completely reported after 1880—with high confidence if the shock occurred along Utah's main seismic belt. Looking at figure E-25, where in the UTR could one arguably "hide" a shock of **M** 5.45 in 1880? At that time, besides the population distribution we described earlier, there were at least six established communities in the Uintah Basin (locality 8), at least 11 established communities in the coal-mining areas of east-central Utah (locality 11), and a few small communities in southeastern Utah. Conceivably, a shock of **M** 5.45 in the interior of the Colorado Plateau (locality 10) might have had ground shaking of MMI IV or larger insufficiently sampled to estimate the shock's true size, but such an earthquake likely would have been reported felt (because of a predicted felt radius of 207 km).

t_0 from Other Arguments (1850, 1860, 1880)

The BEM catalog contains only four mainshocks of **M** ≥ 5.95 in the UTR, too few to produce informative CRCs, leaving us to make assessments of t_0 solely on the basis of other arguments. For the WGUEP Region, we have confidence in choosing 1850 as t_0 for **M** ≥ 5.95. This choice is based on the population distribution that we described earlier, the 1850 start date for Utah's first newspaper, and the size of A_{IV} compared to the geography of the WGUEP Region (figure E-25).

Isoseismal maps for the 1962 **M** 5.75 Cache Valley, Utah, earthquake and the 1975 **M** 6.02 Pocatello Valley, Idaho, earthquake (Hopper, 2000) strongly argue against the possibility that any shock of **M** ≥ 5.95 in the WGUEP Region in 1850 or later could escape reporting or not have its size reasonably estimated from felt reports.

For the Utah Region as a whole, we are not confident that the population distribution before 1880 was adequate to ensure reasonable sampling of A_{IV} for any shock of **M** ≥ 5.95 (figure E-25). We judge that population distribution was sufficient in 1880, however, and we assign that date as t_0 for the **M** 5.95 threshold in the UTR. For higher magnitude thresholds (**M** 6.35 and **M** 6.45), the expected sizes of A_{IV} and FA are so large (figure E-25, table E-17) that we believe the distribution of Mormon settlements in 1860 justifies assigning that date as t_0 for those size thresholds in the UTR.

*N** VALUES AND SEISMICITY RATE PARAMETERS

The culmination of all the described preceding steps is the calculation of seismicity rate parameters for background earthquake models for the WGUEP and Utah regions. Recall that our goal is to achieve unbiased estimates of seismicity rate parameters. We do this by using the *N** approach developed by Tinti and Mulargia (1985) that was outlined in figure E-2.

*N** Values

*N** is a count of earthquakes in a specified magnitude interval, adjusted for magnitude uncertainty bias, that is used to compute unbiased earthquake recurrence parameters. We followed the EPRI/DOE/NRC (2012) steps of (1) calculating *N** from σ on an earthquake-by-earthquake basis (using $N^* = \exp\{-(b \ln(10))^2\sigma^2/2\}$), (2) summing *N** for earthquakes within specified magnitude intervals, (3) dividing each *N** sum by the period of completeness for its respective magnitude interval, and (4) using a maximum-likelihood approach to compute seismicity rate parameters from the equivalent *N** counts. For the *N** calculations, we used a *b*-value of 1.05 assessed from preliminary processing of the BEM catalog. For our six magnitude intervals of complete reporting, the observed number of independent mainshocks along with equivalent *N** counts are given in tables E-18 and E-19 for the WGUEP Region and the Utah Region, respectively.

Seismicity Rate Parameters

Background Earthquake Model for the WGUEP (Wasatch Front) Region

The data in table E-18 were used as input to the maximum-likelihood algorithm of Weichert (1980) to solve for unbiased recurrence parameters for the WGUEP Region. The Weichert algorithm has the capability to handle binned magnitude data with variable periods of completeness as well as truncation of the exponential magnitude distribution at an upper limit, m_u. Figure E-28 shows the fit of the WGUEP data to a truncated exponential distribution [equation (E-13)]. The fit is for an m_u of 7.00 corresponding to the upper limit of the largest magnitude bin in table E-18 and consistent with a maximum magnitude of **M** 6.75 ± 0.25. We tested alternative values of m_u from 6.75 to 8.00 and determined that both the seismicity rates and *b*-value were insensitive to the change. For the WGUEP Region background earthquake

model, based on N^*, the cumulative annual rate of independent mainshocks greater than or equal to $m_0 = 2.85$ is 7.70 with a standard error of $\sigma(N(m_0)) = 0.52$. The b-value determined for the model is 1.06 with a standard error of $\sigma(b) = 0.06$. Table E-20 provides rate information for $\mathbf{M} \geq 5.0$ and other magnitude ranges, calculated using these parameters and equation (E-13). This table indicates that potentially damaging background earthquakes of $\mathbf{M} \geq 5.0$ occur in the WGUEP Region on the average of once every 25 years, with 90% confidence limits of once every 17 to 44 years.

The confidence limits on the seismicity rates in table E-20 are based on a 25-point discrete probability distribution for paired $N(m_0)$ and b-values that Robert R. Youngs (AMEC Foster Wheeler, written communication, March 16, 2014) determined for us using equation (E-13) with $m_0 = 2.85$ and $m_u = 7.00$, the data in table E-18, and the same likelihood model used to calculate the best-fit $N(m_0)$ and b-values (Weichert, 1980; Veneziano and Van Dyck, 1985b). The likelihood function is

$$L = \prod_i \frac{(\lambda_i T_i)^{n_i} e^{-\lambda_i T_i}}{n_i!} \qquad \text{(E-14)}$$

where n_i is the observed number of earthquakes in the magnitude range $m_i \leq m < m_{i+1}$, T_i is the time period of completeness for this magnitude range, and λ_i is the predicted rate of earthquakes in this magnitude range for a truncated exponential distribution. In terms of equation (E-13), λ_i can be written as:

$$\lambda_i = N(m_0)\,\frac{10^{-b(m_i - m_0)} - 10^{-b(m_{i+1} - m_0)}}{1 - 10^{-b(m_u - m_0)}} \qquad \text{(E-15)}$$

The following text from Robert Youngs (written communication, May 7, 2014) describes how he used this likelihood function to develop a discrete joint probability distribution for $N(m_0)$ and b:

> The process involves setting up a grid of pairs of $N(m_0)$ and b, computing the likelihood that the observed seismicity in a zone is produced by each pair, and then normalizing these likelihoods to form a discrete joint distribution for $N(m_0)$ and b. This process captures the correlation between $N(m_0)$ and b. The grid of b-values is initially set at values spaced at 0.1 [$\sigma(b)$] over the range of ±2.5 [$\sigma(b)$]. The grid of $N(m_0)$ values consists of 51 points over the range of 0.5% to 99.5% of a chi^2 distribution. The grid of 51x51 pairs is then aggregated at 25 points representing the centers of grid sections dividing the range of $N(m_0)$ and b-values into five sections. The weight assigned to each of the 25 points is the sum of the relative likelihoods in each grid partition.

We used the resulting discrete probability distribution for $N(m_0)$ and b to calculate 90% confidence limits on the cumulative seismicity rates for each of the minimum magnitude values m in table E-20. These calculations involved the following steps: (1) for each pair of $N(m_0)$ and b values, calculate the number of earthquakes per year of magnitude m and greater using equation (E-13); (2) sort the resulting table of earthquake rates, and the associated values of $N(m_0)$, b, and branch weight, in order of increasing rate of $\mathbf{M} \geq$ m earthquakes $N(m)$; (3) calculate the cumulative weight for each rate value, which is the sum of its weight and the weights for all of the lower rates; and (4) interpolate to find the earthquake rate values $N(m)$

corresponding to cumulative weights of 0.05 and 0.95, which constitute the 90% confidence limits on the rates.

After carrying out this four-step procedure for the WGUEP data set, we found that for all m values of 5.0 and larger tested the cumulative weight associated with each $N(m_0)$-b pair in the 25-point discrete probability distribution was the same. We interpolated to find the $N(m_0)$-b pairs corresponding to the 5th and 95th percentile $N(m)$ values for $m \geq 5.0$. For the 5th percentile rates, $N(m_0) = 7.89$ events/yr and $b = 1.18$ and for the 95th percentile rates, $N(m_0) = 8.61$ events/yr and $b = 1.00$. These interpolated values can be used with equation (E-13) to estimate the 90% confidence limits on $N(m)$ for other magnitude ranges above $\mathbf{M} \geq 5.0$ (e.g., $\mathbf{M} \geq 5.25$). This alternative procedure for estimating confidence limits for magnitude ranges above $\mathbf{M} \geq 5.0$ is an empirical result for our specific WGUEP region data set.

Note that the cumulative rates in table E-20 are for independent *background* earthquakes in the WGUEP Region. In order to reliably estimate cumulative rates of all future mainshocks above **M** 5.0 in this region, one must also account for earthquakes expected to occur on identified faults (see, for example, WGUEP, 2015, figures 7.1-2 and 7.1-5).

Background Earthquake Model for the Utah Region

Following the same steps described above, the data in table E-19 were used as input to the maximum-likelihood algorithm of Weichert (1980) to solve for unbiased recurrence parameters for the Utah Region. Figure E-29 shows the fit to the data for an m_u of 7.00. For the background earthquake model, based on N^*, the cumulative annual rate of independent mainshocks greater than or equal to $m_0 = 2.85$ is 18.1 with a standard error of 0.81. The b-value determined for the model is 1.07 with a standard error of 0.04. Table E-21 provides rate information for $\mathbf{M} \geq 5.0$ and other magnitude ranges, calculated using these parameters and equation (E-13). This table indicates that potentially damaging background earthquakes of $\mathbf{M} \geq 5.0$ occur in the Utah region on the average of once every 11 years, with 90% confidence limits of once every 8 to 16 years. Just as for table E-20, we emphasize that the cumulative rates in table E-21 are for independent *background* earthquakes in the Utah Region and do not account for earthquakes expected to occur on identified faults.

The confidence limits on the Utah region seismicity rates in table E-21 were determined using the procedures described above for the WGUEP Region. The 25-point discrete probability distribution for paired $N(m_0)$ and b-values was provided to us by Robert R. Youngs (written communication, November 18, 2014). As was the case with the WGUEP Region, we found that the $N(m)$ percentile associated with each $N(m_0)$-b pair in the 25-point discrete probability distribution was the same for $m \geq 5.0$. Consequently, one can estimate the 90% confidence limits on $N(m)$ for any magnitude range above $\mathbf{M} \geq 5.0$ by using the following interpolated values for $N(m_0)$ and b in equation (E-13): $N(m_0) = 18.4$ events/yr with $b = 1.15$ for the 5th percentile rate and $N(m_0) = 18.7$ events/yr with $b = 1.01$ for the 95th percentile rate. Although we have found empirically that this alternative procedure for estimating confidence limits for magnitude ranges over **M** 5.0 is applicable to both our Utah and WGUEP region data sets, it may not be applicable to other data sets.

Some caution is warranted regarding use of the UTR background earthquake model. The Working Group on Utah Earthquake Probabilities made the decision to treat the WGUEP Region

as a single domain for constructing a background earthquake model. For this appendix we similarly treated the UTR as a single domain for modeling earthquake rates. The background earthquake model provides a good first-order representation of earthquake occurrence in the UTR, but it primarily reflects earthquake activity within the region's main seismic belt. For site-specific seismic hazard and risk analyses in the UTR, model components such as earthquake counts and periods of completeness should be re-assessed on a finer scale to account for the spatial inhomogeneity of seismicity in the UTR.

ACKNOWLEDGMENTS

We are indebted to colleagues at the U.S. Geological Survey's National Earthquake Information Center (USGS/NEIC) in Golden, Colorado, for data, information, and helpful discussions that enabled us to develop the unified earthquake catalog for the Extended Utah Region. In particular, we thank C.S. Mueller for providing key USGS earthquake catalogs and for sharing his *cat3w* declustering algorithm; J.W. Dewey, for information relating to m_b PDE and m_b ISC; and B.W. Presgrave, for information relating to M_L GS. We are also indebted to R.R. Youngs of AMEC Foster Wheeler, and G.R. Toro of Lettis Consultants International, Inc., for invaluable discussions and helpful guidance relating to methodology for achieving unbiased estimates of seismicity rate parameters. We accept full responsibility for any errors we may have made. R.R. Youngs also kindly generated probability distributions to aid our evaluation of confidence intervals on predicted seismicity rates. We thank the staff of the University of Utah Seismograph Stations for their supportive involvement, particularly P.M. Roberson for major help with the illustrations, S.N. Whittaker for help with ArcGIS analyses of isoseismal maps, and K.M. Whidden for providing her moment-tensor data. C.S. Mueller and J.W. Dewey of the USGS provided valuable review comments that helped improve this appendix.

REFERENCES

(including citations in the Electronic Supplements)

Ake, J., Mahrer, K., O'Connell, D., and Block, L., 2005, Deep-injection and closely monitored induced seismicity at Paradox Valley, Colorado: Bulletin of the Seismological Society of America, v. 95, no. 2, p. 664–683, doi: 10.1785/0120040072.

Anadarko Petroleum Corporation, 2005, Known sodium leasing area (KSLA) map: Online, http://www.wma-minelife.com/trona/tronmine/graphics/KSLA2005.pdf, accessed Feb. 14, 2014.

Arabasz, W.J., 1979, Historical review of earthquake-related studies and seismographic recording in Utah, *in* Arabasz, W.J., Smith, R.B., and Richins, W.D., editors, Earthquake studies in Utah 1850 to 1978: Salt Lake City, University of Utah Seismograph Stations, Department of Geology and Geophysics, p. 33–56.

Arabasz, W.J., Burlacu, R., and Pankow, K.L., 2007, An overview of historical and contemporary seismicity in central Utah, *in* Willis, G.C., Hylland, M.D., Clark, D.L., and Chidsey, T.C., Jr., editors, Central Utah—Diverse Geology of a Dynamic Landscape: Utah Geological Association Publication 36, p. 237–25.

Arabasz. W.J., and Julander, D.R., 1986, Geometry of seismically active faults and crustal deformation within the Basin and Range-Colorado Plateau transition in Utah, *in* Mayer, L., editor, Extensional tectonics of the southwestern United States—a perspective on processes and kinematics: Geological Society of America Special Paper 208, p. 43–74.

Arabasz, W.J., and McKee, M.E., 1979, Utah earthquake catalog, 1850–June 1962, *in* Arabasz, W.J., Smith, R.B., and Richins, W.D., editors, Earthquake studies in Utah 1850 to 1978: Salt Lake City, University of Utah Seismograph Stations, Department of Geology and Geophysics, p. 119–121, 131–143.

Arabasz, W.J., Nava, S.J., McCarter, M.K., Pankow, K.L., Pechmann, J.C., Ake, J., and McGarr, A.M., 2005, Coal-mining seismicity and ground-shaking hazard—a case study in the Trail Mountain area, Emery County, Utah: Bulletin of the Seismological Society of America, v. 95, no. 2, p. 18–30, doi: 10.1785/0120040045.

Arabasz, W.J., Nava, S.J., and Phelps, W.T., 1997, Mining seismicity in the Wasatch Plateau and Book Cliffs coal mining districts, Utah, USA, *in* Gibowicz, S.J., and Lasocki, S., editors, Rockbursts and seismicity in mines, Proceedings of the 4th International Symposium on Rockbursts and Seismicity in Mines, Krakow, Poland: Rotterdam, A.A. Balkema, p. 111–116.

Arabasz, W.J., and Pechmann, J.C., 2001, Seismic characterization of coal-mining seismicity in Utah for CTBT monitoring: Technical Report to Lawrence Livermore National Laboratory, LLNL Research Agreement No. B344836, variously paginated: Online, http://www.quake.utah.edu/Reports/llnl2001/LLNLRept.pdf, accessed Feb. 14, 2014.

Arabasz, W.J., Pechmann, J.C., and Brown, E.D., 1992, Observational seismology and the evaluation of earthquake hazards and risk in the Wasatch front area, Utah, *in* Gori, P.L., and Hays, W.W., editors, Assessment of regional earthquake hazards and risk along the Wasatch Front, Utah: U. S. Geological Survey Professional Paper 1500-A-J, p. D-1–36.

Arabasz, W.J., Richins, W.D., and Langer, C.J., 1981, The Pocatello Valley (Idaho-Utah border) earthquake sequence of March to April, 1975: Bulletin of the Seismological Society of America, v. 71, no. 3, p. 803–826.

Arabasz, W.J., Smith, R.B., and Richins, W.D., editors, 1979, Earthquake studies in Utah 1850 to 1978: Salt Lake City, University of Utah Seismograph Stations, Department of Geology and Geophysics, 552 p.

Arrington, L.J., 1994, Colonization of Utah, *in* Powell, A.K., editor, Utah History Encyclopedia: Salt Lake City, Utah, University of Utah Press: Online, http://www.onlineutah.com/colonizationhistory.shtml, accessed April 11, 2014.

Atkinson, G.M., and Wald, D.J., 2007, "Did you feel it?" intensity data: A surprisingly good measure of earthquake ground motion: Seismological Research Letters, v. 78, no. 3, p. 362–368, doi: 10.1785/gssrl.78.3.362.

Bache, T.C., Lambert, D.G., and Barker, T.G., 1980, A source model for the March 28, 1975, Pocatello Valley earthquake from time-domain modeling of teleseismic P waves: Bulletin of the Seismological Society of America, v. 70, no. 2, p. 405–418.

Bakun, W.H., 2006, MMI attenuation and historical earthquakes in the Basin and Range Province: Bulletin of the Seismological Society of America, v. 96, no. 6, p. 2206–2220, doi: 10.1785/0120060045.

Bakun, W.H., and Wentworth, C.M., 1997, Estimating earthquake location and magnitude from seismic intensity data: Bulletin of the Seismological Society of America, v. 87, no. 6, p. 1502–1521.

Barrientos, S.E, Ward, S.N., Gonzalez-Ruiz, J.R., and Stein, R.S., 1985, Inversion for moment as a function of depth from geodetic observations and long period body waves of the 1983 Borah Peak, Idaho earthquake: U. S. Geological Survey Open-File Report OF 85-0290-A, p. 485–518.

Battis, T.C., and Hill, K., 1977, Analysis of seismicity and tectonics of the central and western United States: Interim Scientific Report #1, AFSOR Contract # F44620-76-0063, Texas Instruments, Inc., Dallas, Texas, 109 p.

Benjamin, J.R., and Cornell, C.A., 1970, Probability, statistics, and decision for civil engineers: New York, McGraw Hill Book Company, 684 p.

Black, B.D., Hecker, S., Hylland, M.D., Christenson, G.E., and McDonald, G.N., 2003, Quaternary fault and fold database and map of Utah: Utah Geological Survey Map 193DM, scale 1:500,000, CD-ROM.

Black, B.D, Mulvey, W.E., Lowe, M., and Solomon, B.J., 1995, Geologic effects, *in* Christenson, G.E., editor, The September 2, 1992 M_L 5.8 St. George earthquake, Washington County, Utah: Utah Geological Survey Circular 88, p. 2–11.

Block, L., Yeck, W., King, V., Derouin, S., and Wood, C., 2012, Review of geologic investigations and injection well site selection, Paradox Valley Unit, Colorado: U.S. Bureau of Reclamation Technical Memorandum No. 86-68330-2012-27, 71 p.

Bodle, R.R., 1941, United States earthquakes 1939: U.S. Coast and Geodetic Survey, Serial 637, 69 p.

Bodle, R.R., 1944, United States earthquakes 1942: U.S. Coast and Geodetic Survey, Serial 662, 38 p.

Bodle, R.R., and Murphy, L.M., 1947, United States earthquakes 1945: U.S. Coast and Geodetic Survey, Serial 699, 38 p.

Braunmiller, J., Deichmann, N., Giardini, D., Wiemer, S., and the SED Magnitude Working Group, 2005, Homogeneous moment-magnitude calibration in Switzerland: Bulletin of the Seismological Society of America, v. 95, no. 1, p. 58–74, doi: 10.1785/0120030245.

Brazee, R.J., and Cloud, W.K., 1958, United States earthquakes 1956: U.S. Coast and Geodetic Survey, 78 p.

Brazee, R.J., and Cloud, W.K., 1959, United States earthquakes 1957: U.S. Coast and Geodetic Survey, 108 p.

Brazee, R.J., and Cloud, W.K., 1960, United States earthquakes 1958: U.S. Coast and Geodetic Survey, 76 p.

Brumbaugh, D.A., 2001, The 1994 Draney Peak, Idaho, earthquake sequence: Focal mechanisms and stress field inversion: M.S. thesis, University of Utah, 157 p.

Carver, D., Richins, W.D., and Langer, C.J., 1983, Details of the aftershock process following the 30 September 1977 Uinta Basin, Utah, earthquake: Bulletin of the Seismological Society of America, v. 73, no. 2, p. 435–448.

Case, W.F., 1988, Geologic effects of the 14 and 18 August, 1988 earthquakes in Emery County, Utah: Survey Notes, Utah Geological Survey, v. 22, no. 1, 2, p. 8–15: Online, www.seis.utah.edu/lqthreat/nehrp_htm/1988sanr/1988sanr.shtml, accessed March 20, 2014.

Castellaro, S., and Bormann, P., 2007, Performance of different regression procedures on the magnitude conversion problem: Bulletin of the Seismological Society of America, v. 97, no. 4, p. 1167–1175, doi: 10.1785/0120060102.

Castellaro, S., Mulargia, F., and Kagan, Y.Y., 2006, Regression problems for magnitudes: Geophysical Journal International, v. 165, p, 913–930.

Chapman, D.G., and Schaufele, R.A., 1970, Elementary probability models and statistical inference: Waltham, Massachusetts, Xerox College Publishing Company, 358 p.

Cheng, C-L, and Van Ness, J., 1999, Statistical regression with measurement error: London, Edward Arnold Publishers Ltd, 262 p.

Chidsey, T.C., Jr., Morgan, C.D., and Bon, R., 2003, Major oil plays in Utah and vicinity: Utah Geological Survey Quarterly Technical Progress Report, Contract No. DE-FC26-02NT15133, 14 p.

Clark, R., 2012, Rangely Weber sand unit case history (RWSU): Online, http://www.uwyo.edu/eori/_files/co2conference12/rory_rangelycasehistory.pdf, accessed Feb. 11, 2014.

Coffman, J.L., and Stover, C.W., 1977, United States earthquakes 1975: U.S. National and Atmospheric Administration and U.S. Geological Survey, 136 p.

Coffman, J.L., and Stover, C.W., 1979, United States earthquakes 1977: U.S. National and Atmospheric Administration and U.S. Geological Survey, 81 p.

Coffman, J.L., and von Hake, C.A., 1972, United States earthquakes 1970: U.S. National and Atmospheric Administration, 81 p.

Committee on Induced Seismicity Potential in Energy Technologies, 2013, Induced seismicity potential in energy technologies: National Research Council, Washington, DC: Online, https://dels.nas.edu/Report/Induced-Seismicity-Potential-Energy-Technologies/13355, accessed Feb. 14, 2014.

Cook, K.L., and Nye, R.K., 1979, Effects of the Pocatello Valley (Idaho-Utah border) earthquake of March 28, 1975 (UTC), *in* Arabasz, W.J., Smith, R.B., and Richins, W.D., editors, Earthquake studies in Utah 1850 to 1978: Salt Lake City, University of Utah Seismograph Stations, Department of Geology and Geophysics, p. 445–457.

Cook, K.L., and Smith, R.B., 1967, Seismicity in Utah, 1850 through June 1965: Bulletin of the Seismological Society of America, v. 57, no. 4, p. 689–718.

dePolo, C., and Pecoraro, B., 2011, Modified Mercalli Intensity Maps for the February 21, 2008 Wells, Nevada earthquake: *in* dePolo, C. M,, and LaPointe, D. D., editors, The 21 February 2008 M_w 6.0 Wells, Nevada, earthquake—a compendium of earthquake-related investigations prepared by the University of Nevada, Reno (online version): Nevada Bureau of Mines and Geology Special Publication36: Online, http://www.nbmg.unr.edu/Pubs/sp/sp36/, accessed Feb. 14, 2014.

Dewey, J.W., Earle, P.S., and Presgrave, B.W, 2003, Four decades of PDE mb [abs]: Seismological Research Letters, v. 74, no. 2, p. 249.

Dewey, J.W., Earle, P.S., and Presgrave, B.W, 2004, Quantifying year-to-year drifts in PDE mb and explaining their causes [abs.]: Seismological Research Letters, v. 75, no. 2, p. 275.

Dewey, J.W., Presgrave, B.W., and Earle, P.S., 2011, Variations of mb(PDE): 1976–2010 [abs.]: Seismological Research Letters, v. 82, no. 2, p. 295.

Doser, D.I., 1985, Source parameters and faulting processes of the 1959 Hebgen Lake, Montana, earthquake sequence: Journal of Geophysical Research, v. 90, no. B6, p. 4537–4555.

Doser, D.I., 1989, Extensional tectonics in northern Utah-southern Idaho, U.S.A., and the 1934 Hansel Valley sequence: Physics of the Earth and Planetary Interiors, v. 54, p. 120–134.

Doser, D. I., and Kanamori, H., 1987, Long-period surface waves of four western United States earthquakes recorded by the Pasadena strainmeter: Bulletin of the Seismological Society of America, v. 77, no. 1, p. 236–243.

Doser, D.I., and Smith, R.B., 1982, Seismic moment rates in the Utah region: Bulletin of the Seismological Society of America, v. 72, no. 2, p. 525–551.

Doser, D.I., and Smith, R.B., 1985, Source parameters of the 28 October 1983 Borah Peak, Idaho, earthquake from body wave analysis: Bulletin of the Seismological Society of America, v. 75, no. 4, p. 1041–1051.

Dziewonski, A.M., Ekström, G., and Salganik, M.P., 1993, Centroid-moment-tensor solutions for October–December 1992: Physics of the Earth and Planetary Interiors, v. 80, no. 3-4, p. 89–103.

Dziewonski, A.M., Ekström, G., Woodhouse, J.H., and Zwart, G., 1990, Centroid-moment-tensor solutions for January–March 1989, Physics of the Earth and Planetary Interiors, v. 59, no. 4, p. 233–242.

Ekström, G., and Dziewonski, A.M., 1985, Centroid-moment-tensor solutions for 35 earthquakes in western North America (1977–1983): Bulletin of the Seismological Society of America, v. 75, no. 1, p. 23–39.

Ekström, G., and Nettles, M., undated, Global CMT web page: Online, http://www.globalcmt.org/, accessed March 21, 2014.

Electric Power Research Institute (EPRI), 1988, Seismic hazard methodology for the central and eastern United States: 10 volumes, EPRI-NP-4726, Palo Alto, California.

Electric Power Research Institute (EPRI), U.S. Department of Energy (DOE), and U.S. Nuclear Regulatory Commission (NRC), 2012, Technical Report: Central and Eastern United States

Seismic Source Characterization for Nuclear Facilities, v. 1, EPRI, Palo Alto, California: Online: www.ceus-ssc.com/index.htm, accessed Feb. 14, 2014.

Ellsworth, W.L., 2013, Injection-induced earthquakes: Science, v. 341, 1225942, doi: 10.1126/science.1225942.

Energy and Minerals Field Institute (EMFI), 2005, ChevronTexaco's Rangely Oil Field Operations: Online, emfi.mines.edu/emfi2005/ChevronTexaco.pdf, accessed Feb. 11, 2014.

Eppley, R.A., and Cloud, W.K., 1961, United States earthquakes 1959: U.S. Coast and Geodetic Survey, 115 p.

Evans, J.P., Martindale, D.C., and Kendrick, R.D., Jr., 2003, Geologic setting of the 1884 Bear Lake, Idaho, earthquake: Rupture in the hanging wall of a Basin and Range normal fault revealed by historical and geological analyses: Bulletin of the Seismological Society of America, v. 93, no. 4, p. 1621–1632.

Felzer, K.R., 2007, Calculating California seismicity rates: Appendix I *in* Working Group on California Earthquake Probabilities, The Uniform California Earthquake Rupture Forecast, Version 2 (UCERF 2): U.S. Geological Survey Open-File Report 2007-1437I, and California Geological Survey Special Report 203-I.

Felzer, K.R., and Cao, T., 2007, WGCEP historical California earthquake catalog: Appendix H *in* Working Group on California Earthquake Probabilities, The Uniform California Earthquake Rupture Forecast, Version 2 (UCERF 2): U.S. Geological Survey Open-File Report 2007-1437H, and California Geological Survey Special Report 203-H.

Fuller, W.A., 1987, Measurement error models: New York, John Wiley & Sons, 440 p.

Frankel, A., 1994, Implications of felt area-magnitude relations for earthquake scaling and the average frequency of perceptible ground motion: Bulletin of the Seismological Society of America, v. 84, no. 2, p. 462–465.

Gardner, J.K., and Knopoff, L., 1974, Is the sequence of earthquakes in southern California, with aftershocks removed, Poissonian?: Bulletin of the Seismological Society of America, v. 64, no. 5, p. 1363–1367.

Gasperini, P., and Lolli, B., 2014, Comment on "General Orthogonal Regression Relations between Body-Wave and Moment Magnitudes" by Ranjit Das, H.R. Wason, and M.L. Sharma: Seismological Research Letters, v. 85, no. 2, p. 351, doi: 10.1785/0220130096.

Gibbs, J.F., Healy, J.H., Raleigh, C.B., and Coakley, J., 1973, Seismicity in the Rangely, Colorado, area: 1962–1970: Bulletin of the Seismological Society of America, v. 63, no. 5, p. 1557–1570.

Griscom, M., and Arabasz, W.J., 1979, Local magnitude (M_L) in the Wasatch Front and Utah region: Wood-Anderson calibration, coda-duration estimates of M_L, and M_L versus m_b, *in* Arabasz, W.J., Smith, R.B., and Richins, W.D., editors, Earthquake studies in Utah 1850 to 1978: Salt Lake City, University of Utah Seismograph Stations, Department of Geology and Geophysics, p. 433–443.

Grünthal, G., Mayer-Rosa, D., and Lenhardt, W., 1998, Abschätzung der Erdbebengefährdung für die D-A-CH-Staaten—Deutschland, Österreich, Schweitz: Bautechnik, v.75 no. 10, p. 753–767.

Gurland, J., and Tripathi, R.C., 1971, A simple approximation for unbiased estimation of the standard deviation: American Statistician, v. 25, p. 30–32.

Gutenberg, B., and Richter, C.F., 1942, Earthquake magnitude, intensity, energy, and acceleration: Bulletin of the Seismological Society of America, v. 32, no. 3, p. 163–191.

Gutenberg, B., and Richter, C.F., 1949, Seismicity of the Earth and associated phenomena: Princeton, New Jersey, Princeton University Press, 273 p.

Gutenberg, B., and Richter, C.F., 1956, Earthquake magnitude, intensity, energy, and acceleration (Second Paper): Bulletin of the Seismological Society of America, v. 46, no. 2, p. 105–145.

Hakimhashemi, A.H., and Grünthal, G., 2012, A statistical method for estimating catalog completeness applicable to long-term nonstationary seismic data: Bulletin of the Seismological Society of America, v. 102, no. 6, p. 2530–2546, doi: 10.1785/0120110309.

Hanks, T.C., Hileman, J.A., and Thatcher, W., 1975, Seismic moments of the larger earthquakes of the southern California region: Geological Society of America Bulletin, v. 86, p. 1131–1139.

Hanks, T.C., and Johnston, A.C., 1992, Common features of the excitation and propagation of strong ground motion for North American earthquakes: Bulletin of the Seismological Society of America, v. 82, no. 1, p. 1–23.

Hanks, T.C., and Kanamori, H., 1979, A moment magnitude scale: Journal of Geophysical Research, v. 84, no. B5, p. 2348–2350.

Herrmann, R.B., Benz, H., and Ammon, C.J., 2011, Monitoring the earthquake source process in North America: Bulletin of the Seismological Society of America, v. 101, no. 6, p. 2609–2625, doi: 10.1785/0120110095.

Hileman, J.A., Allen, C.R., and Nordquist, J.M., 1973, Seismicity of the southern California region, 1 January 1932 to 31 December, 1972: Pasadena, Seismological Laboratory, California Institute of Technology, variously paginated.

Hopper, M.G., 2000, Isoseismals of some historical earthquakes affecting the Wasatch Front area, Utah, *in* Gori, P.L., and Hays, W.W., editors, Assessment of regional earthquake hazards and risk along the Wasatch Front, Utah: U.S. Geological Survey Professional Paper 1500-K-R, p. Q-1–25.

International Seismological Centre, 2010, On-line Bulletin: www.isc.ac.uk, accessed July 11, 2012.

Jibson, R.W., and Harp, E.L., 1995, The Springdale landslide, *in* Christenson, G., editor, The September 2, 1992 M_L 5.8 St. George earthquake, Washington County, Utah: Utah Geological Survey Circular 88, p. 21–30.

Jones, A.E., 1975, Recording of earthquakes at Reno, 1916–1951: University of Nevada Reno, Bulletin of the Seismological Laboratory, 199 p.

Kagan, Y.Y., 2002, Modern California earthquake catalogs and their comparison: Seismological Research Letters, v. 73, no. 6, p. 921–929.

Kagan, Y.Y., 2003, Accuracy of modern global earthquake catalogs: Physics of the Earth and Planetary Interiors, v. 135, p. 173–209, doi: 10.1016/S0031-9201(02)00214-5.

Lander, J.F., and Cloud, W.K., 1962, United States earthquakes 1960: U.S. Coast and Geodetic Survey, 90 p.

Lander, J.F., and Cloud, W.K., 1963, United States earthquakes 1961: U.S. Coast and Geodetic Survey, 106 p.

Lander, J.F., and Cloud, W.K., 1963, United States earthquakes 1961: U.S. Coast and Geodetic Survey, 106 p.

Lander, J.F., and Cloud, W.K., 1964, United States earthquakes 1962: U.S. Coast and Geodetic Survey, 114 p.

Lolli, B., and P. Gasperini, 2012, A comparison among general orthogonal regression methods applied to earthquake magnitude conversions: Geophysical Journal International, v. 190, p. 1135–1151, doi: 10.1111/j.1365-246X.2012.05530.x.

McCarter, M.K., 2001, Documentation of ground truth for significant seismic events related to underground mining in Utah and Wyoming, *in* Arabasz, W.J., and Pechmann, J.C., 2001, Seismic characterization of coal-mining seismicity in Utah for CTBT monitoring: Technical Report to Lawrence Livermore National Laboratory, LLNL Research Agreement No. B344836, Appendix C: Online, http://www.quake.utah.edu/Reports/llnl2001/LLNLRept.pdf, accessed Feb. 14, 2014.

Mendoza, C., and Hartzell, S.H., 1988, Inversion for slip distribution using teleseismic P waveforms; North Palm Springs, Borah Peak, and Michoacan earthquakes: Bulletin of the Seismological Society of America, v. 78, no.3, p. 1092–1111.

Moran, R., 2007, Earthquakes at Rangely, Colorado: Online, http://academic.emporia.edu/aberjame/student/moran4/index.htm, accessed Feb. 11, 2014.

Murphy, L.M., and Cloud, W.K., 1953, United States earthquakes 1951: U.S. Coast and Geodetic Survey, Serial 762, 49 p.

Murphy, L.M., and Cloud, W.K., 1957, United States earthquakes 1955: U.S. Coast and Geodetic Survey, 83 p.

Murphy, L.M., and Ulrich, F.P., 1951, United States earthquakes 1949: U.S. Coast and Geodetic Survey, Serial 748, 63 p.

Murphy, L.M., and Ulrich, F.P., 1952, United States earthquakes 1950: U.S. Coast and Geodetic Survey, Serial 755, 47 p.

Musson, R.M.W., 2012, The effect of magnitude uncertainty on earthquake activity rates: Bulletin of the Seismological Society of America, v. 102, no. 6, p. 2771–2775, doi: 10.1785/0120110224.

Nabelek, J., Eyidogan, H, and Toksoz, M.N., 1985, Source parameters of the Borah Peak, Idaho, earthquake of October 28, 1983 from body-wave inversion: Eos, Transactions, American Geophysical Union, v..66, no. 18, p. 308.

Neumann, F., 1936, United States earthquakes 1934: U.S. Coast and Geodetic Survey, Serial 593, 101 p.

Neumann, F., 1940a, United States earthquakes 1937: U.S. Coast and Geodetic Survey, Serial 619, 55 p.

Neumann, F., 1940b, United States earthquakes 1938: U.S. Coast and Geodetic Survey, Serial 629, 59 p.

Olig, S.S., 1995, Ground shaking and Modified Mercalli intensities, *in* Christenson, G., editor, The September 2, 1992 M_L 5.8 St. George earthquake, Washington County, Utah: Utah Geological Survey Circular 88, p. 12–20.

Oregon State University (OSU), 1998, Moment tensors: online catalog at http://quakes.oce.orst.edu/moment-tensor/, accessed May 10, 2012.

Pack, F.J., 1921, The Elsinore earthquakes in central Utah, September 29 and October 1, 1921: Bulletin of the Seismological Society of America, v. 11, nos. 3 and 4, p. 157–165.

Pancha, A., Anderson, J.G., and Kreemer, C., 2006, Comparison of seismic and geodetic scalar moment rates across the Basin and Range Province: Bulletin of the Seismological Society of America, v. 96, no. 1, p. 11–32, doi: 10.1785/0120040166.

Patton, H.J., and Zandt, G., 1991, Seismic moment tensors of Western U.S. earthquakes and implications for the tectonic stress field: Journal of Geophysical Research, v. 96, no. B11, p. 18,245–18,259.

Pechmann, J.C., and Arabasz, W.J., 1995, The problem of the random earthquake in seismic hazard analysis—Wasatch Front region, Utah, *in* Lund, W.R., editor, Environmental and engineering geology of the Wasatch Front region: Utah Geological Association Publication 24, p. 77–93.

Pechmann, J.C., Arabasz, W.J., and Nava, S.J., 1994, Refined analysis of the 1992 M_L 5.8 St. George, Utah, earthquake and its aftershocks [abs.]: Seismological Research Letters, v. 65, no. 2, p. 32.

Pechmann, J.C., Arabasz, W.J., Pankow, K.L., Burlacu, R., and McCarter, M.K., 2008, Seismological report on the 6 August 2007 Crandall Canyon mine collapse in Utah: Seismological Research Letters, v. 79, no. 5, p.620–636, doi: 10.1785gssrl.79.5.620.

Pechmann, J.C., Bernier, J.C., Nava, S.J., and Terra, F.M., 2010, Correction of systematic time-dependent coda magnitude errors in the Utah and Yellowstone National Park region earthquake catalogs, 1981–2001: Online, www.quake.utah.edu/Reports/mcpaper.BSSA2010sub.pdf, accessed Feb. 25, 2014.

Pechmann, J.C., Brumbaugh, D.A., Nava, S.J., Skelton T.G., Fivas, G.P., and Arabasz, W.J., 1997, The 1994 Draney Peak, ID, earthquake and its aftershocks [abs.]: Eos (Transactions American Geophysical Union), v. 78, no. 46 (Supplement), p. F480.

Pechmann, J.C., Nava, S.J., and Arabasz, W.J., 1991, Seismological analysis of four recent moderate (M_L 4.8 to 5.4) earthquakes in Utah: Technical report to the Utah Geological Survey, Contract No. 89-3659, 107 p.

Pechmann, J.C., Nava, S.J., Terra, F.M., and Bernier, J., 2007, Local magnitude determinations for Intermountain Seismic Belt earthquakes from broadband digital data: Bulletin of the Seismological Society of America, v. 97, no. 2, p. 557–574, doi: 10.1785/0120060114.

Pechmann, J.C., Walter, W.R., Nava, S.J., and Arabasz, W.J., 1995, The February 3, 1995, M_L 5.1 seismic event in the trona mining district of southwestern Wyoming: Seismological Research Letters, v. 66, no. 3, p. 25–34.

Pechmann, J.C., and Whidden, K.M., 2013, The relation of University of Utah local and coda magnitudes to moment magnitudes: The sequel [abs.]: Seismological Research Letters, v. 84, no. 2, p. 299.

Petersen, M.D., Frankel, A.D., Harmsen, S.C., Mueller, C.S., Haller, K.M., Wheeler, R.L., Wesson, R.L., Zeng, Y., Boyd, O.S., Perkins, D.M., Luco, N., Field, E.H., Wills, C.J., and Rukstales, K.S., 2008, Documentation for the 2008 update of the United States National Seismic Hazard Maps: U.S. Geological Survey Open-File Report 2008-1128, 61 p.

Raleigh, C.B., Healy, J.H., and Bredehoeft, J.D., 1976, An experiment in earthquake control at Rangely, Colorado: Science, v. 191, p. 1230–1237.

Richins, W.D., Pechmann, J.C., Smith, R.B., Langer, C.J., Goter, S.K., Zollweg, J.E., and King, J.J., 1987, The 1983 Borah Peak, Idaho, earthquake and its aftershocks: Bulletin of the Seismological Society of America, v. 77, p. 694-723.

Richter, C.F., 1958, Elementary seismology: San Francisco, W.H. Freeman and Company, 768 p.

Rohlf, F.J., and Sokal, R.R., 1981, Statistical Tables: W. H. Freeman and Company, New York, 219 p.

Rogers, A.M., Algermissen, S.T., Hays, W.W., and Perkins, D.M., 1976, A study of earthquake losses in the Salt Lake City, Utah, area: U.S. Geological Survey Open-File Report 76-89, 357 p.

Rogers, A.M., Harmsen, S.C., Corbett, E.J., Priestley, K., and dePolo, D., 1991, The seismicity of Nevada and some adjacent parts of the Great Basin, *in* Slemmons, D.B., Engdahl, E.R., Zoback, M.D., and Blackwell, D.D., editors, Neotectonics of North America: Geological Society of America, Decade Map Volume 1, p. 153–184.

Schuh, M.L., 1993, Red Wash, *in* Hill, B.G., and Bereskin, S.R., editors, Oil and gas fields of Utah: Utah Geological Association Publication 22, non-paginated.

Shemeta, J.E., 1989, New analyses of three-component digital data for aftershocks of the 1983 Borah Peak, Idaho, earthquake source parameters and refined hypocenters: Salt Lake City, Utah, University of Utah, M.S. thesis, 126 p.

Shenon, P.J., 1936, The Utah earthquake of March 12, 1934 (extracts from unpublished report), *in* Neumann, F., United States earthquakes 1934: U.S. Coast and Geodetic Survey, Serial 593, p. 43–48.

Simpson, D.W., 1976, Seismicity changes associated with reservoir loading: Engineering Geology, v. 10, p. 123–150.

Sipkin, S.A, 1986, Estimation of earthquake source parameters by the inversion of waveform data; global seismicity, 1981–1983: Bulletin of the Seismological Society of America, v. 76, no. 6, p. 1515–1541.

Slemmons, D.B., Jones, A.E., and Gimlett, J.I., 1965, Catalog of Nevada earthquakes, 1852–1960: Bulletin of the Seismological Society of America, v. 55, no. 2, p. 519–565.

Smith, R.B., and Arabasz, W.J., 1991, Seismicity of the Intermountain seismic belt, *in* Slemmons, D.B., Engdahl, E.R., Zoback, M.D., and Blackwell, D.D., editors, Neotectonics of North America: Geological Society of America, Decade Map Volume 1, p. 185–228.

Smith, K., Pechmann, J., Meremonte, M., and Pankow, K., 2011, Preliminary analysis of the M_w 6.0 Wells, Nevada, earthquake sequence: *in* dePolo, C.M,, and LaPointe, D.D., editors., The 21 February 2008 M_w 6.0 Wells, Nevada, earthquake—a compendium of earthquake-related investigations prepared by the University of Nevada, Reno (online version): Nevada Bureau of Mines and Geology Special Publication36: Online www.nbmg.unr.edu/Pubs/sp/sp36/, accessed Feb. 14, 2014.

Stover, C.W., 1985, United States earthquakes, 1982: U.S. Geological Survey Bulletin 1655, 141 p.

Stover, C.W., editor, 1987, United States earthquakes, 1983: U.S. Geological Survey Bulletin 1698, 196 p.

Stover, C.W., and Coffman, J.L., 1993, Seismicity of the United States, 1568–1989 (Revised): U.S. Geological Survey Professional Paper 1527, 418 p.

Stover, C.W., Reagor, B.G., and Algermissen, S.T., 1986, Seismicity map of the state of Utah: U.S. Geological Survey Miscellaneous Field Studies Map MF-1856, including data compilation.

Stover, C.W., and von Hake, C.A., editors, 1982, United States earthquakes, 1980: U.S. Geological Survey and U.S. National Oceanic and Atmospheric Administration, 182 p.

Talley, H.C., Jr., and Cloud, W.K., 1962, United States earthquakes 1960: U.S. Coast and Geodetic Survey, 90 p.

Taylor, J.R., 1982, An introduction to error analysis: Mill Valley, California, University Science Books, 270 p.

Tinti, S., and Mulargia, F., 1985, Effects of magnitude uncertainties on estimating the parameters in the Gutenberg-Richter frequency-magnitude law: Bulletin of the Seismological Society of America, v. 75, no. 6, p. 1681–1697.

Toppozada, T.R., 1975, Earthquake magnitude as a function of intensity data in California and western Nevada: Bulletin of the Seismological Society of America, v. 65, no. 5, p. 1223–1238.

Toppozada, T.R., and Branum, D., 2002, California $M \geq 5.5$ earthquakes: Their history and the areas damaged, *in* Lee, W. H., Kanamori, H., and Jennings, P., editors, International Handbook of Earthquake and Engineering Seismology, International Association of Seismology and Physics of the Earth's Interior, Academic Press, New York (full paper on CD-ROM).

U.S. Geological Survey/National Earthquake Information Center (USGS/NEIC), 2012, USGS/NEIC PDE catalog: Online, earthquake.usgs.gov/earthquakes/eqarchives/epic/, accessed May 18, 2012.

van Stiphout, T., Zhuang, J., and Marsan, D., 2012, Seismicity declustering: Community Online Resource for Statistical Seismicity Analysis, doi: 10.5078/corssa-52382934: Online, www.corsa.org, accessed Feb. 14, 2014.

Veneziano, D., and Van Dyck, J., 1985a, Statistical discrimination of "aftershocks" and their contribution to seismic hazard: Appendix A-4 *in* McGuire, R.K., project manager, Seismic hazard methodology for nuclear facilities in the eastern United States, v. 2, Appendix A: Electric Power Research Institute Project No. P101-29, EPRI/Seismicity Owners Group Draft 85-1 (April 30, 1985), p. A-120–186.

Veneziano, D., and Van Dyck, J., 1985b, Analysis of earthquake catalogs for incompleteness and recurrence rates: Appendix A-6 *in* McGuire, R.K., project manager, Seismic hazard methodology for nuclear facilities in the eastern United States, v. 2, Appendix A: Electric Power Research Institute Project No. P101-29, EPRI/Seismicity Owners Group Draft 85-1 (April 30, 1985), p. A-220–297.

von Hake, C.A., and Cloud, W.K., 1965, United States earthquakes 1963, U.S. Coast and Geodetic Survey, 69 p.

von Hake, C.A., and Cloud, W.K., 1968, United States earthquakes 1966, U.S. Coast and Geodetic Survey, 110 p.

von Hake, C.A., and Cloud, W.K., 1969, United States earthquakes 1967, U.S. Coast and Geodetic Survey, 90 p.

Wahlquist, W.L., editor, 1981, Atlas of Utah: Provo, Utah, Brigham Young University Press and Weber State College, 300 p.

Wald, D.J., Quitoriano, V., Dengler, L.A., and Dewey J.W., 1999, Utilization of the Internet for rapid Community Intensity Maps, Seismological Research Letters, v. 70, no. 6, p. 680-697.

Wallace, T.C., Helmberger, D.V., and Mellman, G.R., 1981, A technique for the inversion of regional data in source parameter studies: Journal of Geophysical Research, v. 86, no. B3, p. 1679–1685.

Weichert, D.H., 1980, Estimation of the earthquake recurrence parameters for unequal observation periods for different magnitudes: Bulletin of the Seismological Society of America, v. 70, no. 4, p. 1337–1346.

Westaway, R., and Smith, R.B., 1989, Source parameters of the Cache Valley (Logan), Utah, earthquake of 30 August 1962: Bulletin of the Seismological Society of America, v. 79, no. 5, p. 1410–1425.

Whidden, K.M., and Pankow, K.L., 2012, A catalog of regional moment tensors in Utah from 1998 to 2011: Seismological Research Letters, v. 83, no. 5, p. 775–783, doi: 10.1785/0220120046.

Williams, B.R., 1979, M_0 calculations from a generalized AR parameter method for WWSSN instruments: Bulletin of the Seismological Society of America, v. 69, no.2, p. 329–351.

Williams, J.S., and Tapper, M.L., 1953, Earthquake history of Utah, 1850–1949: Bulletin of the Seismological Society of America, v. 43, no. 3, p. 191–218.

Wong, I.G., 1993, Tectonic stresses in mine seismicity—are they significant?, *in* Youngs, R.P., editor, Rockbursts and seismicity in mines 93—Proceedings of the 3rd International Symposium on Rockbursts and Seismicity in Mines, Ontario, Canada: Rotterdam, A.A. Balkema, p. 273–278.

Wood, H.O., 1947, Earthquakes in southern California with geologic relations, Part Two: Bulletin of the Seismological Society of America, v. 37, no. 3, p. 217–258.

Wood, H.O., and Neumann, F., 1931, Modified Mercalli intensity scale of 1931: Bulletin of the Seismological Society of America, v. 21, no. 4, p. 277–283.

Working Group on Utah Earthquake Probabilities (WGUEP), 2016, Earthquake probabilities for the Wasatch Front region in Utah, Idaho, and Wyoming: Utah Geological Survey Miscellaneous Publication 16-3, variously paginated.

Youngs, R.R., and Coppersmith, K.J., 1985, Implications of fault slip rates and earthquake recurrence models to probabilistic seismic hazard estimates: Bulletin of the Seismological Society of America, v. 75, no. 4, p. 939–964.

Youngs, R.R., Swan, F.H., Power, M.S., Schwartz, D.P., and Green, R.K., 1987, Probabilistic analysis of earthquake ground shaking hazards along the Wasatch Front, Utah, *in* Gori, P.L., and Hays, W.W., editors, Assessment of regional earthquake hazards and risk along the Wasatch Front, Utah, Volume II: U.S. Geological Survey Open-file Report 87-585, p. M-1–110.

Youngs, R.R., Swan, F.H., Power, M.S., Schwartz, D.P., and Green, R.K., 2000, Probabilistic analysis of earthquake ground shaking hazards along the Wasatch Front, Utah, *in* Gori, P.L., and Hays, W.W., editors, Assessment of regional earthquake hazards and risk along the Wasatch Front, Utah: U.S. Geological Survey Professional Paper 1500-K-R, p. M-1–74.

Table E-1. *Coordinates (in degrees of latitude N and longitude W) defining catalog domains and areas of non-tectonic and human-triggered seismicity shown on figure E-1.*

Catalog Domain/Area	Boundary				Center Point[1]			WP-BC Polygon[2]	
	North	South	West	East	North	West	Radius (km)	North	West
Extended Utah Region (UTREXT)[3]	43.500	36.000	115.000	108.000	------	------	------	39.1667	111.3000
Utah Region (UTR)[4]	42.500	36.750	114.250	108.750	------	------	------	39.5833	111.3000
WGUEP Study Region (WGUEP)[5]	42.500	39.000	113.250	110.750	------	------	------	39.6333	111.3667
Southern Fuel Co. MIS area (SUFCO)	39.033	38.903	111.483	111.267	------	------	------	39.7500	111.3667
SW Wyoming trona mining (TRONA)	41.800	41.300	110.000	109.550	------	------	------	39.8333	111.2333
Paradox Valley (PV)	------	------	------	------	38.297	108.895	25.0	39.8333	110.5000
Rangely oil field (R)	------	------	------	------	40.113	108.861	25.0	39.6333	110.2333
Red Wash oil field (RW)	------	------	------	------	40.189	109.313	25.0	39.3667	110.1667
								39.3667	110.5167
								39.5167	110.5500
								39.5833	110.6500
								39.5833	110.9500
								39.1667	110.9500
								39.1667	111.3000

[1] For PV, the location of the U.S. Bureau of Reclamation's deep disposal well operated as part of the Paradox Valley Unit saltwater injection project; for R, the center of the Rangely oil field taken from Gibbs and others (1973); for RW, the Red Wash field's geocode coordinates.

[2] Polygon outlining the Wasatch Plateau (WP)-Book Cliffs (BC) coal-mining region

[3] Area = 498,360 km^2

[4] Area = 300,850 km^2

[5] Area = 82,060 km

Table E-2. *Overview of merged source catalogs by time period.*

Subcatalog	**UUSS Historical** ALL	**USGS SRA** ALL	**USGS WMM** ALL	**Stover and Coffman (1993)** $I_0 \geq 6$, $M \geq 4.5$	**UUSS Instrumental** $M \geq 2.45$	**USGS PDE** ALL
A. Jan 1850–June 1962	X	X	X	X		
B. July 1962–Dec 1986		X	X	X	X	X[3]
C. Jan 1987–Sept 2012			X[1]	X[2]	X	X

[1] The USGS (WMM) catalog received from C.S. Mueller, USGS, extended only through 2010; according to C.S. Mueller (USGS, oral communication, 2013) the USGS PDE catalog provides the basis for extending the WMM catalog beyond 2010.
[2] The compilation of Stover and Coffman (1993) ends in 1989.
[3] The USGS PDE catalog begins on January 1, 1973.

Table E.3. *Seismic events in the trona-mining district of southwestern Wyoming (M ≥ 2.45, July 1962–September2012) that were removed from the merged earthquake catalog as non-tectonic events.*

Year	MoDay	Hr:Min Sec (UTC)	Long. W	Lat. N	Depth[1] (km)	Magnitude and Type[2]		Note
1985	0320	01:37 10.53	109.653	41.611	8	3.20	Mc UU	
1986	0605	19:34 02.49	109.667	41.384	7	3.00	Mc UU	
1994	0625	10:07 28.77	109.698	41.609	5	3.58	Mc UU	3
1995	0203	15:26 13.25	109.815	41.526	4	5.18	ML UU	4
1998	0113	05:41 48.21	109.958	41.718	5	2.47	ML UU	
1998	1110	10:14 15.60	109.897	41.672	5	2.90	ML GS	
2000	0130	02:05 32.34	109.776	41.521	7	4.25	ML UU	5
2000	0716	02:05 32.34	109.878	41.621	1	3.06	ML UU	
2000	0817	23:02 30.21	109.700	41.554	7	3.08	ML UU	
2007	0605	03:28 42.45	109.973	41.693	1	3.10	ML UU	
2007	0605	03:29 06.92	109.908	41.588	5	3.42	ML UU	
2007	1122	02:29 36.46	109.736	41.633	5	3.42	ML UU	
2007	1222	05:59 46.45	109.918	41.627	7	2.59	ML UU	
2008	0209	17:41 49.85	109.889	41.668	2	3.32	ML UU	
2009	0307	02:45 10.18	109.923	41.670	5	3.61	ML UU	
2012	0225	06:15 16.00	109.884	41.647	2	2.51	ML UU	

[1] Focal-depth control for this region in the source catalogs is very poor.
[2] Magnitudes and types here are from the original source catalogs.
[3] Suspected mining-related event (Pechmann and others, 1995).
[4] Documented mining-related event (Pechmann and others, 1995).
[5] Documented mining-related event (McCarter, 2001).

Table E-4. *Suspected injection-induced earthquakes in the circular areas demarcated on figure E-1 for Paradox Valley and the Rangely and Red Wash oil fields that were removed from the declustered catalog of independent mainshocks before calculating seismicity rates for the Utah Region.*

Year	MoDay	Hr:Min Sec (UTC)	Long. W	Lat. N	Depth[1] (km)	Magnitude and Type[2]		Note
Paradox Valley[3]								
1997	1215	09:18 47.00	109.080	38.319	0	3.22	BEM	
1998	0410	06:52 16.40	108.827	38.268	5	3.14	BEM	
1998	0508	19:45 00.60	109.102	38.317	3	3.04	BEM	
1999	0204	13:38 55.20	108.920	38.286	3	3.00	BEM	
1999	0321	06:14 24.90	109.050	38.311	0	2.76	BEM	
1999	0603	15:35 34.20	108.940	38.261	1	3.66	BEM	
1999	0706	22:05 45.00	108.879	38.276	1	3.69	BEM	
1999	0916	00:35 03.00	108.907	38.310	5	3.02	BEM	
1999	1011	21:43 05.00	108.888	38.273	1	2.74	BEM	
1999	1104	11:00 19.00	108.814	38.242	5	2.71	BEM	
2000	0315	12:14 27.60	108.911	38.277	2	3.23	BEM	
2000	0527	21:58 19.00	108.881	38.301	3	3.80	BEM	
2002	0606	12:29 11.00	108.941	38.326	2	3.20	BEM	
2004	1107	06:54 59.70	108.911	38.245	1	3.68	BEM	
2005	0807	22:12 13.30	108.914	38.259	1	3.05	BEM	
2007	0801	07:46 08.20	108.985	38.378	4	3.00	BEM	
2009	0419	13:34 52.90	108.918	38.273	2	2.89	BEM	
2009	0430	08:50 34.20	108.914	38.258	0	2.79	BEM	
2009	1117	19:44 38.00	108.870	38.360	5	3.21	BEM	
Rangely Oil Field[4]								
1966	0706	05:47 08.40	108.948	40.090	7	3.78	BEM	
1967	0215	03:28 03.50	109.054	40.113	7	4.02	BEM	5
1970	0421	08:53 53.10	109.008	40.055	7	3.93	BEM	
1979	0319	14:59 30.20	108.859	40.044	7	3.66	BEM	
1993	0513	16:13 24.50	108.884	40.111	0	3.31	BEM	
1995	0320	12:46 16.30	108.820	40.125	3	4.26	BEM	
2007	0907	13:51 26.40	108.904	40.160	0	2.97	BEM	
Red Wash Oil Field								
1967	0215	03:28 03.50	109.054	40.113	7	4.02	BEM	5
1990	0407	15:37 54.50	109.474	40.116	2	3.92	BEM	
1991	0302	08:41 36.60	109.427	40.127	1	3.66	BEM	
1991	1108	13:15 04.70	109.242	40.127	1	3.46	BEM	
2000	1111	21:17 52.70	109.194	40.246	1	3.66	BEM	

[1] Focal-depth control in the source catalogs is fair to good for most of the events in the Paradox Valley area but poor for the areas of the Rangely and Red Wash oil fields.

[2] All magnitudes are best-estimate moment magnitudes from the BEM declustered catalog, into which original source catalogs contributed seismic events of ~M 2.5 and larger.

[3] The following dependent events removed by declustering are not included:
1998 0516 04:30 (**M** 2.50); 1999 0320 15:12 (**M** 2.59).

[4] The following dependent events removed by declustering are not included:
1966 0705 18:26 (**M** 3.38); 1966 0705 20:02 (**M** 3.46); 1967 0215 04:33 (**M** 2.99); 1970 0421 15:05 (**M** 3.55); 1979 0329 22:07 (**M** 2.82); 1995 0320 13:16 (**M** 2.97); 1995 0320 14:33 (**M** 2.77); 1995 0323 03:31 (**M** 3.14); 1995 0401 05:22 (**M** 3.25).

[5] This same event appears in the 25-km radial sorts for both the Rangely and Red Wash oil fields.

Table E-5. *Directly-determined magnitude uncertainties, from sets of earthquakes with three or more station measures for the given magnitude type, using the average-standard-error approach.*

Catalog	**Mag. Type,** ***M***	**No. of Earthquakes**	**Time Period**	**Region**	$\sigma[M]$[1] (± 1 s.d.)	**Single-Station Mag. Uncertainty**[2] (± 1 s.d.)
UUSS	M_L	2517	1996-2012	UTR	0.10 (± 0.06)	0.21 (± 0.10)
UUSS	M_L	41	1962-1980	UTR	0.16 (± 0.10)[3]	0.29 (± 0.17)
UUSS	M_C	873	1986-2000	UTR	0.10 (± 0.04)	0.31 (± 0.10)
ISC	m_b[4]	34	1966-2008	UTREXT	0.12 (± 0.06)	0.38 (± 0.10)

[1] Based on the average standard error of event magnitudes, $\overline{SE_{em}}$, for the total sample of earthquakes.

[2] Population standard deviation estimated from the average of sample standard deviations for event magnitudes (corrected for sample size), $STDEV_{\text{corrected}}$, for all the earthquakes in the sample.

[3] Many values of M_L in the UUSS catalog for this period are based on less than three station measures; for the 299 M_L event magnitudes during 1962-1980, an average value of $\sigma[M_L\,UU]$ of 0.24 was calculated using the single-station magnitude uncertainty of 0.29 and the number of station measures entering into each event M_L value.

[4] Based on five or more station measures.

Table E-6. *Indirectly-determined magnitude uncertainties from the standard deviation of the magnitude difference, $\sigma_{\Delta M}$, in two catalogs.*[1]

Catalogs	Mag. Type	No. of Earthquakes	Time Period	Region	$\sigma_{\Delta M}$	σ_{M1}	σ_{M2}
UUSS, SLU[2]	**M**	36	1998–2013	Intermountain Seismic Belt	0.071	0.05 UUSS	0.05 SLU
SLU, GCMT[2]	**M**	24	2001–2013	Western U.S.[3] (shallow)	0.076	0.05 SLU	0.06 GCMT[4]
UUSS, USGS/PDE	M_L	44	1996–2012	UTR	0.187	0.10 UUSS	0.16 USGS
UUSS, USGS/PDE	M_L	334	1994–2012	UTREXT	0.248	0.10 UUSS	0.23 USGS
USGS/PDE, ISC[5]	m_b	15	1978–2008	UTREXT	0.177	0.13 USGS	0.13 ISC

[1] Where $\sigma_{M1} = \sigma_{M2}$ in the table, the two values were assumed to be equal *a priori.*

[2] Data in this row are revised from Pechmann and Whidden (2013).

[3] 31°–49° N. latitude, 105°–125° W. longitude, depth < 33 km.

[4] From magnitude-difference data in Kagan (2003, Table 5) and the linear combination of squared uncertainties, we derived the following time-varying values of σ_M for reported values of **M** in the GCMT catalog prior to 2001:

σ_M = 0.10 for global earthquakes 0–70 km depth during 1980–1994,

σ_M = 0.06 for global earthquakes 0–70 km depth during 1995–2000.

[5] Based on five or more station measures.

Table E-6a. *Addendum—Summary of uncertainties assessed for original catalog magnitudes.*

Local Magnitude, Coda Magnitude, and Body-Wave Magnitude

Catalog	Mag. Type	CR ID[1]	Time Period[2]	Region[3]	$\sigma[M]$[4]	Reference
UUSS	M_L	2	1962-1980	UTR	**0.24**	table E-5, footnote 3
UUSS	M_L	1#	1981-1995	UTR	**0.21**	table E-8, footnote 2 and addendum
UUSS	M_L	1	1996-2012	UTR	0.10	table E-5 (see also table E-8, addendum)
UUSS	M_L	1#	1981-1993	EBR	**0.21**	table E-8, footnote 2 and addendum (same $\sigma[M]$ for UTR assumed for EBR)
UUSS	M_L	1	1994-2012	EBR	0.10	table E-5 (see also table E-8, addendum; same $\sigma[M]$ for UTR assumed for EBR)
UUSS	M_C[5]	3	1981-2012	UTR	0.10	table E-5
USGS	M_L	6	1974-2012	UTR	0.16	table E-6
USGS	M_L	7	1981-2012	EBR	0.23	table E-6 ($\sigma[M]$ determined from UTREXT applied only to EBR)
USGS	m_b	10	1963-1977	UTR	*0.19*	table E-10, footnote 4
USGS	m_b	9	1978-1990	UTREXT	*0.14*	table E-10, footnote 3
USGS	m_b	8	1991-2012	UTREXT	*0.14*	table E-10, footnote 3
ISC	m_b	11	1964-2012	UTREXT	0.12	table E-5 (see also table E-6)

[1] ID number for conversion relationship (CR) listed in table E-8.

[2] The listed time periods cover the ranges indicated for the corresponding conversion relationships in table E-8; the time periods of data contributing to $\sigma[M]$ may differ, as indicated in the references.

[3] Unless otherwise indicated, the source domain of data used for the listed $\sigma[M]$.

[4] Bolded values are used in propagating uncertainties in two-step regressions; italicized values are used as estimates of σ_x in general orthogonal regressions (see table E-10).

[5] UUSS coda magnitudes prior to 1981 were based on "network" formulas rather than single-stations formulas (Griscom and Arabasz, 1979); $\sigma[M]$ was not assessed for M_C UU2 and M_C UU3, only $\sigma[M_L$ UU1$|$ M_C UU2] and $\sigma[M_L$ UU1$|$ M_C UU3] (see table E-8).

Moment Magnitude **(M_{obs})**[6]

Catalog	Mag. Type	CR ID	Time Period[7]	Region[8]	σ[**M**]	Reference
UUSS	**M**	n/a	1998–2013	ISB	0.05	table E-6
SLU	**M**	n/a	1998–2013	ISB	0.05	table E-6
GCMT	**M**	n/a	1980–1994	global	0.10	table E-6, footnote 4; Kagan (2003)
GCMT	**M**	n/a	1995–2000	global	0.06	table E-6, footnote 4; Kagan (2003)
GCMT	**M**	n/a	2001-2013	WUS	0.06	table E-6

[6] See the "Explanation of Columns" sheet in Electronic Supplement E-2 for σ[**M**] associated with other values of $\mathbf{M}_{obs}$ not listed here.

[7] Time period of data contributing to σ[**M**].

[8] Source domain of data used for the listed σ[**M**]: ISB = Intermountain Seismic Belt; global = global earthquakes 0–70 km depth; WUS = Western U.S. (shallow).

Table E-7. *Sources of M_{obs} used in this study.*

Source of Reported Seismic Moment, M_0	Number of M_{obs} Values
1989 and Later	
Global Centroid Moment Tensor (GCMT) catalog	7
Whidden and Pankow (2012)	43
Whidden (University of Utah, unpublished data)	13
St. Louis University (SLU): Herrmann and others (2011), SLU online moment tensor catalog	30
Oregon State University (OSU) online moment tensor catalog	7
Pre-1989	
Battis and Hill (1977)	1
Doser (1989)	2
Patton and Zandt (1991)	8
Other (geometric mean of multiple M_0's)	3
TOTAL	114

Table E-8. *Conversion relationships to a predicted "best-estimate" uniform moment magnitude,* $\boldsymbol{M}_{pred}$*, based on general orthogonal regression. (Unless otherwise noted, relationships were developed for the Utah Region; use in the Extended Utah Region is provisional.)*

Size Measure		Conversion Relationship (CR)		$\sigma[\mathbf{M}\|X]$[1]
Notation	**Description and Applicable Period**	**ID**	**Relationship**	
M_L UU1	M_L Univ. of Utah (1981–2012) [see addendum on following page]	1	$\mathbf{M}_{pred} = 0.791\ (M_L\ UU1) + 0.851$	0.139[2]
M_L UU2	M_L Univ. of Utah (July 1962–Dec 1980)	2	***Two-step:*** M_L UU1 = M_L UU2 ± 0.24 (see footnote 3, table E-5), where 0.24 = $\sigma_{MLUU1\|MLUU2}$, and use CR-1	0.229
M_C UU1	M_C Univ. of Utah (1981–2012)	3	$\mathbf{M}_{pred} = 0.929\ (M_C\ UU1) + 0.227$	0.225
M_C UU2	M_C Univ. of Utah (Oct 1974–Dec 1980)	4	***Two-step:*** M_L UU1 = M_C UU2 ± 0.27 (see Griscom and Arabasz, 1979), where 0.27 = $\sigma_{MLUU1\|McUU2}$, and use CR-1	0.249
M_C UU3	M_C Univ. of Utah (July 1962–Sept 1974)	5	***Two-step:*** M_L UU1 = M_C UU3 ± 0.28 (see Griscom and Arabasz, 1979), where 0.28 = $\sigma_{MLUU1\|McUU3}$, and use CR-1	0.256
M_L GS	M_L USGS (1974–2012), Utah Region (UTR)	6	***Two-step:*** M_L UU1 = M_L GS – 0.11 and use CR-1	0.232
M_L GS	M_L USGS (1981–2012), Extended Border Region (EBR)	7	***Two-step:*** M_L UU1 = M_L GS + 0.09 and use CR-1	0.230
m_b PDE1 > 3.5	m_b USGS/PDE (1991–2012), Extended Utah Region (UTREXT)	8	$\mathbf{M}_{pred} = 1.078\ (m_b\ PDE1) – 0.427$	0.207
m_b PDE2 ≥ 3.5	m_b USGS/PDE (1978–1990)	9	***Two-step:*** $M_{L,C}$ UU = 1.088 m_b PDE2 – 0.652 and use CR-1	0.362
m_b PDE3 3.3–5.0	m_b CGS/USGS/PDE (1963–1977)	10	***Two-step:*** $M_{L,C}$ UU = 1.697 m_b PDE3 – 3.557 and use CR-1	0.443
m_b ISC	m_b ISC, Nsta ≥ 5 (1964–2012)	11	$\mathbf{M}_{pred} = 1.162\ m_b\ ISC –0.740$	0.295
ln(FA)	ln(FA), in km^2, where FA is the total felt area (1850–2012)	12	$\mathbf{M}_{pred} = 0.00 + 0.415 \times \ln(FA) + 0.0015\ (FA)^{1/2}$	0.339
$I_0 \geq V$	Epicentral value of Modified Mercalli Intensity, MMI ≥ V (1850–2012)	13	$\mathbf{M}_{pred} = 0.764\ I_0 + 0.229$	0.5[3]
$I_0 < V$	Epicentral value of MMI < V (1850–2012)	14	$\mathbf{M}_{pred} = 0.386\ I_0 + 2.126$	0.5[3]

(continued on next page)

Size Measure		Conversion Relationship (CR)		σ[**M**|X][1]
Notation	**Description and Applicable Period**	**ID**	**Relationship**	
A_{VII}	Extent of area shaken, in km^2, at or greater than MMI VII (1850–2012)	15	$\mathbf{M}_{pred} = 1.619 \log_{10}(A_{VII}) + 0.802$	0.35[4]
A_{VI}	Extent of area shaken, in km^2, at or greater than MMI VI (1850–2012)	16	$\mathbf{M}_{pred} = 1.341 \log_{10}(A_{VI}) + 0.535$	0.35[4]
A_{V}	Extent of area shaken, in km^2, at or greater than MMI V (1850–2012)	17	$\mathbf{M}_{pred} = 1.445 \log_{10}(A_{V}) - 0.809$	0.35[4]
A_{IV}	Extent of area shaken, in km^2, at or greater than MMI IV (1850–2012)	18	$\mathbf{M}_{pred} = 1.306 \log_{10}(A_{IV}) - 0.345$	0.35[4]

[1] Standard deviation of the normally distributed error in **M** when estimated from size measure X. Uncertainties in $\mathbf{M}_{pred}$ are adjusted for the variance in the observed values of **M**, $\mathbf{M}_{obs}$, used in the regression of $\mathbf{M}_{obs}$ versus X; uncertainties for two-step regressions account for the propagation of uncertainties.

[2] The 1981 start date for M_L UU1 is based on Pechmann et al. (2007), but the value of 0.139 for σ[**M**|M_L UU1] is based mostly on M_L observations from multi-station digital data after 1996. Because M_L values in the University of Utah catalog from 1981 until the early 1990s are based on two stations (with an average standard error of 0.21 vs. 0.10 for later M_L UU1), a larger two-step uncertainty of 0.209 for σ[**M**|M_L UU1] is applied to the UTR for 1981–1995 and to the EBR for 1981–1993.

[3] Adopted nominal value.

[4] Adopted generic value.

Addendum to CR-1

For clarity, the instructions below make explicit how CR-1 for M_L Univ. of Utah was applied to the BEM catalog by time period and by region, based on the information provided in footnote 2 above.

Size Measure		Conversion Relationship (CR)		σ[**M**|X][1]
Notation	**Description and Applicable Period**	**ID**	**Relationship**	
M_L UU1	M_L Univ. of Utah (1996–2012), UTR	1	$\mathbf{M}_{pred} = 0.791\ (M_L\ UU1) + 0.851$	0.139
M_L UU1[#]	M_L Univ. of Utah (1981–1995), UTR	1[#]	***Two-step:*** M_L UU1 = M_L UU1[#] ± 0.21, where 0.21 = $\sigma_{MLUU1\|MLUU1\#,}$ and use CR-1	0.209
M_L UU1	M_L Univ. of Utah (1994–2012), EBR	1	$\mathbf{M}_{pred} = 0.791\ (M_L\ UU1) + 0.851$	0.139
M_L UU1[#]	M_L Univ. of Utah (1981–1993), EBR	1[#]	***Two-step:*** M_L UU1 = M_L UU1[#] ± 0.21, where 0.21 = $\sigma_{MLUU1\|MLUU1\#}$, and use CR-1	0.209

Table E-9. *Conversion relationships to a uniform estimate of moment magnitude, E[**M**], based on least squares regression. (Unless otherwise noted, relationships were developed for the Utah Region; use in the Extended Utah Region is provisional.)*

Size Measure		Conversion Relationship (CR)		$\sigma[\mathbf{M}\|\mathbf{X}]$[1]
Notation	**Description and Applicable Period**	**ID**	**Relationship**	
M_L UU1	M_L Univ. of Utah (1981–2012) [see addendum on following page]	1a	$E[\mathbf{M}] = 0.769\ (M_L\ UU1) + 0.941$	0.137[2]
M_L UU2	M_L Univ. of Utah (July 1962–Dec 1980)	2a	***Two-step:*** M_L UU1 = M_L UU2 ± 0.24 (see footnote 3, table E-5), where $0.24 = \sigma_{MLUU1\|MLUU2}$, and use CR-1	0.223
M_C UU1	M_C Univ. of Utah (1981–2012)	3a	$E[\mathbf{M}] = 0.838\ (M_C\ UU1) + 0.603$	0.216
M_C UU2	M_C Univ. of Utah (Oct 1974–Dec 1980)	4a	***Two-step:*** M_L UU1 = M_C UU2 ± 0.27 (see Griscom and Arabasz, 1979), where $0.27 = \sigma_{MLUU1\|McUU2}$, and use CR-1	0.243
M_C UU3	M_C Univ. of Utah (July 1962–Sept 1974)	5a	***Two-step:*** M_L UU1 = M_C UU3 ± 0.28 (see Griscom and Arabasz, 1979), where $0.28 = \sigma_{MLUU1\|McUU3}$, and use CR-1	0.249
M_L GS	M_L USGS (1974–2012), Utah Region (UTR)	6a	***Two-step:*** M_L UU1 = M_L GS – 0.11 and use CR-1	0.227
M_L GS	M_L USGS (1981–2012), Extended Border Region (EBR)	7a	***Two-step:*** M_L UU1 = M_L GS + 0.09 and use CR-1	0.224
m_b PDE1 > 3.5	m_b USGS/PDE (1991–2012), Extended Utah Region (UTREXT)	8a	$E[\mathbf{M}] = 0.974\ (m_b\ PDE1) + 0.036$	0.197
m_b PDE2 ≥ 3.5	m_b USGS/PDE (1978–1990)	9a	***Two-step:*** $M_{L,C}$ UU = 0.668 m_b PDE2 + 1.231 and use CR-1	0.320
m_b PDE3 3.3–5.0	m_b CGS/USGS/PDE (1963–1977)	10a	***Two-step:*** $M_{L,C}$ UU = 1.020 m_b PDE3 – 0.804 and use CR-1	0.378
m_b ISC	m_b ISC, Nsta ≥ 5 (1964–2012)	11a	$E[\mathbf{M}] = 1.037\ m_b\ ISC - 0.148$	0.283
ln(FA)	ln(FA), in km^2, where FA is the total felt area (1850–2012)	12a	$E[\mathbf{M}] = 0.647 + 0.345 \times \ln(FA) + 0.0018\ (FA)^{1/2}$	0.334
$I_0 \geq V$	Epicentral value of Modified Mercalli Intensity, MMI ≥ V (1850–2012)	13a	$E[\mathbf{M}] = 0.654\ I_0 + 0.922$	0.5[3]
$I_0 < V$	Epicentral value of MMI < V (1850–2012)	14a	$E[\mathbf{M}] = 0.349\ I_0 + 2.393$	0.5[3]

(continued on next page)

Size Measure		Conversion Relationship (CR)		$\sigma[\mathbf{M}\|X]$[1]
Notation	**Description and Applicable Period**	**ID**	**Relationship**	
A_{VII}	Extent of area shaken, in km^2, at or greater than MMI VII (1850–2012)	15a	$E[\mathbf{M}] = 1.591 \log_{10}(A_{VII}) + 0.896$	0.35
A_{VI}	Extent of area shaken, in km^2, at or greater than MMI VI (1850–2012)	16a	$E[\mathbf{M}] = 1.230 \log_{10}(A_{VI}) + 0.983$	0.35[4]
A_V	Extent of area shaken, in km^2, at or greater than MMI V (1850–2012)	17a	$E[\mathbf{M}] = 1.290 \log_{10}(A_V) - 0.088$	0.35[4]
A_{IV}	Extent of area shaken, in km^2, at or greater than MMI IV (1850–2012)	18a	$E[\mathbf{M}] = 1.295\log_{10}(A_{IV}) - 0.288$	0.35[4]

[1] Standard deviation of the normally distributed error in **M** when estimated from size measure X. Uncertainties in E[**M**] are adjusted for the variance in the observed values of **M**, $\mathbf{M}_{obs}$, used in the regression of $\mathbf{M}_{obs}$ versus X; uncertainties for two-step regressions account for propagation of uncertainties.

[2] The 1981 start date for M_L UU1 is based on Pechmann et al. (2007), but the value of 0.137 for $\sigma[\mathbf{M}|M_L$ UU1] is based mostly on M_L observations from multi-station digital data after 1996. Because M_L values in the University of Utah catalog from 1981 until the early 1990s are based on two stations (with an average standard error of 0.21 vs. 0.10 for later M_L UU1), a larger two-step uncertainty of 0.205 for $\sigma[\mathbf{M}|M_L$ UU1] should be applied to the UTR for 1981–1995 and to the EBR for 1981–1993.

[3] Adopted nominal value.

[4] Adopted generic value.

Addendum to CR-1a

For clarity, the instructions below make explicit how CR-1a for M_L Univ. of Utah would be applied by time period and by region, based on the information provided in footnote 2 above.

Size Measure		Conversion Relationship (CR)		$\sigma[\mathbf{M}\|X]$[1]
Notation	**Description and Applicable Period**	**ID**	**Relationship**	
M_L UU1	M_L Univ. of Utah (1996–2012), UTR	1a	$E[\mathbf{M}] = 0.769\ (M_L\ UU1) + 0.941$	0.137
M_L UU1$^{\#}$	M_L Univ. of Utah (1981–1995), UTR	1$^{\#}$a	***Two-step:*** M_L UU1 = M_L UU1$^{\#} \pm 0.21$, where $0.21 = \sigma_{MLUU1\|MLUU1\#}$, and use CR-1	0.205
M_L UU1	M_L Univ. of Utah (1994–2012), EBR	1a	$E[\mathbf{M}] = 0.769\ (M_L\ UU1) + 0.941$	0.137
M_L UU1$^{\#}$	M_L Univ. of Utah (1981–1993), EBR	1$^{\#}$a	***Two-step:*** M_L UU1 = M_L UU1$^{\#} \pm 0.21$, where $0.21 = \sigma_{MLUU1\|MLUU1\#}$, and use CR-1	0.205

Table E-10. *Regression statistics for general orthogonal regressions.*

ID	Y	X[1]	Slope (± 1 std. error)	Intercept (± 1 std. error)	N	Uncertainty[2] σ_y	Uncertainty[2] σ_x	η	$S_{y,x}$	σ [M|X][7]	R^2
1	**M**obs	ML UU1	0.791 ± 0.023	0.851 ± 0.096	65	0.05	0.07	0.51	0.1473	0.139	0.950
3	**M**obs	Mc UU1	0.929 ± 0.045	0.227 ± 0.188	63	0.05	0.10	0.25	0.2310	0.225	0.874
8	**M**obs	mb PDE1	1.078 ± 0.083	-0.427 ± 0.375	23	0.06	0.14[3]	0.18	0.2154	0.207	0.889
9	$M_{L,}$ Mc UU	mb PDE2	1.088 ± 0.307	-0.652 ± 1.380	21	0.14	0.14[3]	1.00	0.4292	n/a	0.402
10	$M_{L,}$ Mc UU	mb PDE3	1.697 ± 0.191	-3.557 ± 0.779	103	0.24	0.19[4]	1.60	0.5369	n/a	0.440
11	**M**obs	mb ISC	1.162 ± 0.151	-0.740 ± 0.720	13	0.08	0.10	0.64	0.3053	0.295	0.844
13	**M**obs	$I_0 \geq V$	0.764 ± 0.071	0.229 ± 0.459	24	0.13	0.50[5]	0.07	0.4474	*0.429*	0.841
14	**M**obs	$I_0 < V$	0.386 ± 0.009	2.126 ± 0.044	39	0.10	0.50[5]	0.04	0.3236	*0.308*	0.527[9]
15	**M**obs	$\log(A_{VII})$	1.619 ± 0.126	0.802 ± 0.429	6	0.18	0.18[6]	0.97	0.1406	*(0.141)*[8]	0.976
16	**M**obs	$\log(A_{VI})$	1.341 ± 0.203	0.535 ± 0.828	8	0.16	0.18[6]	0.83	0.3767	*0.339*	0.880
17	**M**obs	$\log(A_V)$	1.445 ± 0.226	-0.809 ± 1.057	9	0.16	0.18[6]	0.76	0.3896	*0.357*	0.855
18	**M**obs	$\log(A_{IV})$	1.306 ± 0.076	-0.345 ± 0.369	6	0.16	0.18[6]	0.81	0.1290	*(0.129)*[8]	0.987
12	**M**obs	ln(FA)	Model: $\mathbf{M} = c_0 + c_1 \ln(FA) + c_2\sqrt{FA}$		26	0.10	-----	-----	0.3535	0.339	
			$c_0 = 0.00$ (constrained to be non-negative) $c_1 = 0.415$ $c_2 = 0.0015$								

[1] X_{min} and X_{max} used in each regression are the same as for the counterpart least squares regression (with "a" appended to the ID) shown in table E-11.

[2] Unless noted otherwise, σ_y and σ_x are the average σ for the individual event magnitudes used in the regression.

[3] Estimated from uncertainties for tabulated event magnitudes of m_b ISC for events of comparable size during the same period; the estimate is supported by an independent one of 0.13 made for m_b PDE, 1978–2008, using a different approach (table E-6).

[4] Estimated by using the single-station σ of 0.38 for m_b ISC in the UTREXT (table E-5) divided by $\sqrt{4}$, where 4 is the average number of station measures reported for m_b PDE3 in the UTR during 1963–1977.

[5] Nominal value for the uncertainty in I_0.

[6] Nominal value for the uncertainty in $\log(A_{IV–VII})$.

[7] Calculated as $\sqrt{S_{y,x}{}^2 - \sigma_y{}^2}$; the italicized values are replaced in table E-8 by either a nominal value, in the case of I_0, or by a generic value, in the case of $\log(A_{IV–VII})$.

[8] Where $\sigma_y{}^2 \geq S_{y,x}{}^2$, the value of $S_{y,x}{}^2$ is shown in parentheses; as indicated above, the value is replaced by a generic value in table E-8.

[9] Constrained case.

Table E-11. *Regression statistics for least squares regressions.*

ID	Y	X	**Slope** (± 1 std. error)	**Intercept** (± 1 std. error)	N	X min, max	$S_{y,x}$	σ [M|X][1]	R^2
1a	**M**obs	ML UU1	0.769 ± 0.022	0.941 ± 0.093	65	2.87, 6.05	0.1462	0.137	0.950
3a	**M**obs	Mc UU1	0.838 ± 0.041	0.603 ± 0.170	63	2.91, 6.06	0.2220	0.216	0.874
8a	**M**obs	mb PDE1	0.974 ± 0.075	0.036 ± 0.339	23	3.6, 5.7	0.2063	0.197	0.889
9a	M_L, Mc UU	mb PDE2	0.668 ± 0.187	1.231 ± 0.845	21	3.5, 5.5	0.3817	n/a	0.402
10a	M_L, Mc UU	mb PDE3	1.020 ± 0.115	-0.804 ± 0.469	103	3.3, 5.0	0.4630	n/a	0.440
11a	**M**obs	mb ISC	1.037 ± 0.134	-0.148 ± 0.641	13	4.00, 5.82	0.2939	0.283	0.844
13a	**M**obs	$I_0 \geq$ V	0.654 ± 0.061	0.922 ± 0.394	24	5, 10	0.4175	*0.397*	0.841
14a	**M**obs	$I_0 <$ V	0.349 ± 0.054	2.393 ± 0.203	39	3, 5	0.2923	*0.275*	0.527
15a	**M**obs	log(A_{VII})	1.591 ± 0.124	0.896 ± 0.421	6	log(A_{VII}): 2.68, 4.01	0.1397	*(0.140)*[2]	0.976
16a	**M**obs	log(A_{VI})	1.230 ± 0.185	0.983 ± 0.757	8	log(A_{VI}): 2.49, 4.90	0.3658	*0.327*	0.880
17a	**M**obs	log(A_V)	1.290 ± 0.201	-0.088 ± 0.939	9	log(A_V): 3.32, 5.40	0.3740	*0.339*	0.855
18a	**M**obs	log(A_{IV})	1.295 ± 0.075	-0.288 ± 0.366	6	log(A_{IV}): 3.54, 5.91	0.1286	*(0.129)*[2]	0.987
12a	**Mobs**	ln(FA)	Model: **M** = c_0 + c_1 ln(FA) + $c_2\sqrt{FA}$		26	ln(FA): 8.24, 13.98	0.3484	0.334	
			c_0 = 0.647 ± 0.956 (± 1 std. error) c_1 = 0.345 ± 0.107 (± 1 std. error) c_2 = 0.0018 ± 0.0007 (± 1 std. error)						

[1] Calculated as $\sqrt{S_{y,x}{}^2 - \sigma_y{}^2}$, where $\sigma_y{}^2$ is the uncertainty in the Y values used in the regression, which is the same as that tabulated in table E-10 for the counterpart general orthogonal regression (whose ID is without an appended "a"); the italicized values are replaced in table E-9 by either a nominal value, in the case of I_0, or by a generic value, in the case of log($A_{IV\text{-}VII}$).

[2] Where $\sigma_y{}^2 \geq S_{y,x}{}^2$, the value of $S_{y,x}{}^2$ is shown in parentheses; as indicated above, the value is replaced by a generic value in table E-9.

Table E-12. *Measurements of A_{MMI} made with a GIS spatial analysis tool and used in either developing or applying magnitude conversion relationships for A_{IV} to A_{VII} (data for A_{MMI} not used for earthquakes after 1962).*

Date (UTC/GMT)	M[1]	Region	Area (km^2) A_{IV}	A_V	A_{VI}	A_{VII}	Source of Isoseismal Map
A_{MMI} used for developing CRs							
Mar. 12, 1934	**6.59**	Hansel Valley, Utah	144,360	66,500	24,060	4240	Hopper (2000)
Aug. 18, 1959	**7.35**	Hebgen Lake, Mont.	816,490	341,170	80,040	10,300	Stover and Coffman (1993)
Aug. 30, 1962	**5.75**	Cache Valley, Utah	----	80,820	6980	830	Hopper (2000)
Oct. 4, 1967	**5.08**	Marysvale, Utah	----	21,660	4900	480	Von Hake and Cloud (1969)
Oct. 1, 1972	**4.35**	Heber City, Utah	3500	2110	310	----	Hopper (2000)
Mar. 28, 1975	**6.02**	Pocatello Valley, Ida.	76,170	----	10,140	2020	Hopper (2000)
Oct. 28, 1983	**6.82**	Borah Peak, Ida.	----	252,000	52,370	5160	Stover and Coffman (1993)
Sept. 2, 1992	**5.50**	St. George, Utah	----	41,630	14,240	----	Olig (1995)
Feb. 3, 1994	**5.66**	Draney Peak, Ida.	48,740	18,350	1080[3]	----	M. Hopper, USGS[5]
Feb. 21, 2008	**5.91**	Wells, Nev.	72,630	31,980	----	----	dePolo and Pecoraro (2011)
A_{MMI} used in applying CRs, contributing to best-estimate moment magnitudes							
Aug. 1, 1900	*4.36*	Eureka, Utah	----	800	500	----	Hopper (2000)
Nov. 1, 1901	*6.63*	Sevier Valley, Utah	----	----	27,260	7250	Hopper (2000)
May 22, 1910	*5.28*	Salt Lake City, Utah	----	9780[2]	3560	240[4]	Hopper (2000)
May 13, 1914	*4.81*	Ogden, Utah	----	4580	820	160	Hopper (2000)
July 15, 1915	*4.34*	Provo, Utah	3,050	1590	660	----	Hopper (2000)
Sept. 29, 1921	*5.45*	Elsinore, Utah	----	----	----	400[6]	Hopper (2000)
Sept. 30, 1921	*4.42*	Elsinore, Utah	----	----	300[6]	----	Hopper (2000)
Oct. 1, 1921	*4.67*	Elsinore, Utah	----	----	300[6]	----	Hopper (2000)
Feb. 22, 1943	*4.24*	Salt Lake City, Utah	5,590	1870	580	----	Hopper (2000)
Feb. 13, 1958	*4.06*	Wallsburg, Utah	3,100	1240	690	----	Hopper (2000)
Sept. 5, 1962	*4.87*	Magna, Utah	----	5190	2090	----	Hopper (2000)
A_{MMI} measured but not used							
Aug. 16, 1966	*5.22*	Nevada-Utah border	----	15,700	----	----	Von Hake and Cloud (1968)
Mar. 9, 1978	*3.38*	Magna, Utah	2200	1140	230	----	Hopper (2000)
Feb. 20, 1981	*3.97*	Orem, Utah	2630	240	----	----	Hopper (2000)
Oct. 8, 1983	*3.92*	West Valley, Utah	5080	920	110	----	Hopper (2000)

[1] Bold values are $\mathbf{M}_{obs}$; italicized values, best-estimate moment magnitudes.

[2] Isoseismal contour completed by extrapolation.

[3] Area smaller than expected: outlier excluded in A_{VI} regression.

[4] Area imprecise.

[5] Isoseismal map for "Modified Mercalli Intensities for Earthquake near Afton, Wyoming, printed April 13, 2000" (M. Hopper, U.S. Geological Survey, written communication, June 2012).

[6] Estimated–but not measured with the GIS spatial analysis tool—using data on isoseismal maps of Hopper (2000).

Table E-13. *Magnitude types termed* ***M˜*** *assumed to be equivalent to* ***M****. These are miscellaneous magnitudes in the merged master catalog that are the sole magnitude available for the indicated number of earthquakes and for which there were inadequate data to develop conversion relationships to* ***M****.*

Mag. Code	Description	a.k.a. (or assumed equivalent)	No.	Mag. Range	Year of Events	Region (No. of Events)	σ	Basis for σ
MsGR	Gutenberg-Richter surface-wave magnitude	------	2	5.25, 5.5	1934	UTR (2)	0.30	Richter (1958) describes uncertainty of at least 0.25 mag. unit for original surface-wave magnitudes
MxJON	Wiechert magnitude at Reno (Jones, 1975)	MxSJG, MLREN	10	4.3–5.5	1917, 1934–1937, 1950	UTR (7), EBR (3)	0.37	Std. error determined by Jones (1975)
MLPAS	ML determined at Pasadena (before 1973)	Ukn PAS (2 events)	65	2.7–5.3,	1936–1967	UTR (19), EBR (46)	0.20	Std. error based on information in Felzer and Cao (2007)
MLBRK	ML determined at Berkeley (before 1973)	------	34	3.6–5.5	1966–1972	UTR (29), EBR (5)	0.20	Std. error based on information in Felzer and Cao (2007)
MLERD	ML determined by Dept. of Energy in Idaho Falls, Idaho	MLAEC, MLERL	4	2.8–3.7	1975–1977	UTR (1), EBR (3)	0.30	Typical single-station std. error for this time period
Ukn UU	Unknown magnitude attributed to Univ. of Utah	------	1	3.5	1962	UTR (1)	0.50	Large std. error assigned because of time period and unknown magnitude type
Miscellaneous Magnitudes Applicable to EBR Only								
MLREN	ML attributed to Nevada Seismological Lab in Reno, Nevada	MDREN (2 events)	39	2.3–4.5	1972–2012	EBR	0.15	Typical std. error for ML (outside California) for this time period
MLBUT	ML attributed to Montana Tech in Butte, Montana	MLMMT	8	2.6–3.6	1988–2011	EBR	0.15	Typical std. error for ML (outside California) for this time period
MDUSBR	MD attributed to U.S. Bureau of Reclamation	------	7	2.3–3.1	1999–2002	EBR	0.15	Typical std. error for this time period
MLPAS	ML determined at Pasadena (after 1972)	------	5	2.5–3.6	1973–2011	EBR	0.10	Std. error based on information in Felzer and Cao (2007)
MLTFO	ML attributed to TFO array in Arizona	------	3	3.8–3.9	1967	EBR	0.30	Typical single-station std. error for this time period
MfaWOO	Magnitude based on felt area estimated by Wood (1947)	------	2	5.0, 5.0	1934, 1940	EBR	0.50	Correlation of M with felt area is approximate and imprecise (see: Wood, 1947; Gutenberg and Richter, 1942)
UKN	Unknown magnitude	UKUKN	2	4.0, 4.0	1934	EBR	0.50	Large std. error assigned because of time period and unknown magnitude type
MLUBO	ML attributed to UBO array in Utah	------	1	4.2	1967	EBR	0.30	Typical single-station std. error for this time period
MLBRK	ML determined at Berkeley (after 1972)	------	1	4.1	1984	EBR	0.10	Std. error based on information in Felzer and Cao (2007)
UK UU	Unknown magnitude attributed to Univ. of Utah	------	1	4.3	1942	EBR	0.50	Large std. error assigned because of time period and unknown magnitude type

(continued on next page)

Mag. Code	Description	a.k.a. (or assumed equivalent)	No.	Mag. Range	Year (No.) of Events	Region (No.) of Events	σ	Basis for σ
UKXXX	Unknown magnitude	------	1	2.7	1966	EBR	0.50	Large std. error assigned because of time period and unknown magnitude type
UNR 1852	Magnitude attributed to Nevada Seismological Lab (abbreviation from Pancha and others, 2006)	------	1	4.9	1952	EBR	0.37	Std. error comparable to that for Wiechert magnitude at UNR for this early time period
ml DNA	Magnitude originating from DNAG catalog	------	1	4.0	1970	EBR	0.50	Large std. error assigned because of time period and unknown magnitude type

Breakdown of $M^{\sim}$ by Region and Event Type

	UTR	WGUEP	EBR
Mainshocks	13	2	76
Dependent Events	46	8	53
Total Number of Events	59	10	129

Table E-14. *Largest mainshocks in the Utah Region, **M** ≥ 4.85, 1850–September 2012.*

ID	Year	MoDay	Hr:Min (UTC/GMT)	Region[1]	M[2]	σ	Long W	Lat N	Depth[3] (km)	BEM Type[4]
1	1884	1110	08:50	*Paris, Idaho*	5.58	0.50	111.400	42.300	-----	Mpred|Io
2	1901	1114	04:39	Tushar Mountains	6.63	0.29	112.400	38.500	-----	Mpred|Xnon
3	1902	1117	19:50	Pine Valley	6.34	0.50	113.520	37.393	-----	Mpred|Io
4	1909	1006	02:41	*Hansel Valley*	5.58	0.50	112.700	41.800	-----	Mpred|Io
5	1910	0522	14:28	*Salt Lake City*	5.28	0.29	111.800	40.700	-----	Mpred|Xnon
6	1921	0929	14:12	Elsinore	5.45	0.29	112.150	38.683	-----	Mpred|Xnon
7	1934	0312	15:05	*Hansel Valley*	**6.59**	0.30	112.795	41.658	9	Mobs
8	1937	1119	00:50	*Idaho-Nevada-Utah tri-state area*	5.40	0.37	113.900	42.100	-----	M~|MxSJG
9	1950	0118	01:55	NW Uinta Basin	5.30	0.20	110.500	40.500	-----	M~|UknPAS
10	1959	0721	17:39	Arizona-Utah border	5.55	0.14	112.370	36.800	-----	Mpred|Xmix
11	1962	0830	13:35	*Cache Valley*	**5.75**	0.15	111.733	41.917	10	Mobs
12	1962	0905	16:04	*Magna*	4.87	0.12	112.089	40.715	7*	Mpred|Xmix
13	1963	0707	19:20	*Juab Valley*	**5.06**	0.15	111.909	39.533	4	Mobs
14	1966	0816	18:02	Nevada-Utah border	5.22	0.20	114.151	37.464	7*	Mpred|Xvar
15	1967	1004	10:20	Marysvale	**5.08**	0.15	112.157	38.543	14	Mobs
16	1975	0328	02:31	*Pocatello Valley, Idaho*	**6.02**	0.06	112.525	42.063	5	Mobs
17	1988	0814	20:03	*San Rafael Swell*	5.02	0.13	110.890	39.133	17	Mpred|Xvar
18	1989	0130	04:06	So. Wasatch Plateau	**5.20**	0.10	111.614	38.823	25	Mobs
19	1992	0902	10:26	St. George	**5.50**	0.10	113.506	37.105	15	Mobs

[1] Unless indicated otherwise, all epicenters are within Utah; italics indicate epicenters within the WGUEP Region.

[2] Bold values are observed moment magnitude, $\mathbf{M}_{obs}$; other values, best-estimate moment magnitudes.

[3] Listed only where there is instrumental focal-depth control; asterisk indicates restricted focal-depth.

[4] Best-estimate moment magnitudes, based either on $\mathbf{M}_{obs}$, $\mathbf{M}^{\sim}$ (a magnitude type assumed to be equivalent to **M**), or $\mathbf{M}_{pred}$ from magnitude conversion relationships. Xnon indicates best estimate from inverse-variance weighting of non-instrumental size measures; Xmix, from non-instrumental and instrumental size measures; Xvar, from instrumental size measures. See text for explanation of other details.

Table E-15. *Summary of declustering results by catalog domain.*

Number	UTREXT	UTR	WGUEP	EBR[1]
Total number of earthquakes	5388	2622	1157	2766
Number of mainshocks	2425	1554	660	871
Number of dependent events	2963	1068	497	1895
Number of mainshocks ≥ **M** 5.0	28	18	8	10

[1] Number in EBR = number in UTREXT – number in UTR

Table E-16. *Completeness periods for the WGUEP and Utah regions (BEM catalog, declustered).*

Magnitude Range	Range for Counts	Completeness Period, T_C Year (Start)[1]	Year (End)	t (years)
WGUEP Region, Magnitude 0.7 Bins				
$2.9 \le M < 3.6$	2.85–3.54	**1986**	2012.75	26.75
$3.6 \le M < 4.3$	3.55–4.24	**1979**	2012.75	33.75
$4.3 \le M < 5.0$	4.25–4.94	**1963**	2012.75	49.75
$5.0 \le M < 5.7$	4.95–5.64	***1908***	2012.75	104.75
$5.7 \le M < 6.4$	5.65–6.34	***1880***	2012.75	132.75
$6.4 \le M < 7.0$	6.35–7.04	*1850*	2012.75	162.75
WGUEP Region, Magnitude 0.5 Bins				
$3.0 \le M < 3.5$	2.95–3.44	**1986**	2012.75	26.75
$3.5 \le M < 4.0$	3.45–3.94	**1979**	2012.75	33.75
$4.0 \le M < 4.5$	3.95–4.44	**1963**	2012.75	49.75
$4.5 \le M < 5.0$	4.45–4.94	**1963**	2012.75	49.75
$5.0 \le M < 5.5$	4.95–5.44	***1908***	2012.75	104.75
$5.5 \le M < 6.0$	5.45–5.94	***1880***	2012.75	132.75
$6.0 \le M < 6.5$	5.95–6.44	*1850*	2012.75	162.75
$6.5 \le M < 7.0$	6.45–6.94	*1850*	2012.75	162.75
Utah Region (UTR), Magnitude 0.7 Bins				
$2.9 \le M < 3.6$	2.85–3.54	**1986**	2012.75	26.75
$3.6 \le M < 4.3$	3.55–4.24	**1986**	2012.75	26.75
$4.3 \le M < 5.0$	4.25–4.94	**1963**	2012.75	49.75
$5.0 \le M < 5.7$	4.95–5.64	***1908***	2012.75	104.75
$5.7 \le M < 6.4$	5.65–6.34	***1880***	2012.75	132.75
$6.4 \le M < 7.0$	6.35–7.04	*1860*	2012.75	152.75
Utah Region (UTR), Magnitude 0.5 Bins				
$3.0 \le M < 3.5$	2.95–3.44	**1986**	2012.75	26.75
$3.5 \le M < 4.0$	3.45–3.94	**1986**	2012.75	26.75
$4.0 \le M < 4.5$	3.95–4.44	**1967**	2012.75	45.75
$4.5 \le M < 5.0$	4.45–4.94	**1963**	2012.75	49.75
$5.0 \le M < 5.5$	4.95–5.44	***1908***	2012.75	104.75
$5.5 \le M < 6.0$	5.45–5.94	***1880***	2012.75	132.75
$6.0 \le M < 6.5$	5.95–6.44	*1880*	2012.75	132.75
$6.5 \le M < 7.0$	6.45–6.94	*1860*	2012.75	152.75

[1] For start dates of completeness periods, bold date was picked from a cumulative recurrence curve (CRC) for the WGUEP and/or the Utah regions; italicized date, based on other arguments; bold italicized date, based on CRC plus other arguments.

Table E-17. *Area of shaking of MMI IV or greater (A_{IV}) and approximate total felt area (FA) expected to be associated with earthquakes of **M** 4.95–6.45 (see figure E-25). Radii of equivalent circular areas are also listed.*

M	**A_{IV}**[1] (km^2)	**Equivalent Radius** (km)	**FA**[2] (km^2)	**Equivalent Radius** (km)
4.95	11,310	60	61,700	140
5.45	27,320	93	134,320	207
5.65	38,860	111	177,900	238
5.95	65,950	145	263,550	290
6.35	133,490	206	422,100	367
6.45	159,230	225	470,710	387

[1] Predicted from a general orthogonal regression of $\log(A_{IV})$ on $\mathbf{M}_{obs}$ using the data shown in figure E-16d for CR-18.

[2] Approximated by inverting conversion relationship CR-12 (table E-8).

Table E-18. *Data for seismicity rate calculations, WGUEP Region (BEM catalog, declustered).*

Magnitude Range	**Year (Start)**[1]	**Year (End)**	***t*** (years)	**No. of Earthquakes**	**Sum *N****[2]
$2.85 \leq$ **M** < 3.55	**1986**	2012.75	26.75	183	170.721
$3.55 \leq$ **M** < 4.25	**1979**	2012.75	33.75	39	37.553
$4.25 \leq$ **M** < 4.95	**1963**	2012.75	49.75	9	8.532
$4.95 \leq$ **M** < 5.65	***1908***	2012.75	104.75	4	3.158
$5.65 \leq$ **M** < 6.35	***1880***	2012.75	132.75	2	1.926
$6.35 \leq$ **M** < 7.00	*1850*	2012.75	162.75	1	0.769

[1] Bold date indicates pick from a cumulative recurrence curve (CRC); italicized date, based on other arguments; bold italicized date, based on CRC plus other arguments.

[2] Sum *N** is the sum of the equivalent number of earthquakes in the specified magnitude interval, corrected for magnitude uncertainty on an earthquake-by-earthquake basis.

Table E-19. *Data for seismicity rate calculations, Utah Region (BEM catalog, declustered, injection-induced earthquakes excluded).*

Magnitude Range	Year (Start)[1]	Year (End)	***t*** (years)	No. of Earthquakes	Sum ***N**** [2]
$2.85 \leq \mathbf{M} < 3.55$	**1986**	2012.75	26.75	428	397.518
$3.55 \leq \mathbf{M} < 4.25$	**1986**	2012.75	26.75	77	74.011
$4.25 \leq \mathbf{M} < 4.95$	**1963**	2012.75	49.75	18	16.942
$4.95 \leq \mathbf{M} < 5.65$	***1908***	2012.75	104.75	12	10.218
$5.65 \leq \mathbf{M} < 6.35$	***1880***	2012.75	132.75	3	2.407
$6.35 \leq \mathbf{M} < 7.00$	*1860*	2012.75	152.75	2	1.555

[1] Bold date indicates the start of the completeness period, T_C, based on a pick from a cumulative recurrence curve (CRC); italicized date, based on other arguments; bold italicized date, based on CRC plus other arguments.

[2] Sum N^* is the sum of the equivalent number of earthquakes in the specified magnitude interval, corrected for magnitude uncertainty on an earthquake-by-earthquake basis.

Table E-20. Cumulative rates of independent background earthquakes, WGUEP Region.

Magnitude Range	**Rate** (events/yr)	**90% Confidence Limits on Rate**	
		Lower (events/yr)	**Upper** (events/yr)
M ≥ 3.00	5.34	4.72	5.92
M ≥ 3.50	1.58	1.30	1.83
M ≥ 4.00	0.465	0.344	0.586
M ≥ 4.50	0.137	0.089	0.192
M ≥ 5.00	0.0402	0.0228	0.0606
M ≥ 5.50	0.0116	0.0058	0.0188
M ≥ 6.00	0.00322	0.00141	0.00552
M ≥ 6.50	0.000734	0.000289	0.001328

Table E-21. Cumulative rates of independent background earthquakes, Utah Region.

Magnitude Range	**Rate** (events/yr)	**90% Confidence Limits on Rate**	
		Lower (events/yr)	**Upper** (events/yr)
M ≥ 3.00	12.5	11.5	13.4
M ≥ 3.50	3.65	3.23	4.05
M ≥ 4.00	1.06	0.88	1.26
M ≥ 4.50	0.310	0.236	0.396
M ≥ 5.00	0.0900	0.0628	0.1227
M ≥ 5.50	0.0258	0.0166	0.0374
M ≥ 6.00	0.00706	0.00419	0.01086
M ≥ 6.50	0.00159	0.00088	0.00258

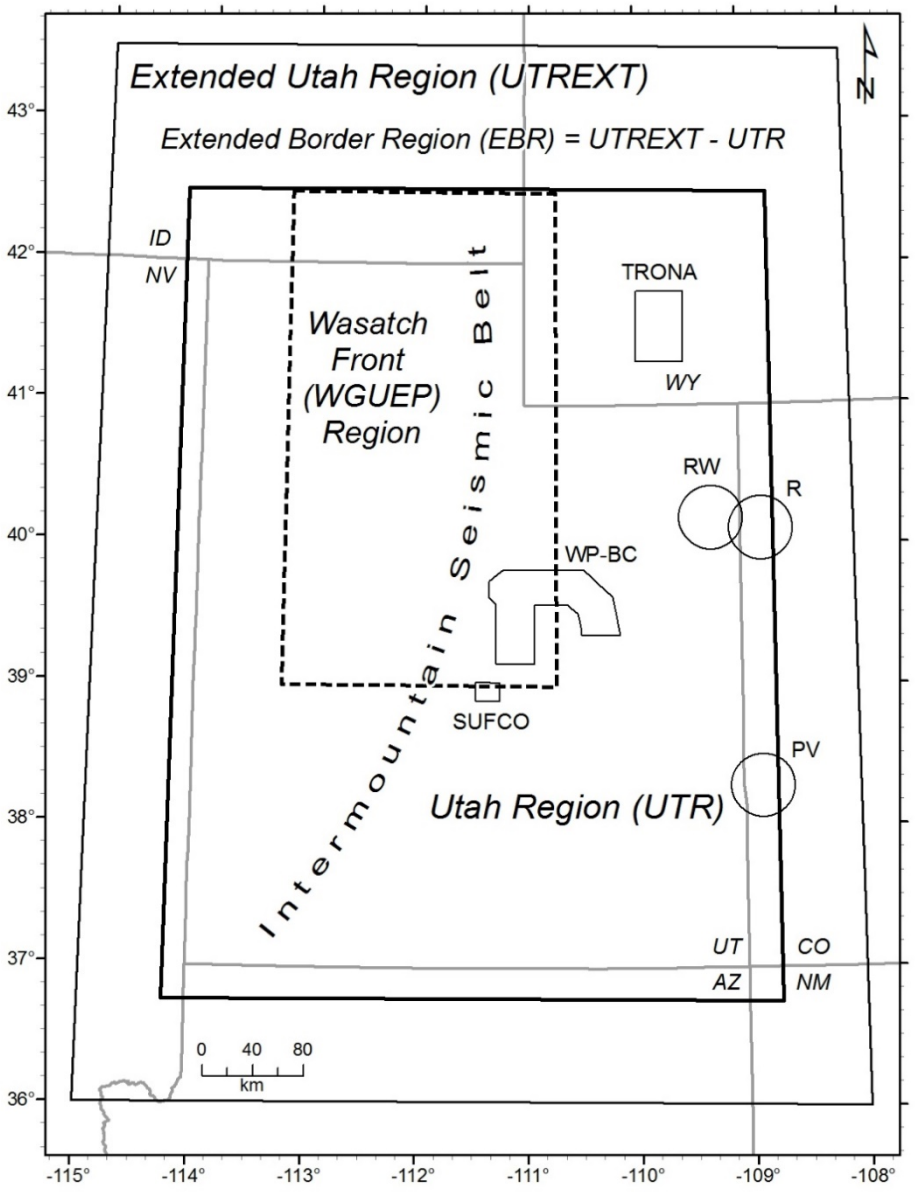

Figure E-1. *Location map. Boundaries of the major catalog domains (table E-1) are shown for the Extended Utah Region, the Utah Region, and the Wasatch Front (WGUEP) Region. Also shown are the outlines of areas demarcated for the removal of non-tectonic and human-triggered seismic events: PV = Paradox Valley, R = Rangely oil field, RW = Red Wash oil field, SUFCO = Southern Fuel Company coal-mining area, TRONA = trona mining district, WP-BC = Wasatch Plateau-Book Cliffs coal-mining region. The general location of the Intermountain Seismic Belt, which transects the study region, is also indicated.*

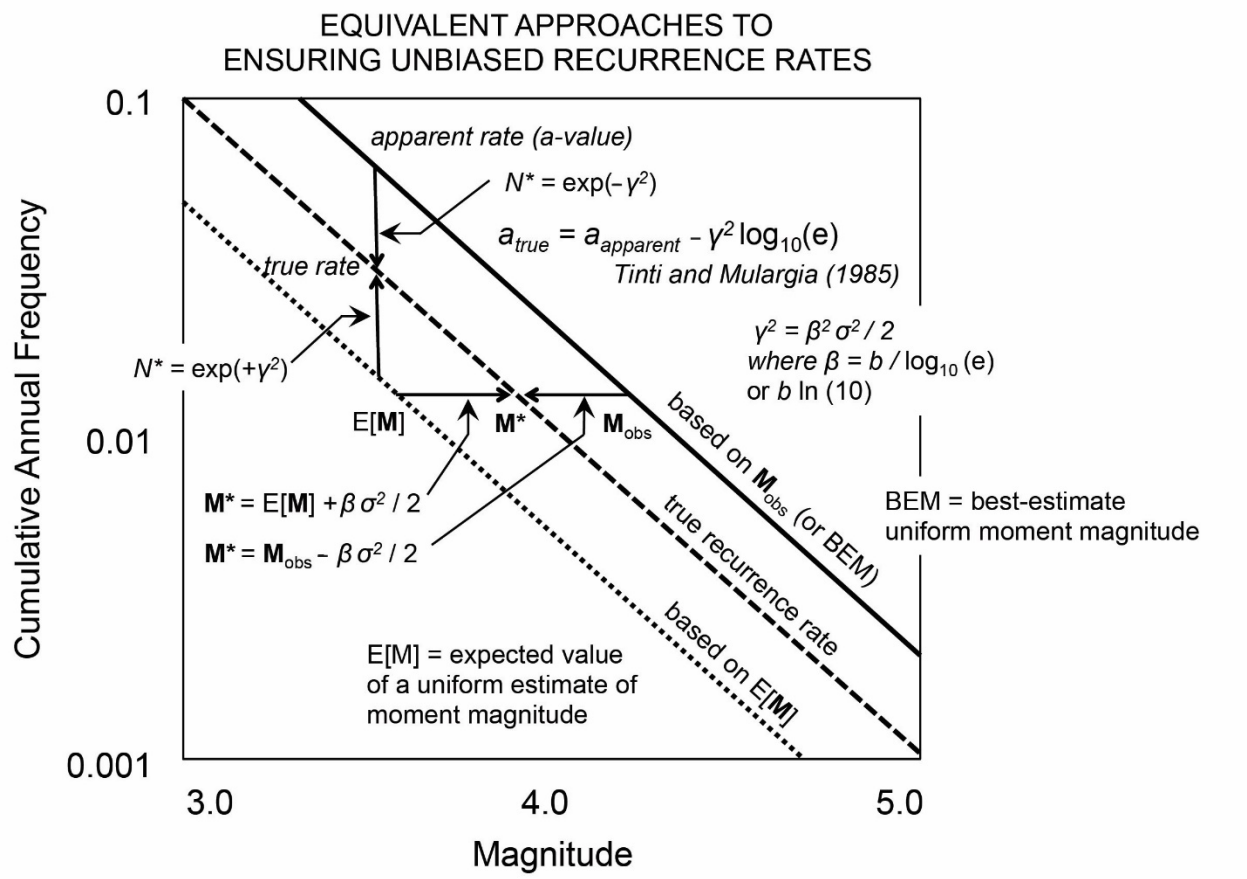

Figure E-2. *Schematic frequency-magnitude diagram showing how unbiased ("true") recurrence rates can be determined by making appropriate corrections in either the x-direction in terms of magnitude,* **M**, *or in the y-direction in terms of rate, expressed here as the cumulative annual rate, a, of earthquakes* ≥ **M**. *Adapted from EPRI/DOE/NRC (2012). N* as defined on the figure is the equivalent count assigned to an individual earthquake.*

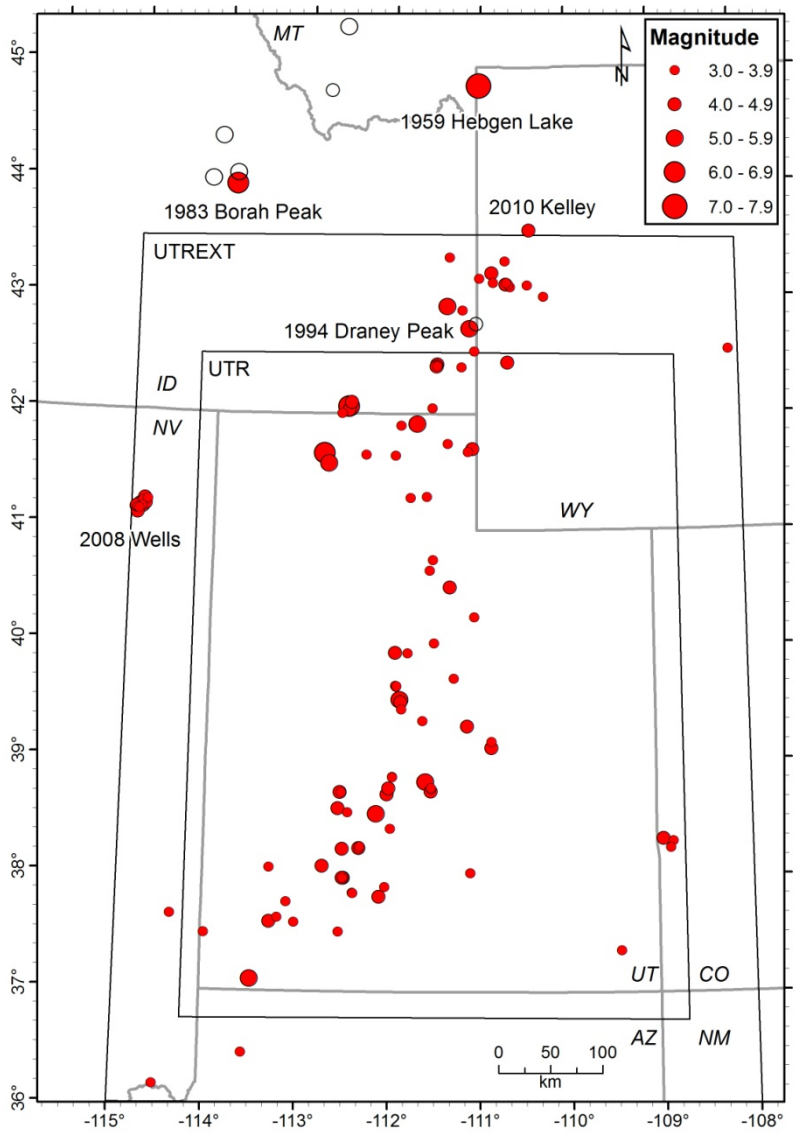

Figure E-3. *Map showing the locations of 114 earthquakes (red dots) for which reliable moment magnitudes were compiled for this study. Boundaries of the UTR and UTREXT as in figure E-1. Magnitudes for the five labeled earthquakes outside the UTR were used to augment data sets for some magnitude conversion relationships developed for the UTR. Data pairs used by Pechmann and Whidden (2013) for regressing* $\boldsymbol{M}_{obs}$ *on* M_L *UU and/or* M_C *UU included data from various earthquakes indicated by red dots plus data from six supplementary earthquakes whose locations are shown by uncolored circles.*

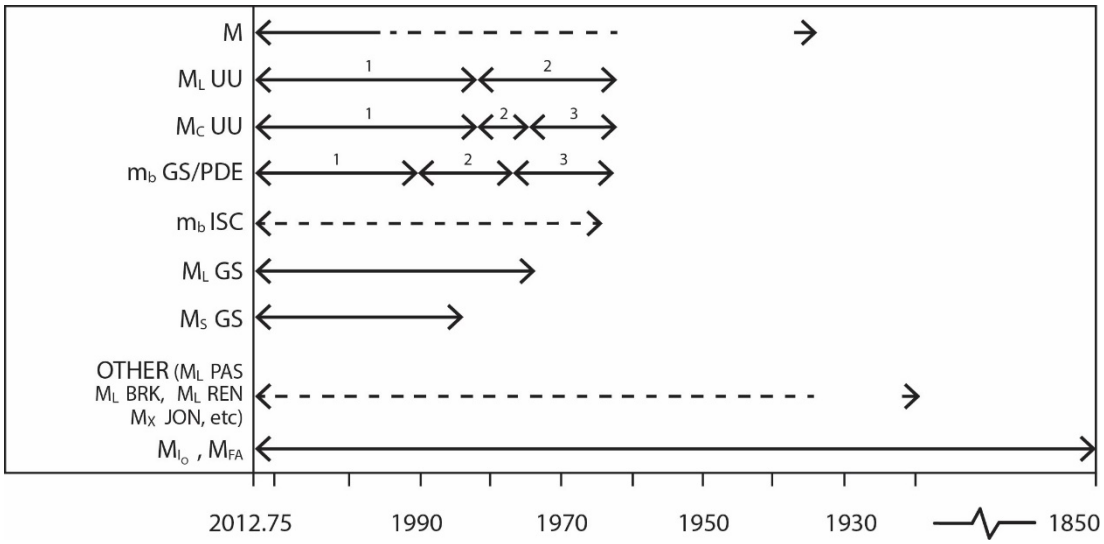

Figure E-4. *Overview of magnitude types reported in the merged source catalogs for the UTREXT. Segmented, numbered timeline for a given magnitude scale (keyed to notation in tables E-8 and E-9) implies time-varying changes in data and/or methods used by a particular agency. Dashed timeline indicates intermittent or sparse data.*

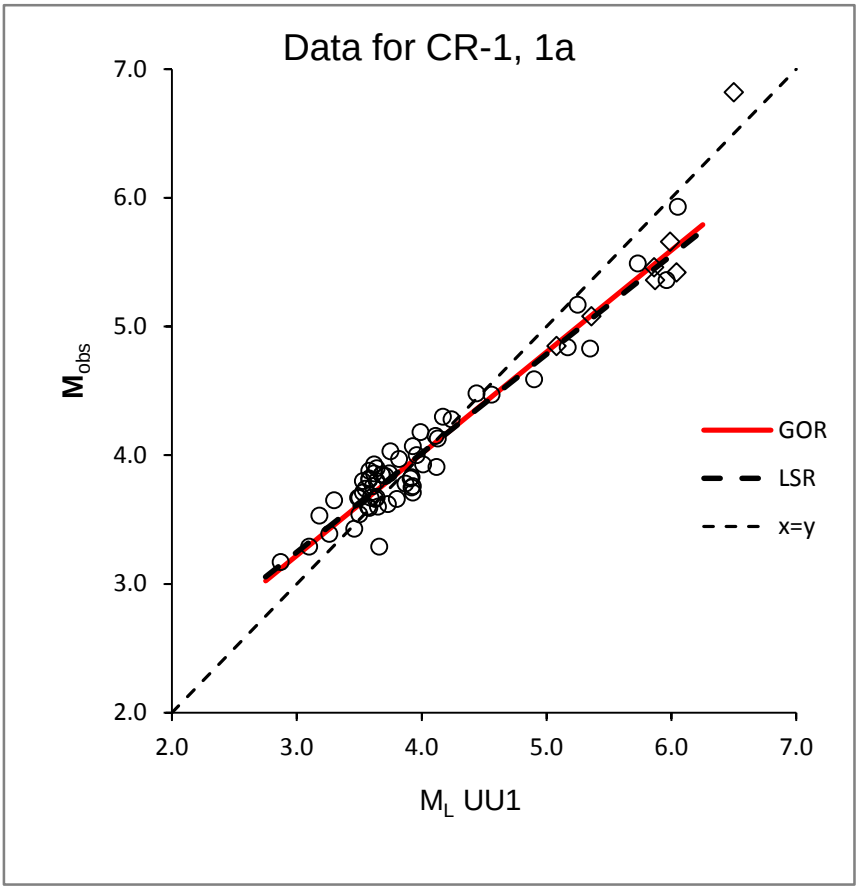

Figure E-5. *Data for general orthogonal regression (GOR) of* $\boldsymbol{M}_{obs}$ *on* M_L *UU1. Least squares regression (LSR) shown for comparison. Modified from original figure of Pechmann and Whidden (2013). Diamonds = non-UUSS* $\boldsymbol{M}_{obs}$*.*

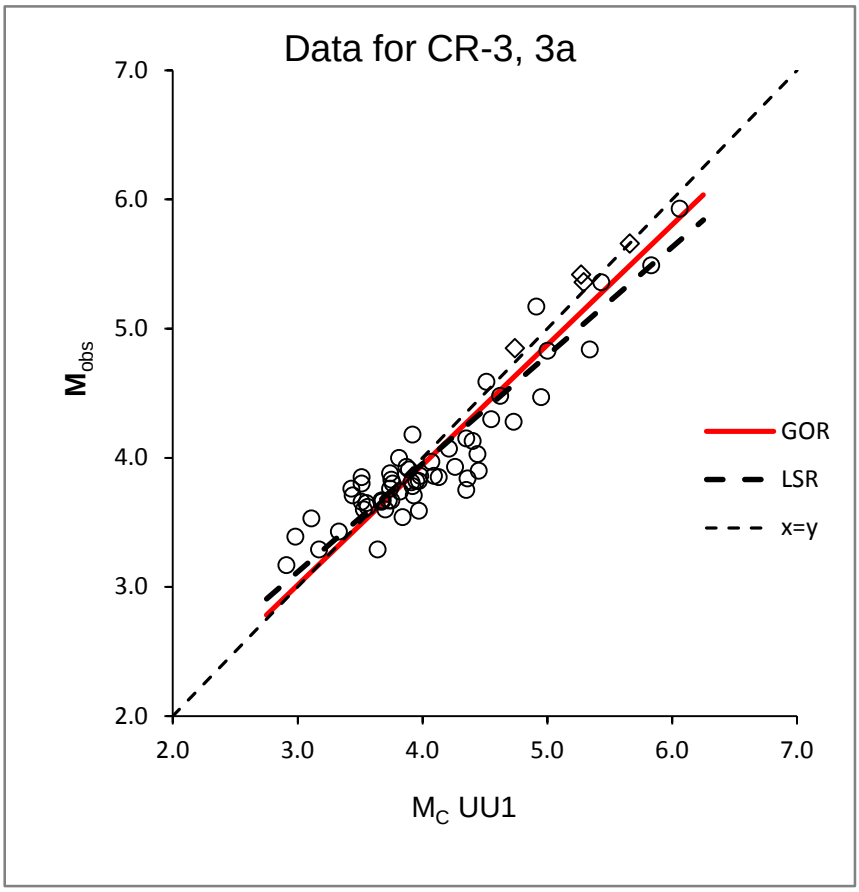

Figure E-6. *Data for general orthogonal regression (GOR) of* $\boldsymbol{M}_{obs}$ *on* M_C *UU1. Least squares regression (LSR) shown for comparison. Modified from original figure of Pechmann and Whidden (2013). Diamonds = non-UUSS* $\boldsymbol{M}_{obs}$.

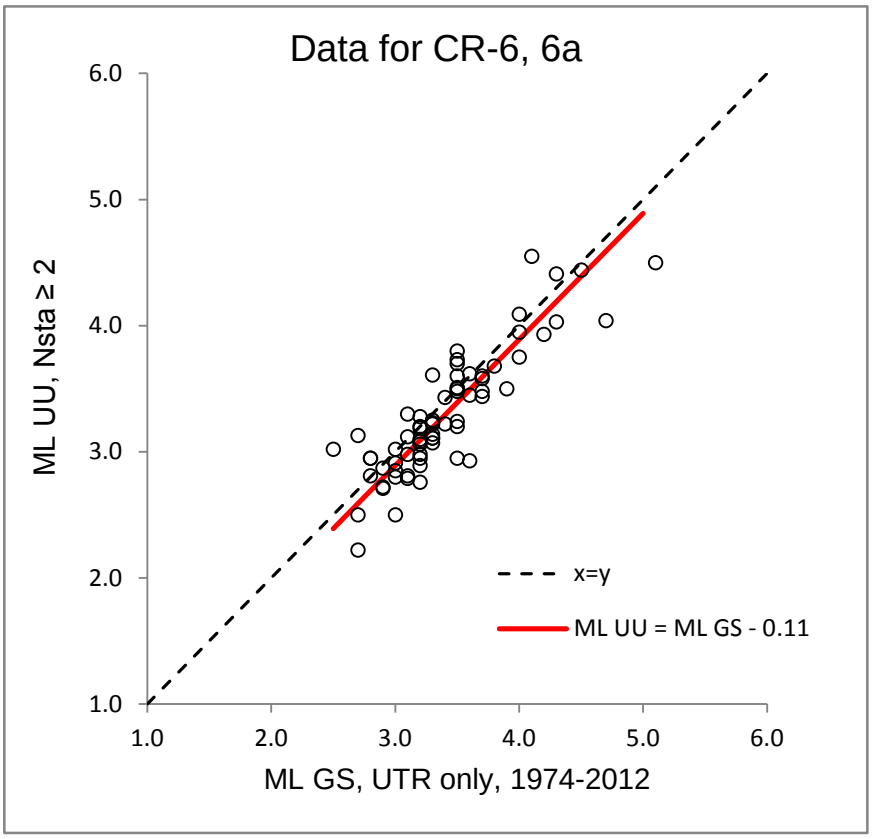

Figure E-7. *Data for the first step of conversion relationships CR-6 (and CR- 6a). Regression, assuming a slope of 1, of M_L UU on M_L GS in the UTR, 1974–2012. Red line shows the offset fit to the data.*

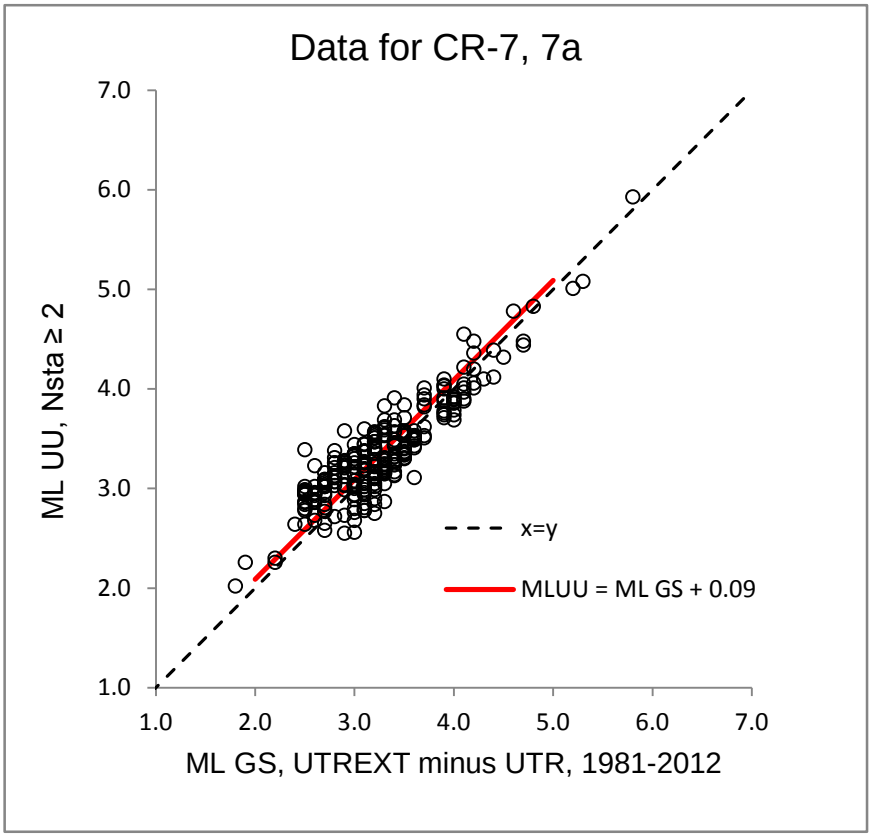

Figure E-8. *Data for the first step of conversion relationship CR-7 (and CR-7a). Regression, assuming a slope of 1, of M_L UU on M_L GS for the Extended Border Region (UTREXT minus UTR), 1981–2012. Red line shows the offset fit to the data.*

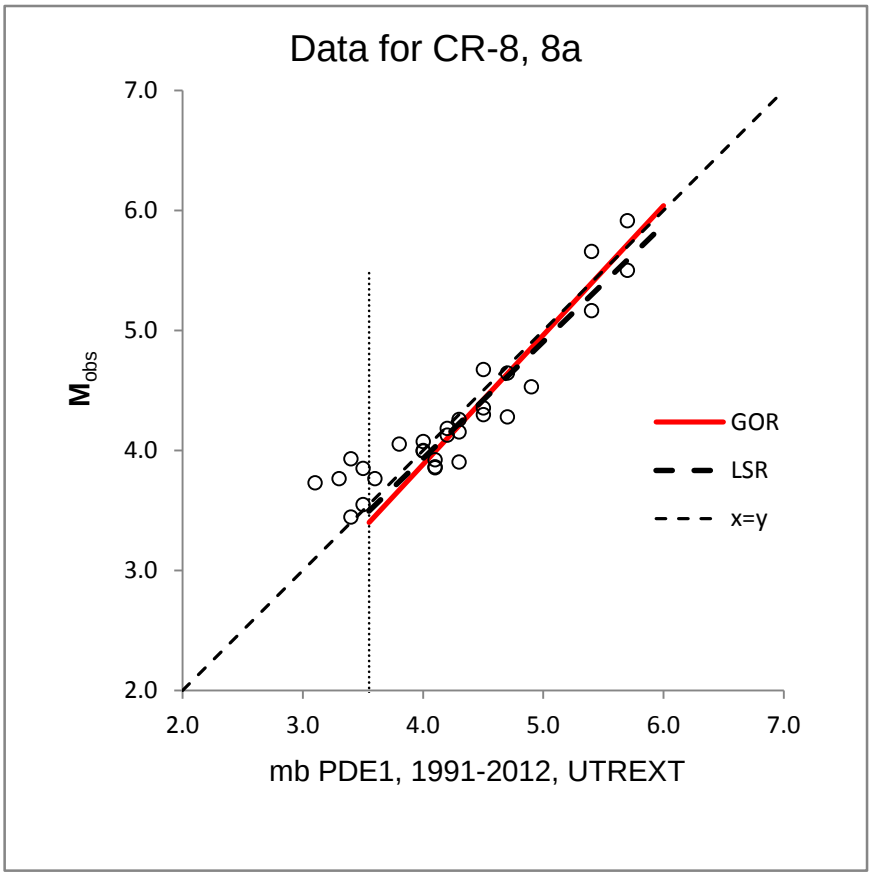

Figure E-9. *Data for general orthogonal regression (GOR) of* $\mathbf{M}_{obs}$ *on* m_b *PDE1 > 3.5 in the UTREXT, 1991–2012. Least squares regression (LSR) shown for comparison.*

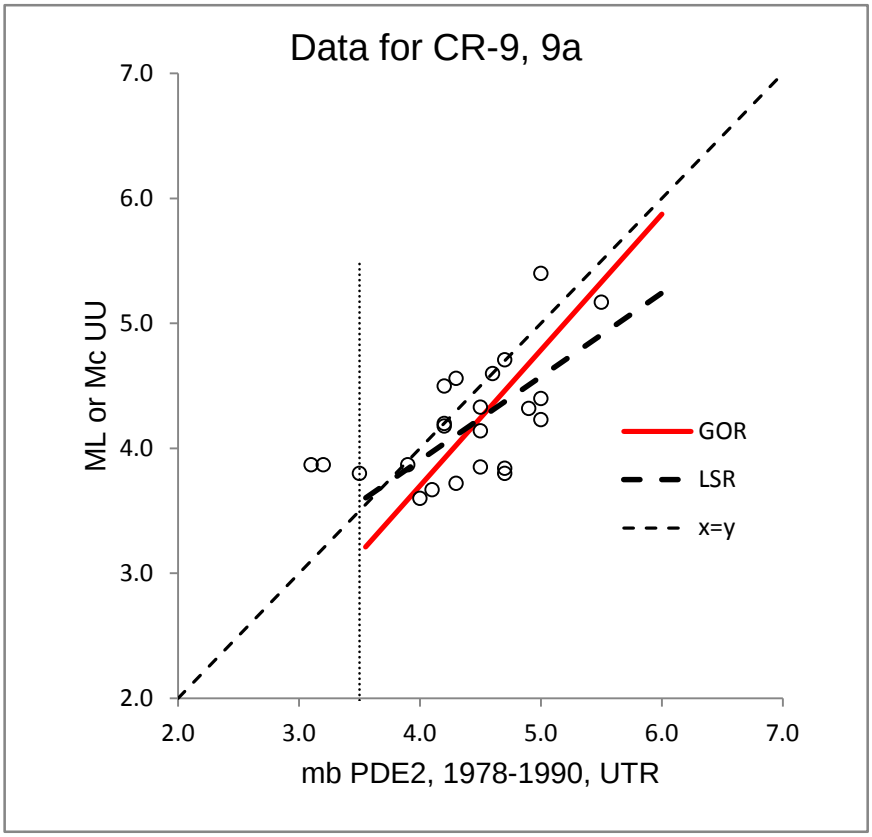

Figure E-10. *Data for the first step of conversion relationship CR-9 (and CR-9a). General orthogonal regression (GOR) of M_L or M_C UU on m_b PDE2 ≥ 3.5 in the UTR, 1978–1990. Least squares regression (LSR) shown for comparison.*

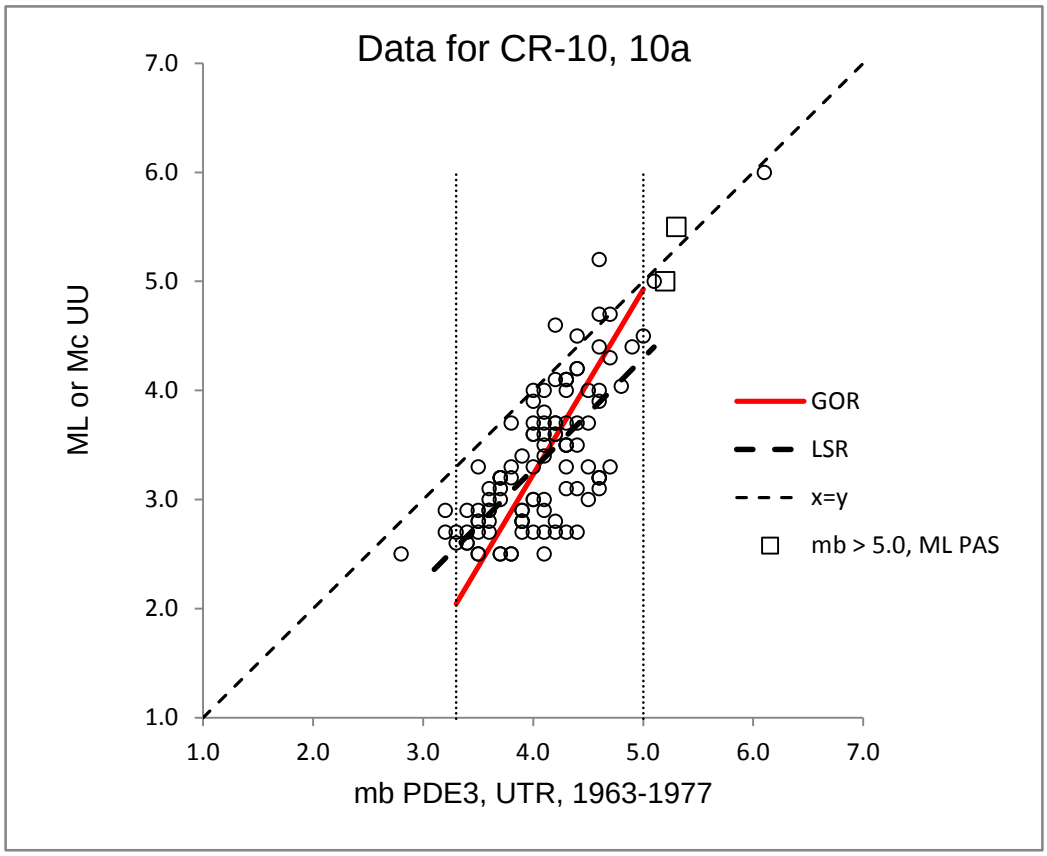

Figure E-11. *Data for the first step of conversion relationship CR-10 (and CR-10a). General orthogonal regression (GOR) of M_L or M_C UU on m_b PDE3 (3.3–5.0) in the UTR, 1963–1977. Least squares regression (LSR) shown for comparison. Squares indicate two earthquakes larger than m_b 5.0 for which the plotted y-value is an M_L from Pasadena.*

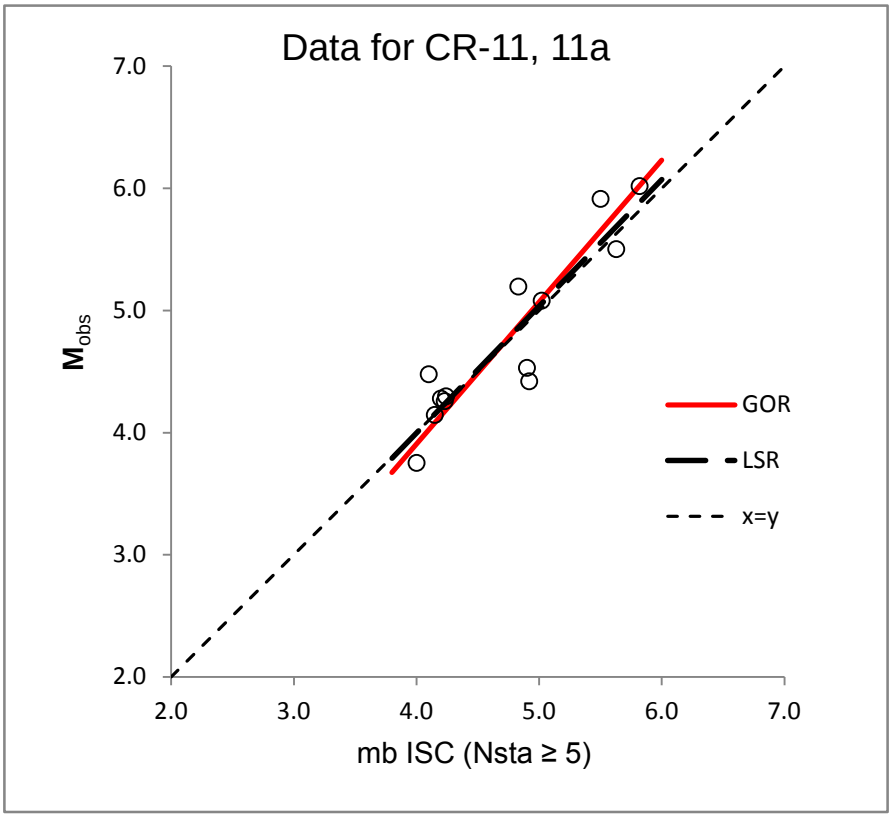

Figure E-12. *Data for general orthogonal regression (GOR) of* $\boldsymbol{M}_{obs}$ *on* m_b *ISC computed from five or more stations. Least squares regression (LSR) shown for comparison.*

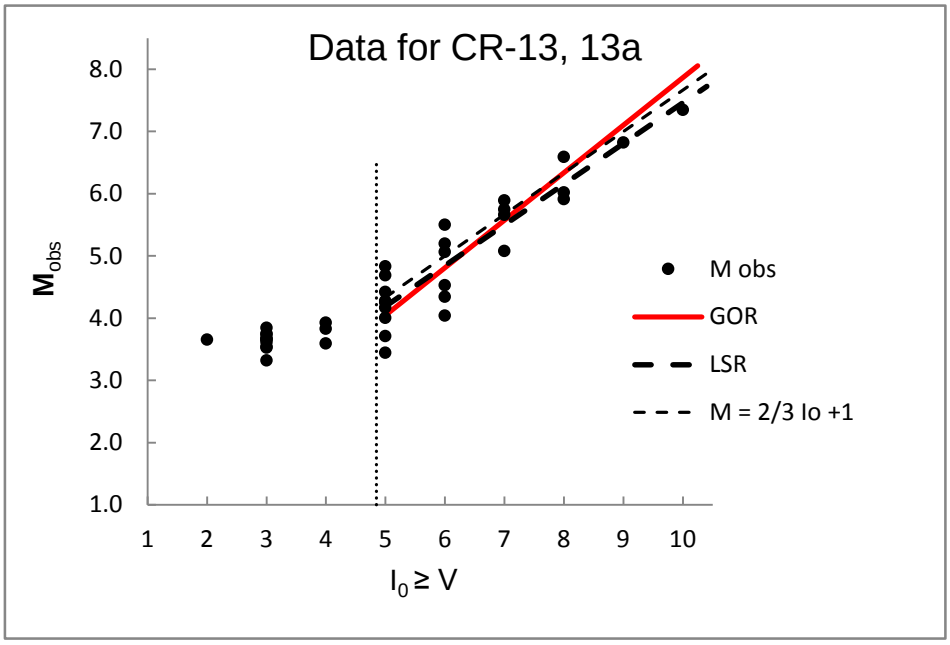

Figure E-13. *Data for conversion relationships CR-13 and CR-13a. Regression of* $\boldsymbol{M}_{obs}$ *on* $I_0 \geq V$. *GOR = general orthogonal regression, LSR = least squares regression. Also shown for reference is Gutenberg and Richter's (1956) relationship,* $M = 2/3\ I_0 + 1$.

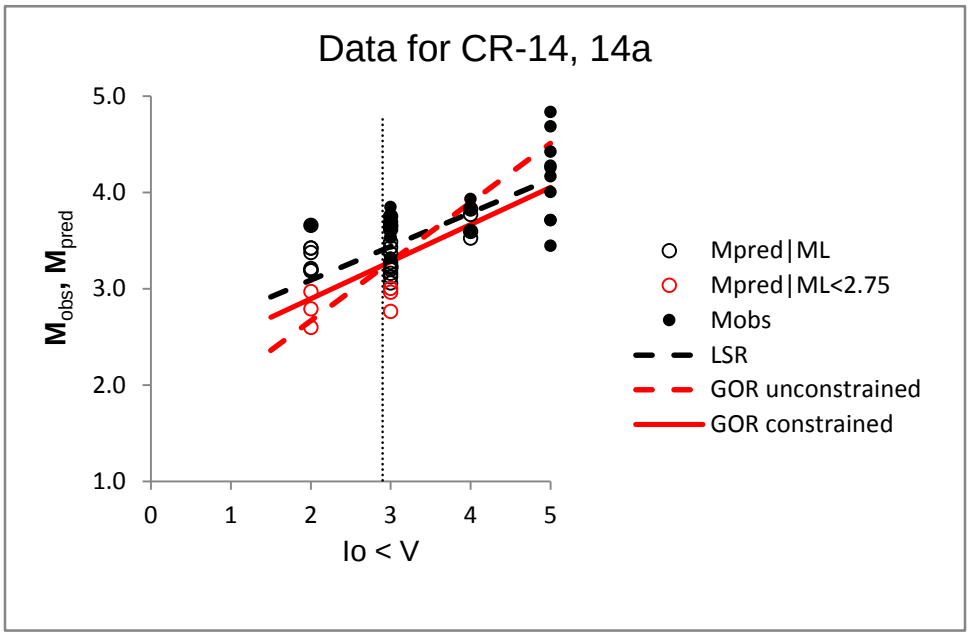

Figure E-14. *Data for provisional conversion relationships CR-14 and CR-14a for $I_o < V$. Regression of $\boldsymbol{M}_{obs}$ and $\boldsymbol{M}_{pred}$ on $I_0 \leq 5$. The regressions exclude data below $I_0 = 3$ and also data based on $\boldsymbol{M}_{pred}|M_L < 2.75$ (red circles); the latter data and the extrapolation of regression lines below $I_0 = 3$ are shown for illustration only. GOR = general orthogonal regression, LSR = least squares regression. The regression for "GOR constrained" was constrained to pass through the same $\boldsymbol{M}_{pred}$ value for $I_0 = 5$ as that for CR-13 for $I_o \geq V$.*

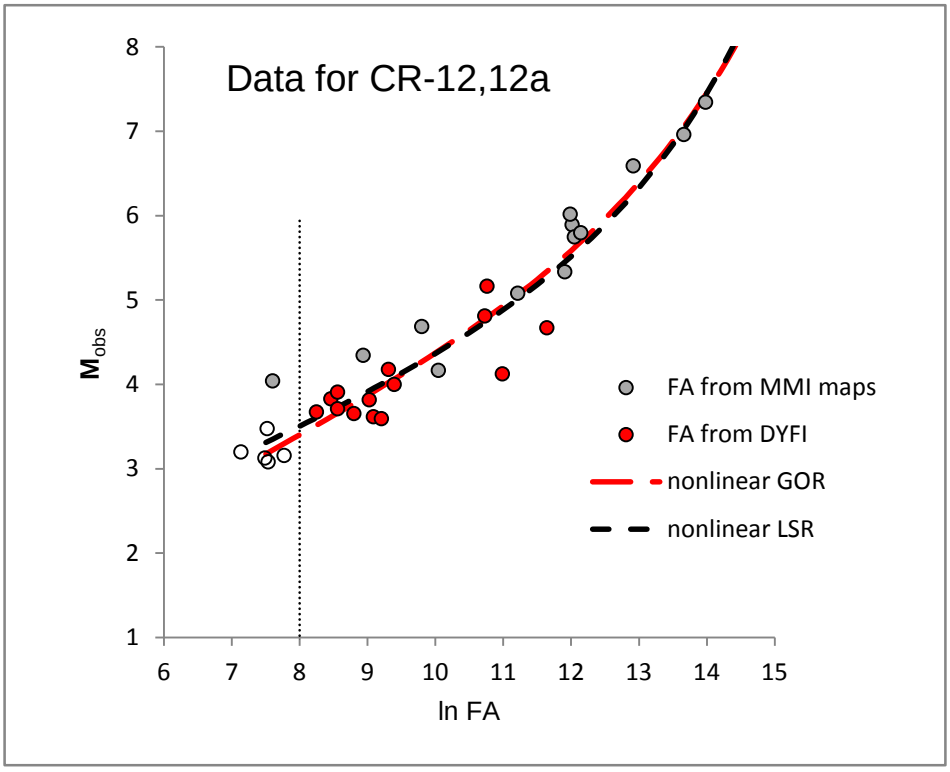

Figure E-15. *Data for conversion relationships CR-12 and CR-12a. Regression of* $\boldsymbol{M}_{obs}$ *on ln(FA) > 8, where FA is in km*^{2}*. GOR = general orthogonal regression, LSR = least squares regression, MMI = Modified Mercalli Intensity, DYFI = Did You Feel It. Data points below ln(FA) = 8 (dotted line) were not used in the regressions and are shown for illustration only; for the open circles, ln(FA) is from DYFI data and the y-value is* $\boldsymbol{M}_{pred}$ *from* M_L *UU using CR-1.*

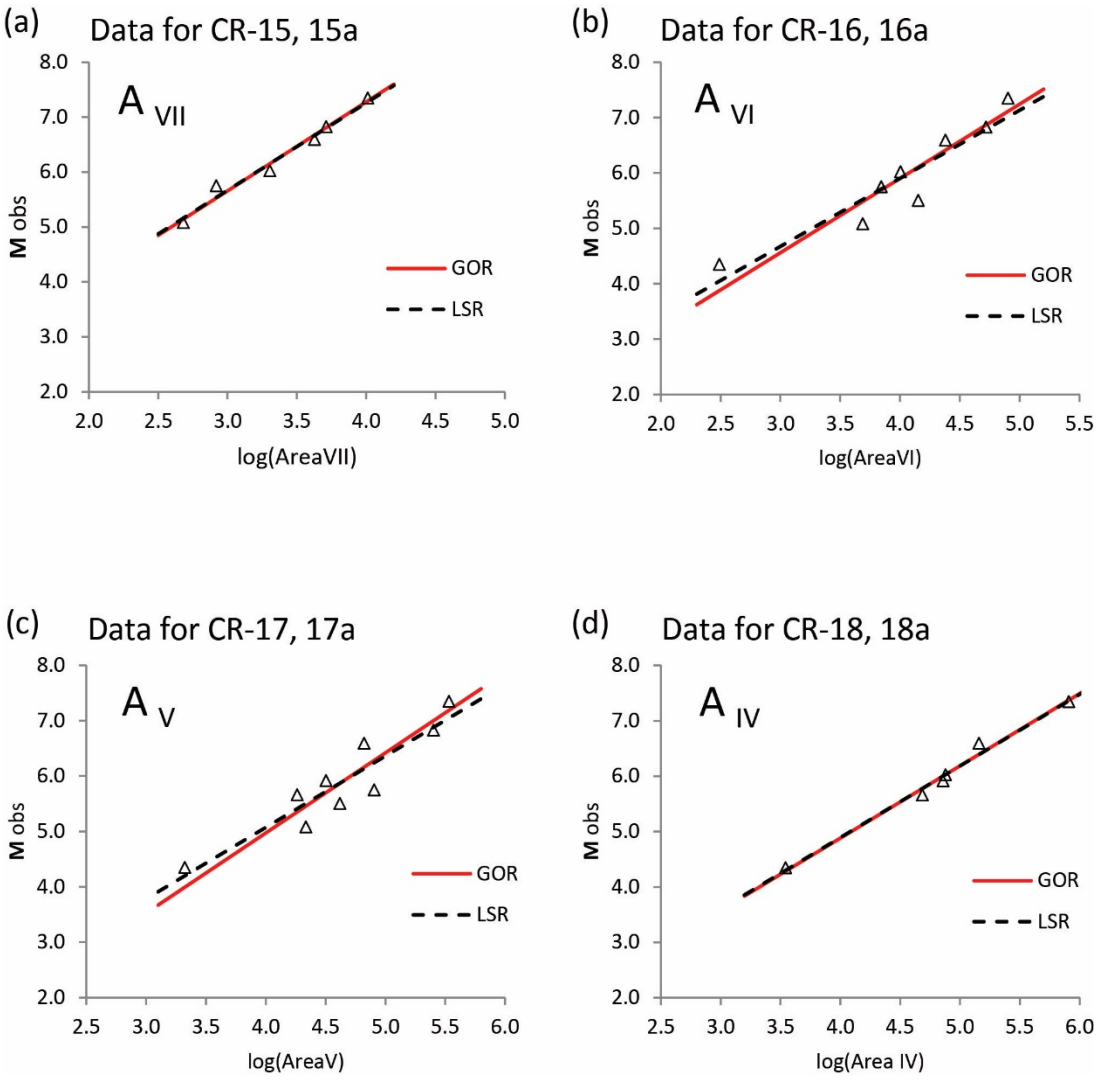

Figure E-16. *Data from general orthogonal regression (GOR) of $\mathbf{M}_{obs}$ on the logarithm of the extent of area shaken, in km^2, at or greater than MMI IV (A_{IV}) to MMI VII (A_{VII}). Least squares regression (LSR) shown for comparison.*

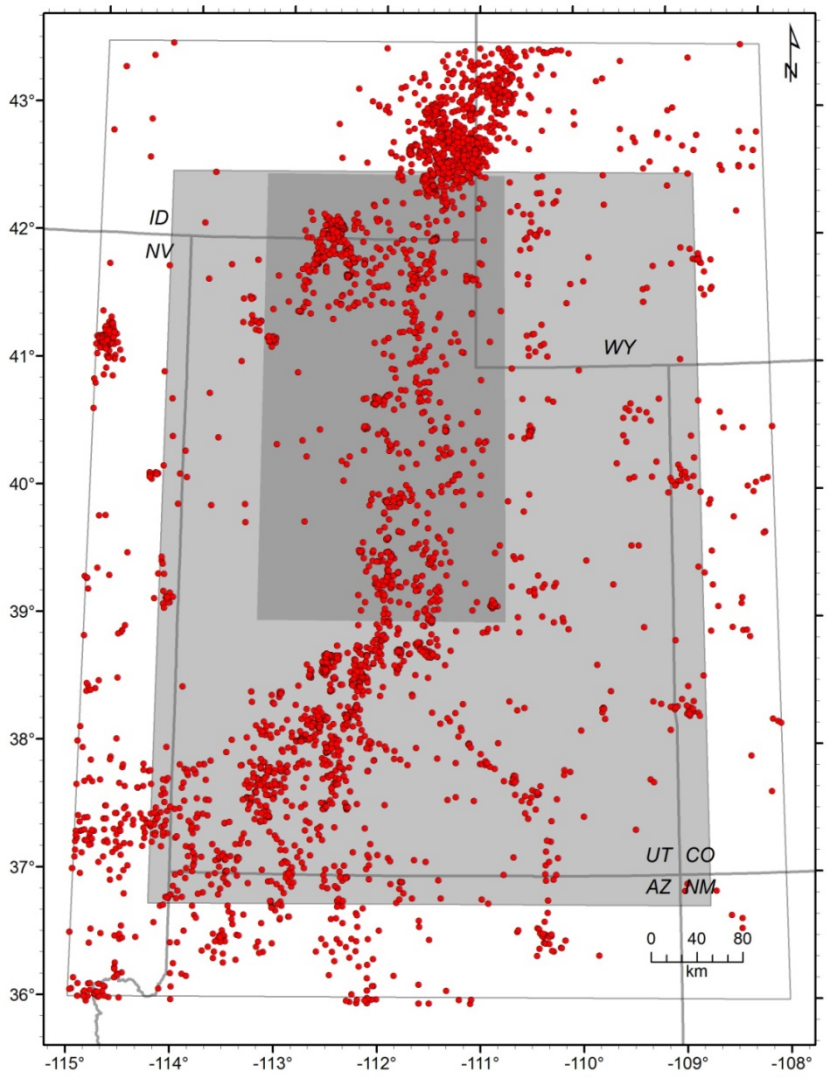

Figure E-17. *Epicenter map of all earthquakes (clustered) in the BEM catalog, 1850 through September 2012, for the entire Extended Utah Region. The WGUEP and Utah regions are shaded in darker and lighter gray, respectively.*

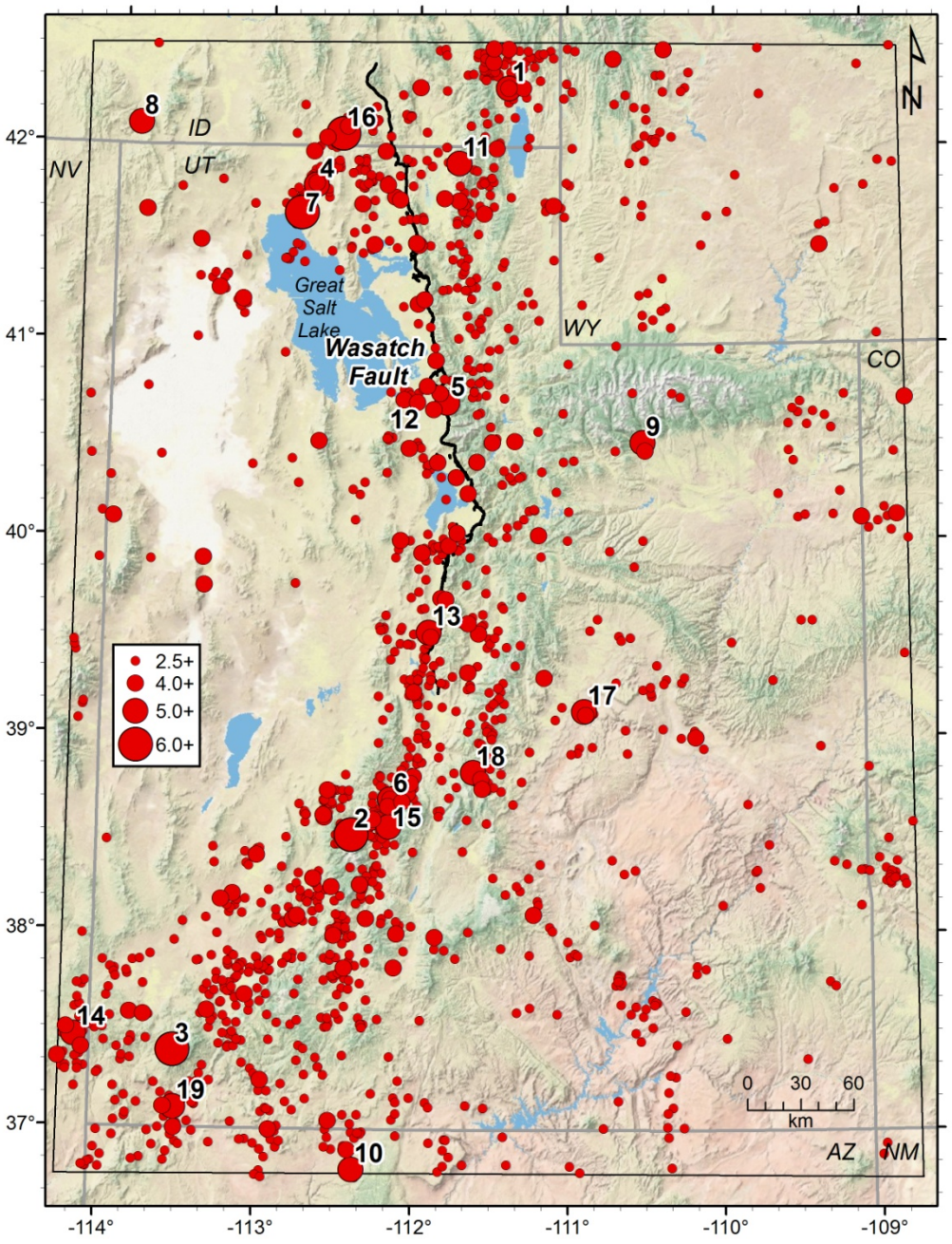

Figure E-18. *Epicenter map of independent mainshocks in the Utah Region, 1850 through September 2012 (BEM catalog, declustered). Epicenters scaled by magnitude. Numbered epicenters (keyed to table E-14) are for earthquakes with* $\boldsymbol{M} \geq 4.85$*. Wasatch fault shown for reference.*

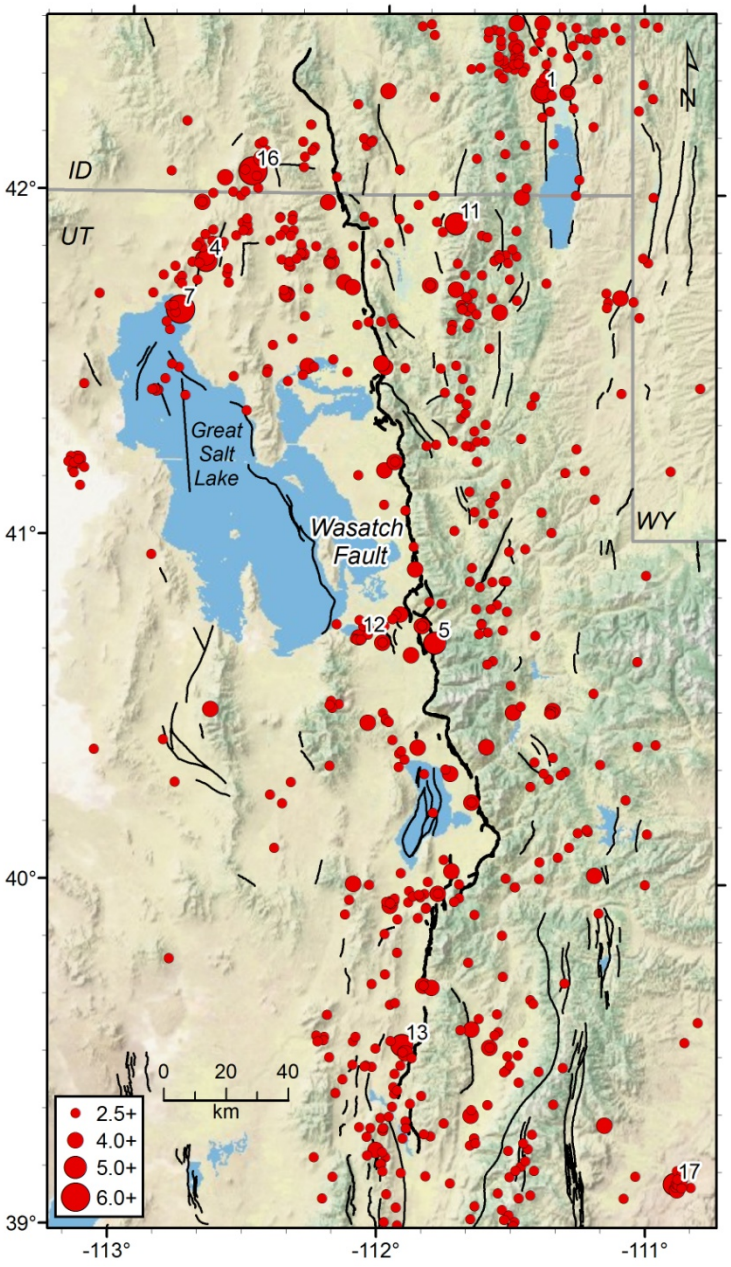

Figure E-19. *Epicenter map of independent mainshocks in the WGUEP Region, 1850 through September 2012 (BEM catalog, declustered). Epicenters scaled by magnitude. Numbered epicenters (keyed to table E-14) are for earthquakes of $M \geq 4.85$). Quaternary faults, after Black and others (2003), shown for reference; Wasatch fault bolded.*

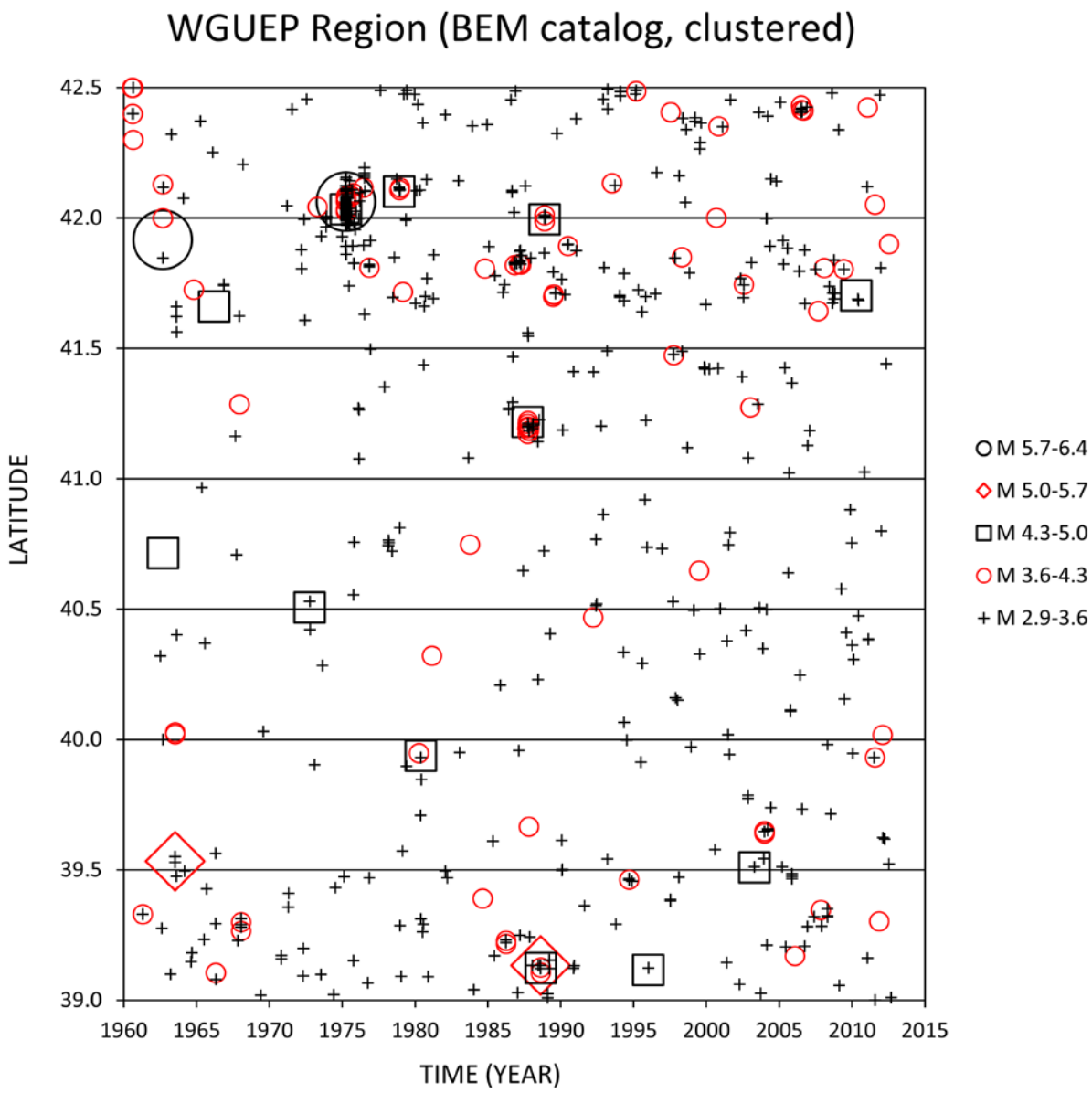

Figure E-20. *Space-time diagram (latitude vs. time since 1960) showing the distribution of earthquakes in the WGUEP Region of* $\boldsymbol{M} \geq 2.9$ *(2.85), differentiated by magnitude bins, for the clustered version of the BEM catalog.*

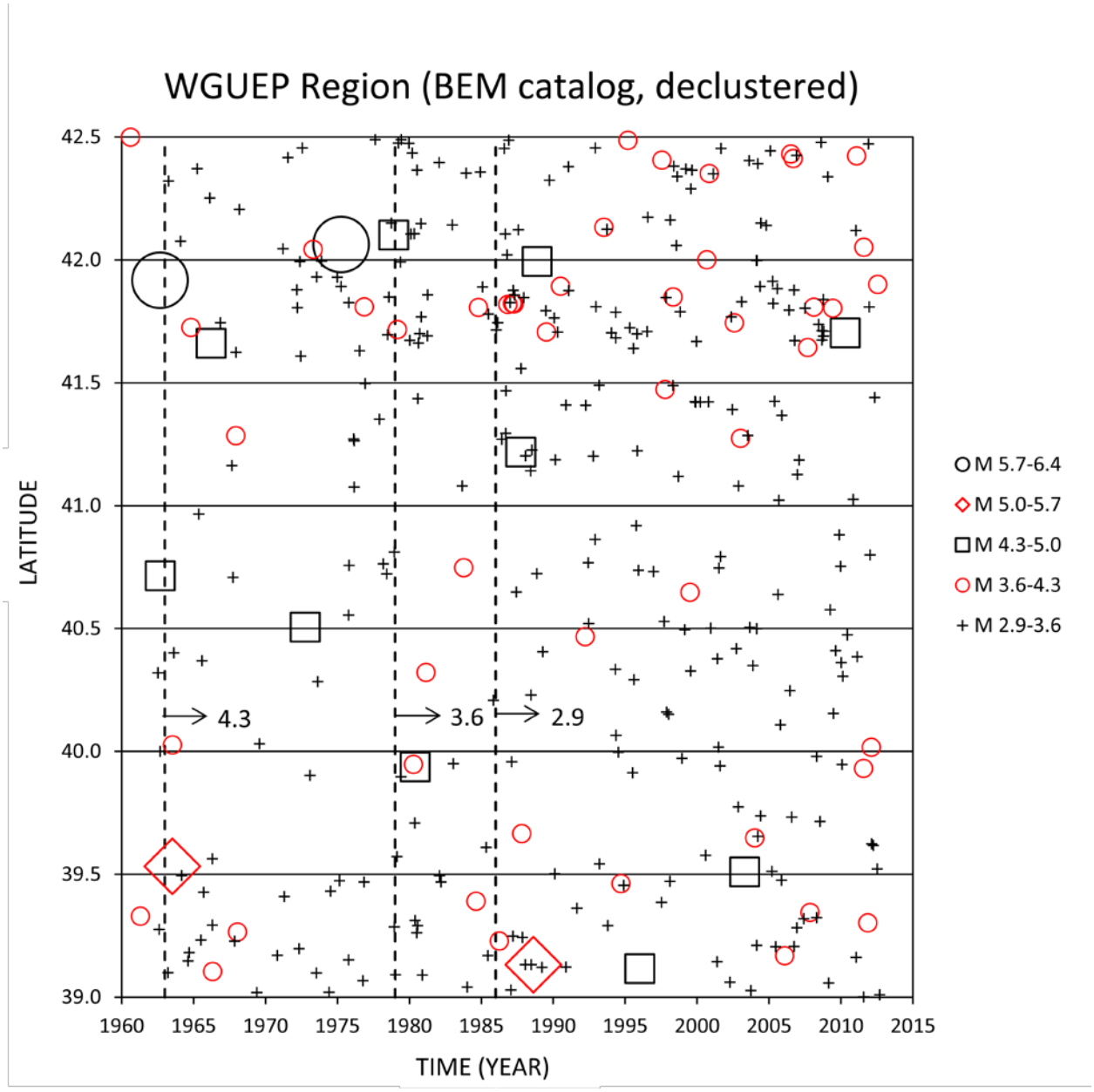

Figure E-21. *Space-time diagram (latitude vs. time since 1960) showing the distribution of mainshocks in the WGUEP Region of* $\mathbf{M} \geq 2.9$ *(2.85), differentiated by magnitude bins, for the declustered version of the BEM catalog. Vertical dashed lines indicate the start of completeness periods for* $\mathbf{M} \geq 4.3$ *(1963),* $\mathbf{M} \geq 3.6$ *(1979), and* $\mathbf{M} \geq 2.9$ *(1986).*

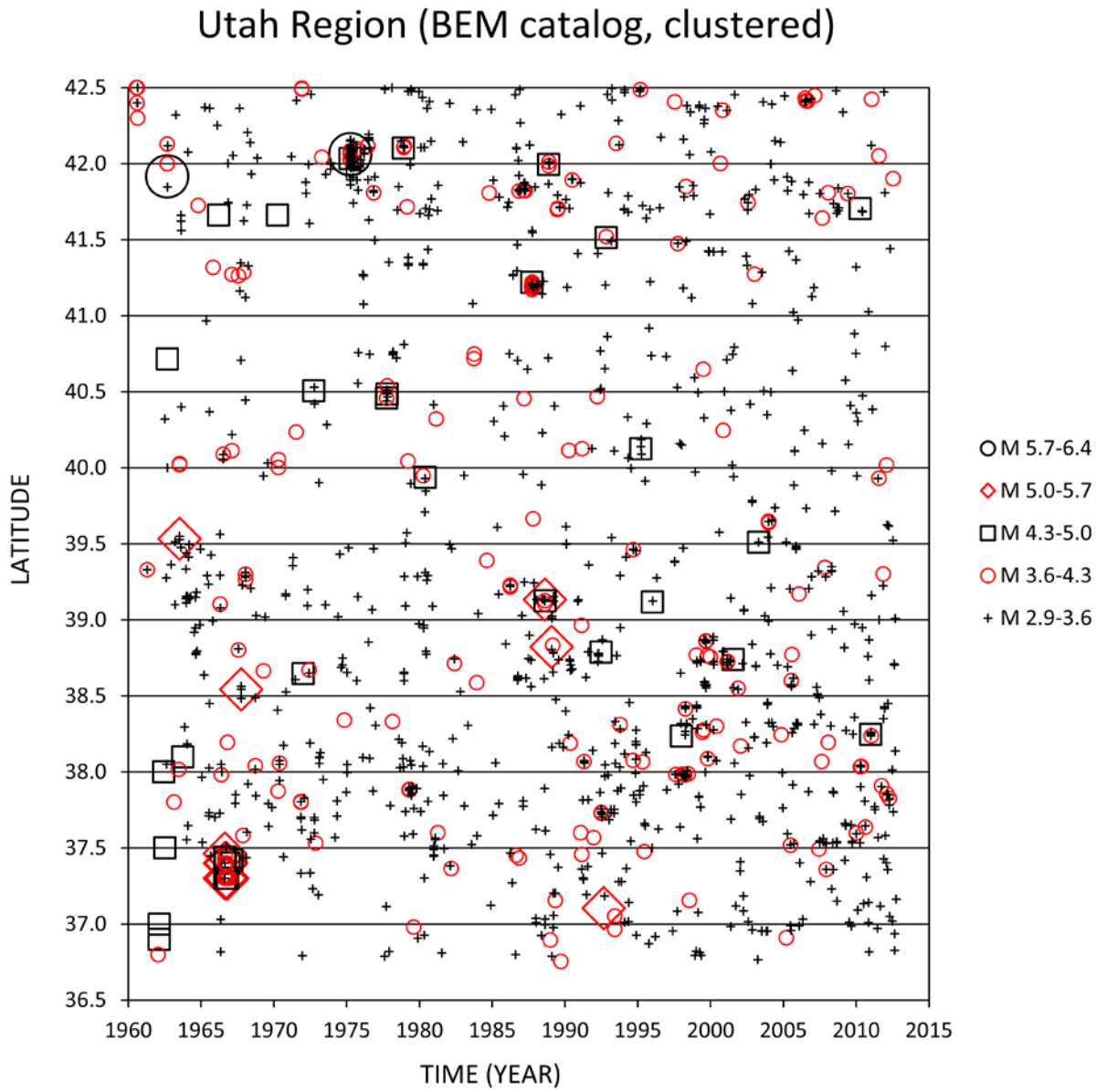

Figure E-22. *Space-time diagram (latitude vs. time since 1960) showing the distribution of earthquakes in the Utah Region of* $\boldsymbol{M} \geq 2.9$ *(2.85), differentiated by magnitude bins, for the clustered version of the BEM catalog. Injection-induced earthquakes (table E-4) are excluded.*

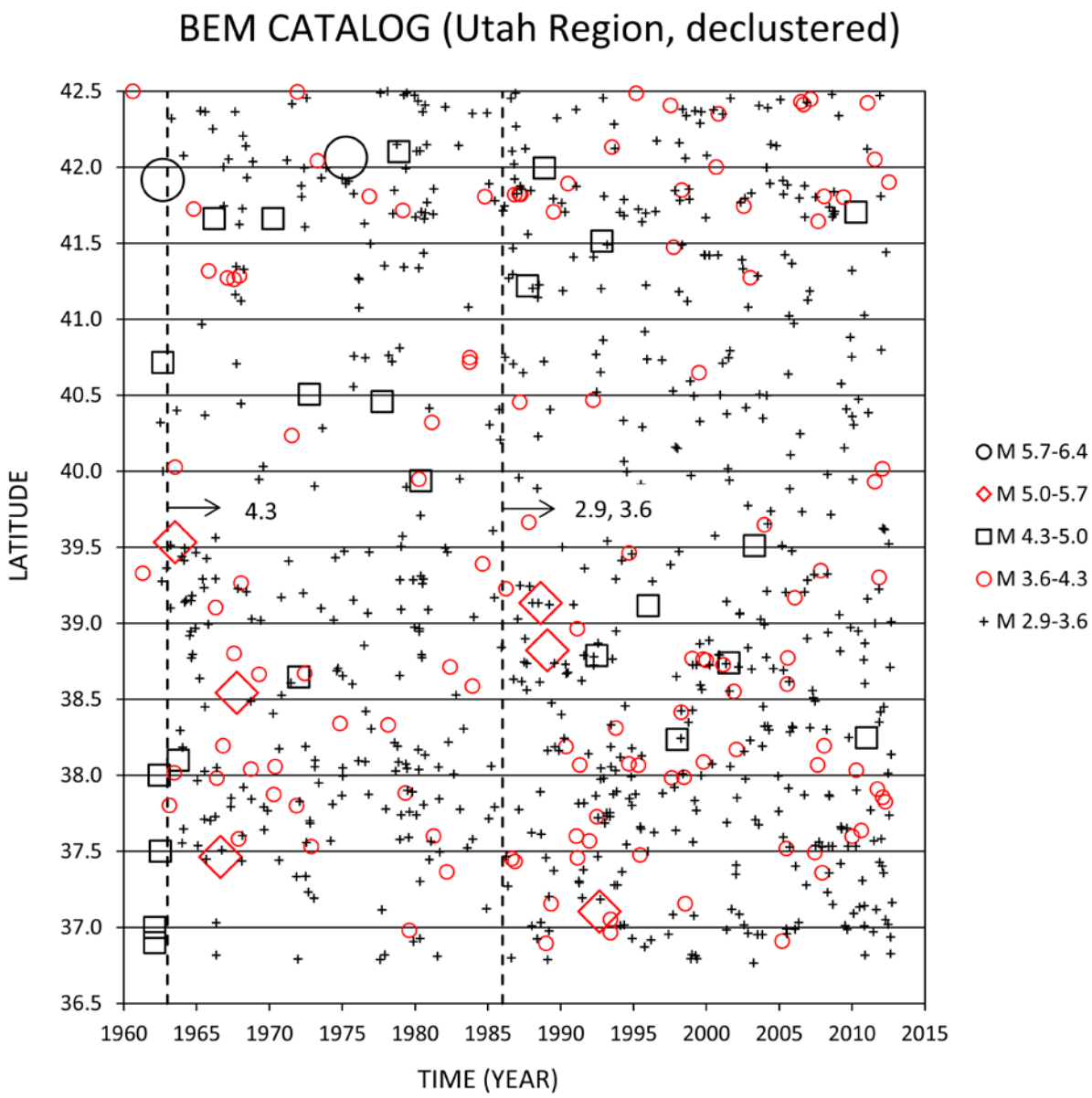

Figure E-23. *Space-time diagram (latitude vs. time since 1960) showing the distribution of mainshocks in the Utah Region of* $\mathbf{M} \geq 2.9$ *(2.85), differentiated by magnitude bins, for the declustered version of the BEM catalog. Injection-induced earthquakes (table E-4) are excluded. Vertical dashed lines indicate the start of completeness periods in 1963 for* $\mathbf{M} \geq 4.3$ *(4.25) and in 1986 for both* $\mathbf{M} \geq 3.6$ *(3.55) and* $\mathbf{M} \geq 2.9$ *(2.85).*

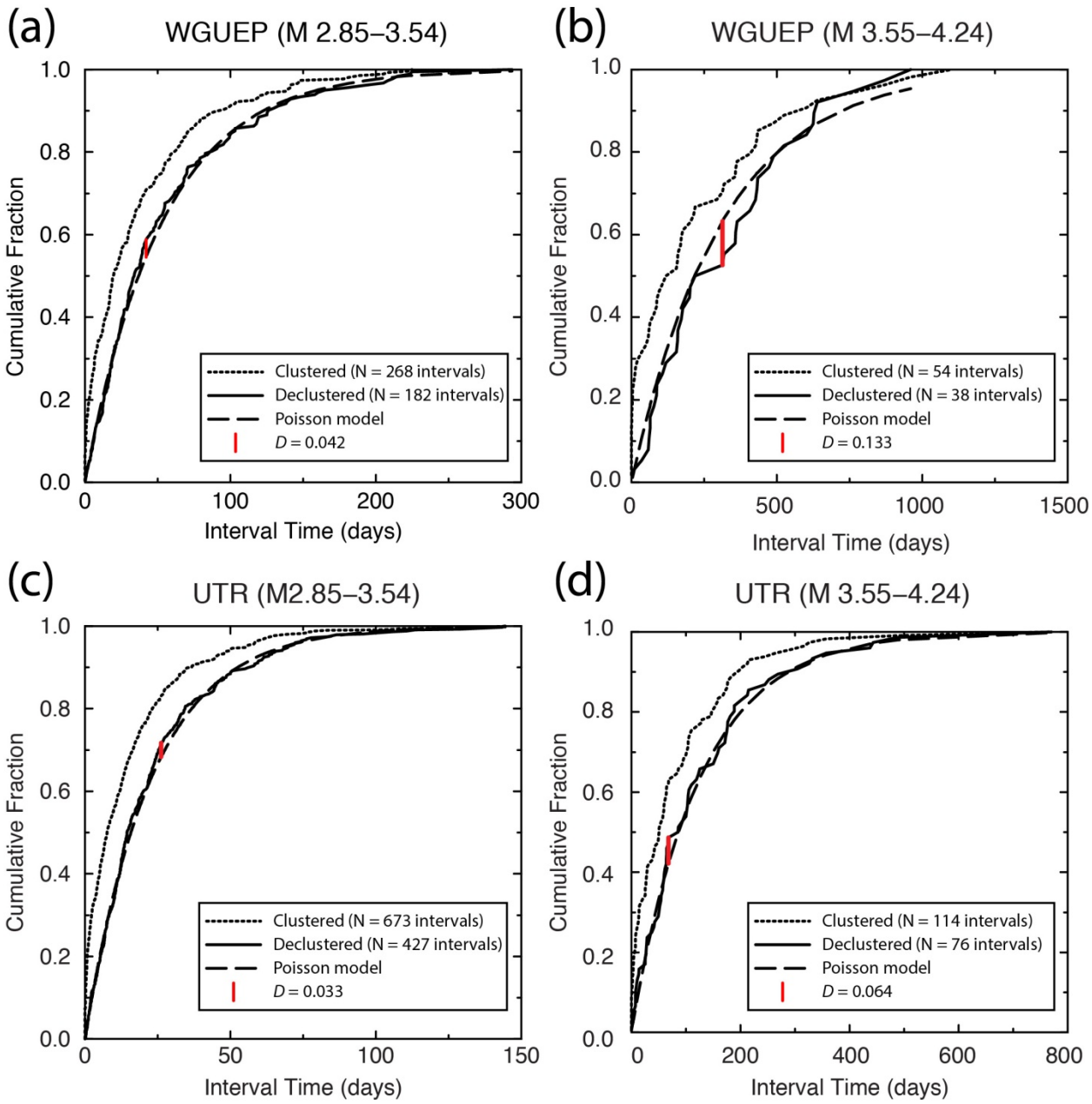

Figure E-24. *Cumulative distribution functions (CDFs) of interval (inter-event) times for earthquakes in selected magnitude bins in the WGUEP Region (a, b) and the Utah Region (c, d). In each panel, CDFs are shown for both the clustered and declustered cases. Data are restricted to the applicable periods of completeness. For the declustered case, the CDF is compared to that expected for a Poisson distribution; the largest absolute difference between the compared CDFs is the K-S statistic, D.*

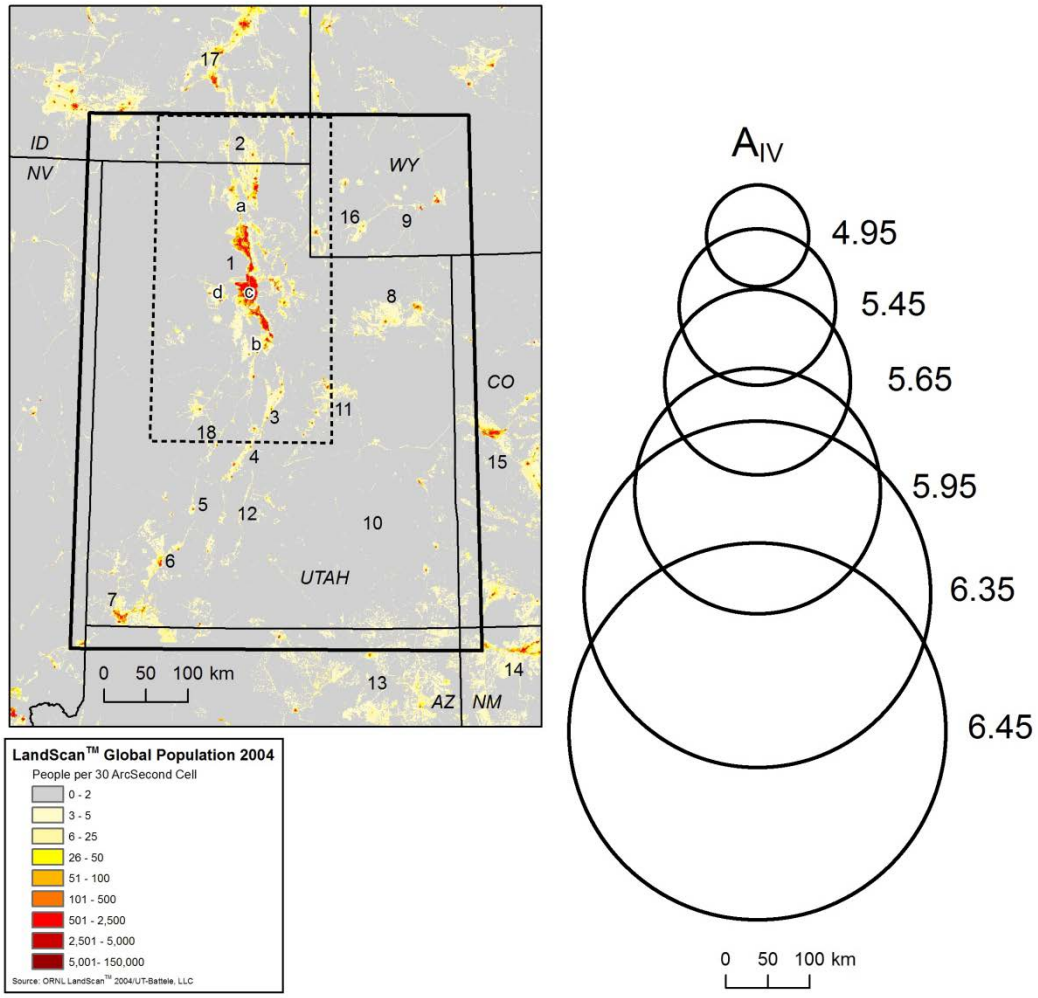

Figure E-25. *(left) Population density map of the Extended Utah Region in 2004 (source: Oak Ridge National Laboratory LandScan™ 2004/UT-Batelle, LLC); one 30 ArcSecond Cell = approx. 0.6 km². The WGUEP and Utah regions are outlined by dashed and bold lines, respectively as in figure E-1. Numbered localities are discussed in the text. For reference, a = Brigham City, b = Payson, c = Salt Lake Valley, d= Tooele Valley. (right) Circles showing the expected area shaken at or greater than MMI IV (A_{IV}) for earthquakes of various magnitudes from* ***M*** *4.95 to* ***M*** *6.45 (radii are given in table E-17).*

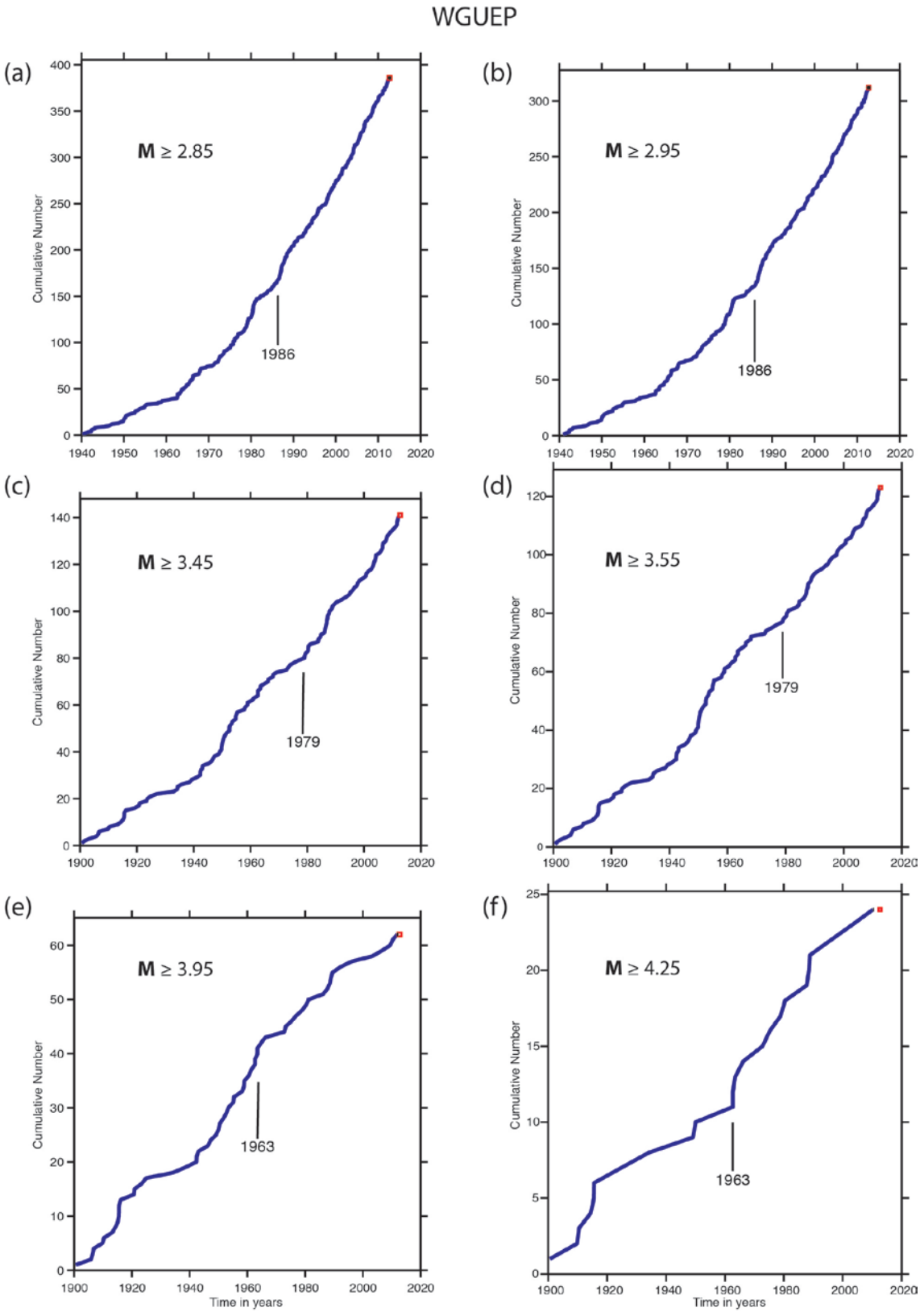
WGUEP
(a)
M ≥ 2.85
1986
(b)
M ≥ 2.95
1986
(c)
M ≥ 3.45
1979
(d)
M ≥ 3.55
1979
(e)
M ≥ 3.95
1963
(f)
M ≥ 4.25
1963
Cumulative Number
Time in years

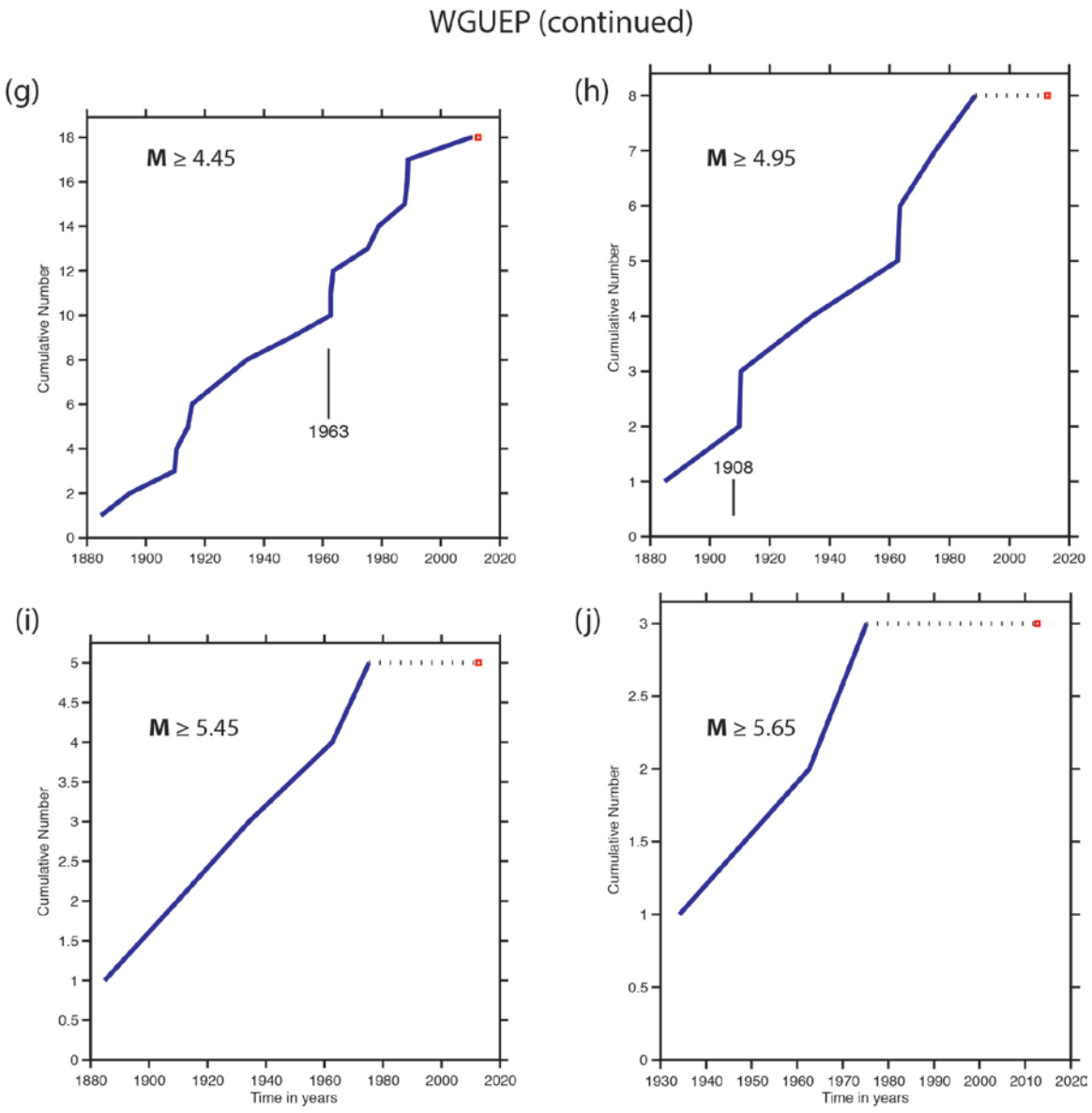

Figure E-26. *Cumulative recurrence curves (CRCs) for declustered earthquakes in the WGUEP Region (BEM catalog) for incremental magnitude thresholds listed in table E-16 from* ***M*** *2.85 to* ***M*** *5.65. Labeled vertical lines in panels (a) to (g) indicate the selected start date of a period of completeness picked from the CRC; that for 1908 in panel (h) is based on other arguments.*

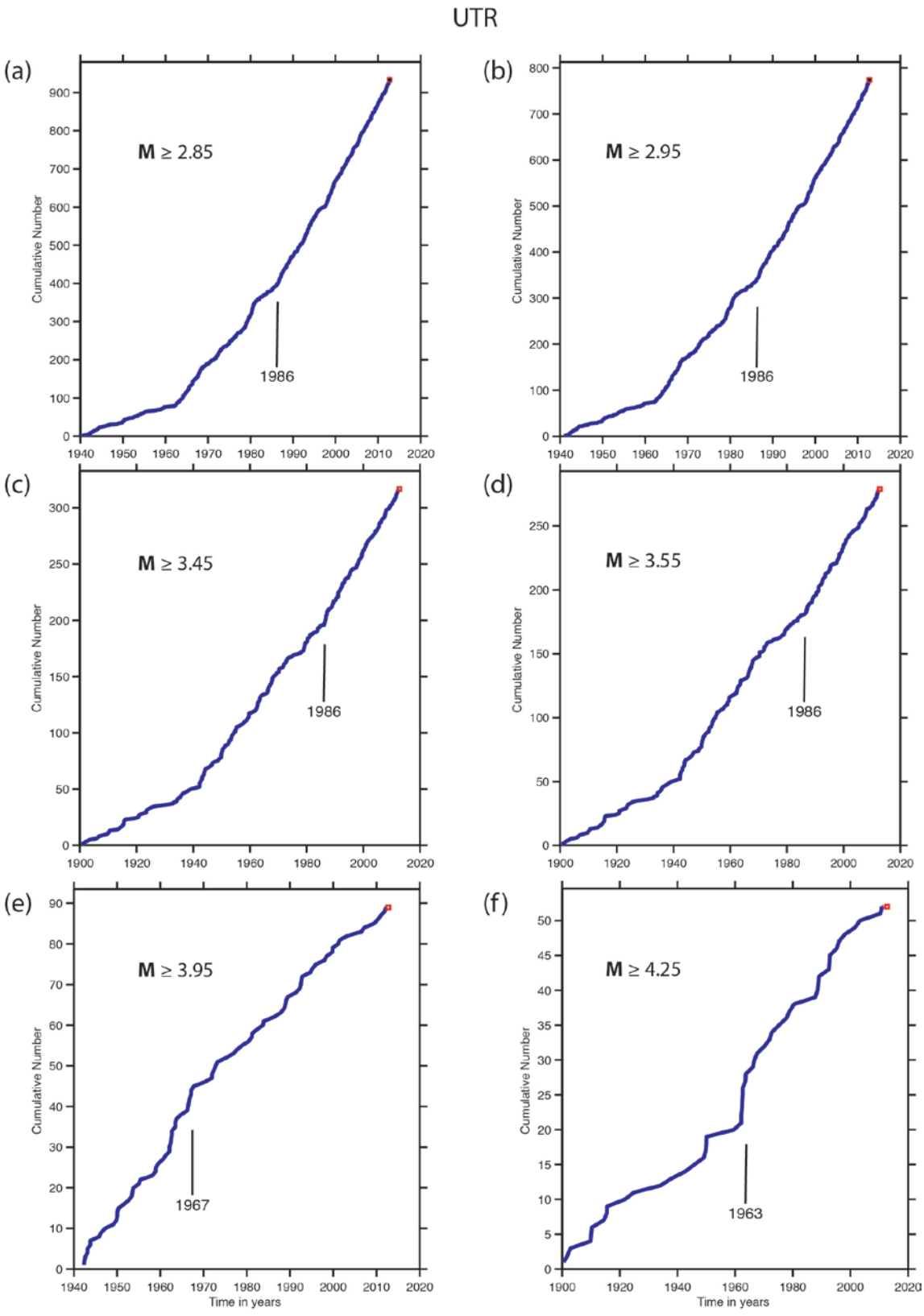
UTR
(a)
M ≥ 2.85
1986
(b)
M ≥ 2.95
1986
(c)
M ≥ 3.45
1986
(d)
M ≥ 3.55
1986
(e)
M ≥ 3.95
1967
(f)
M ≥ 4.25
1963
Cumulative Number
Time in years

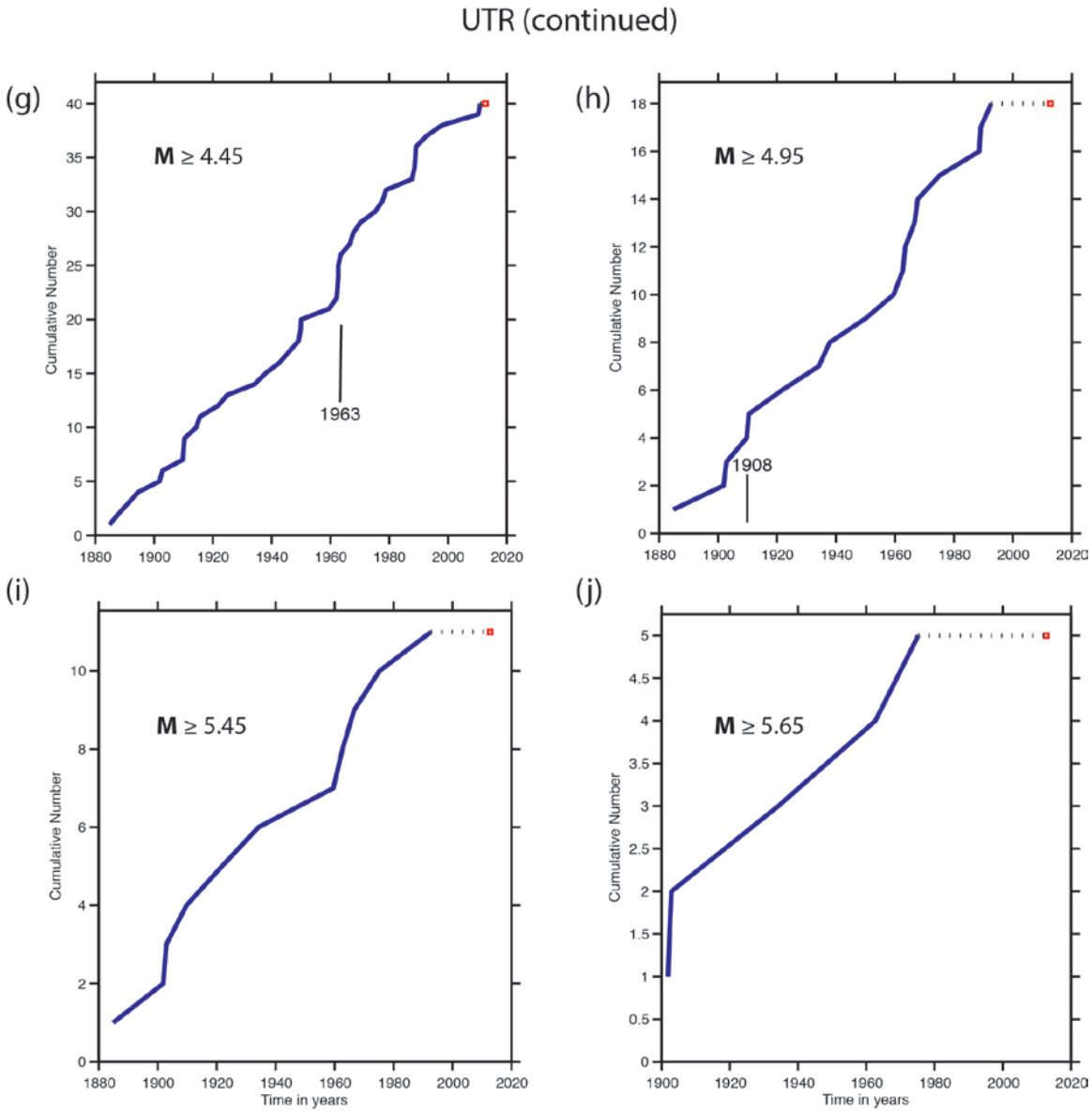

Figure E-27. *Cumulative recurrence curves (CRCs) for declustered earthquakes in the Utah Region (BEM catalog) for incremental magnitude thresholds listed in table E-16 from* ***M*** *2.85 to* ***M*** *5.65. Labeled vertical lines in panels (a) to (g) indicate the selected start date of a period of completeness picked from the CRC; that for 1908 in panel (h) is based on other arguments.*

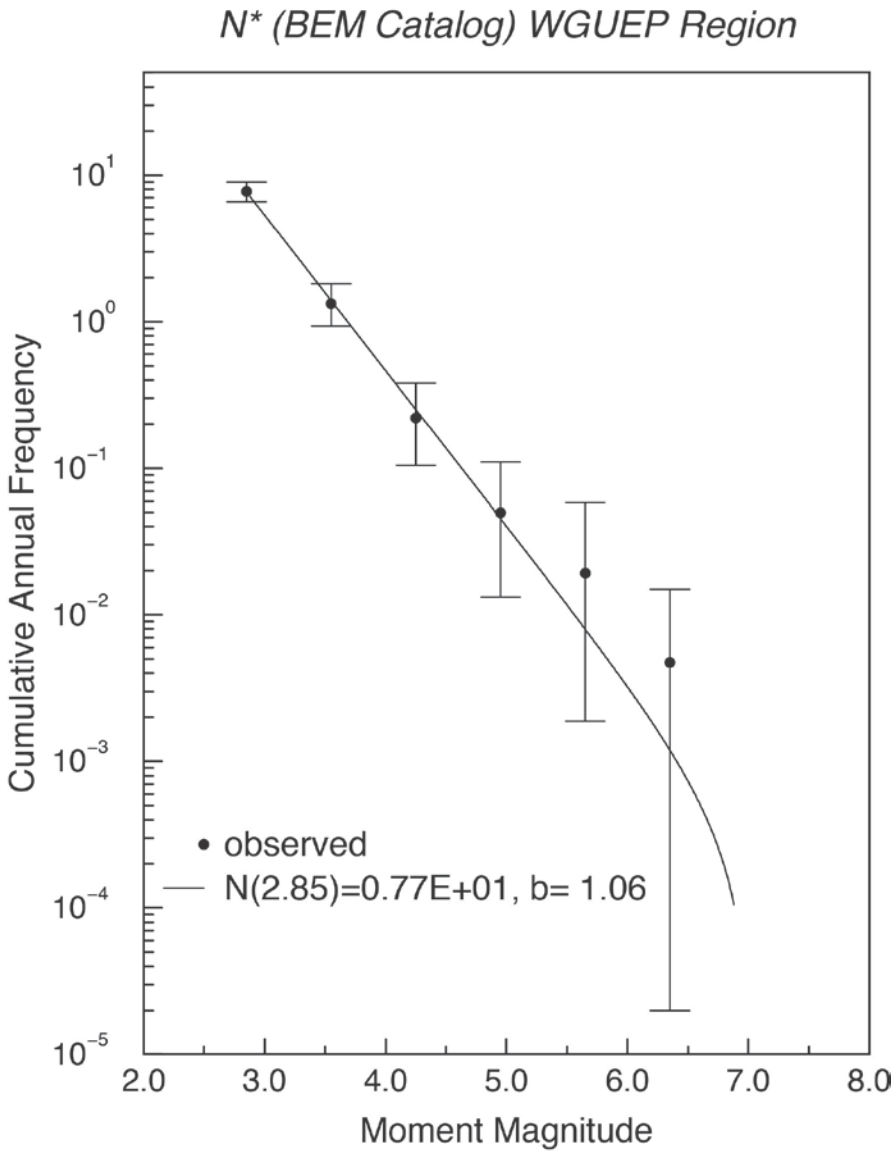

Figure E-28. *Background earthquake model for the WGUEP Region. Frequency-magnitude distribution of independent mainshocks (**M** ≥ 2.85), corrected for magnitude uncertainty and calculated using the maximum-likelihood algorithm of Weichert (1980).*

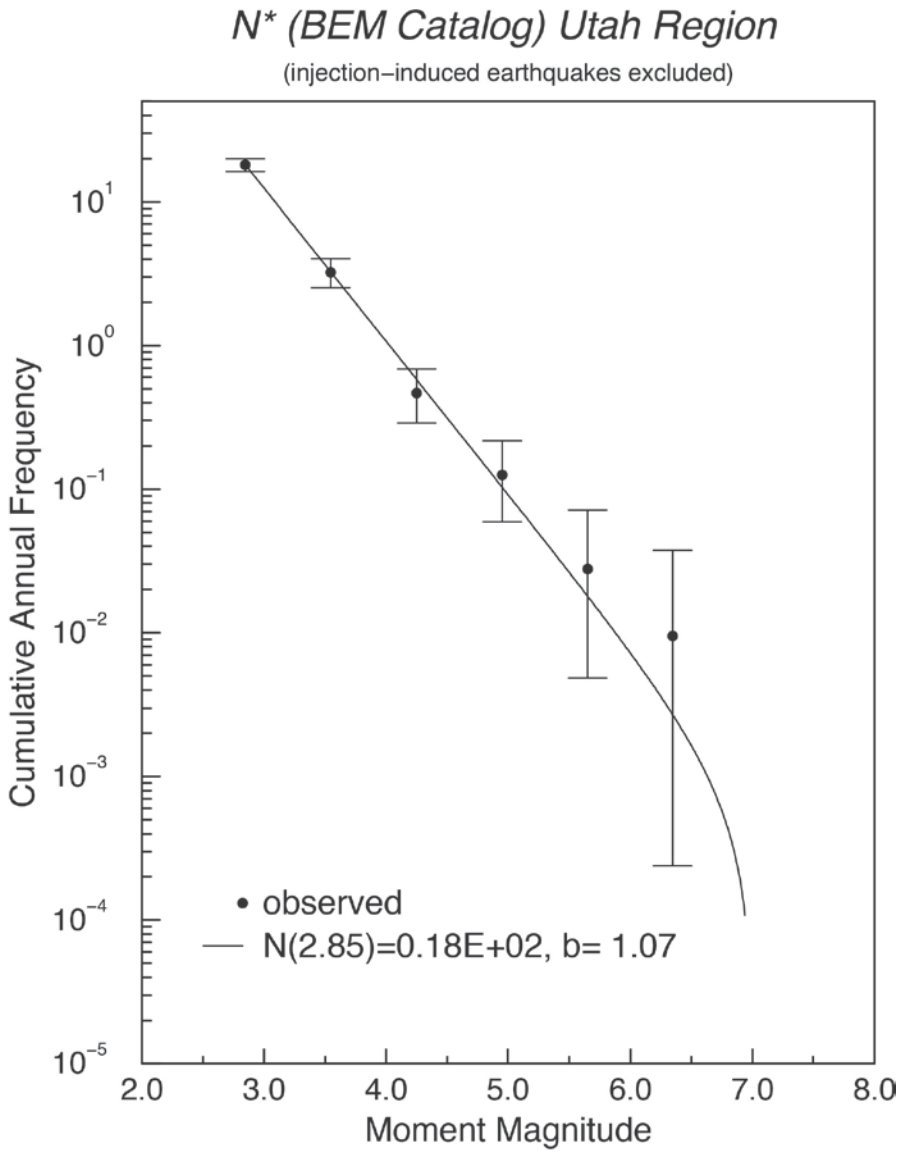

Figure E-29. *Background earthquake model for the Utah Region. Frequency-magnitude distribution of independent mainshocks (**M** ≥ 2.85), corrected for magnitude uncertainty and calculated using the maximum-likelihood algorithm of Weichert (1980). Injection-induced earthquakes listed in table E-4 are excluded from the rate calculation.*